INCORPORATING RISK CONSIDERATIONS IN AIRPORT RUNWAY PAVEMENT MAINTENANCE MANAGEMENT

H.R.PASINDU

NATIONAL UNIVERSITY OF SINGAPORE

2011

INCORPORATING RISK CONSIDERATIONS IN AIRPORT RUNWAY PAVEMENT MAINTENANCE MANAGEMENT

H.R.PASINDU

(B.Sc. (Hons) Engineering, University of Moratuwa, Sri Lanka)

A THESIS SUBMITTED

FOR THE DEGREE OF DOCTOR OF PHILOSOPHY

DEPARTMENT CIVIL AND ENVIRONMENTAL ENGINEERING

NATIONAL UNIVERSITY OF SINGAPORE

2011

ACKNOWLEDGEMENTS

I would like to convey my utmost gratitude to my supervisor, Professor Fwa Tien Fang, for his valuable guidance, encouragement and patience throughout the research. My gratitude also extends to Dr. G.P.Ong and Professor Meng Qiang for their advice.

I am thankful to my colleagues at NUS, Bagus Setiadji, Kumar Anupam, Farhan Javed, Wang Xingchang, Qu Xiaobo, Ju Fenghua, Zhang Lei, Liu Zhiyuan, Wang Qing, Aditya Nugroho and Imran Saikat. I thank the technical staff at Transportation Engineering Laboratory, Mr. Foo Chee Kiong, Mr. Goh Joon Kiat, and Mr. Mohammed Farouk for their assistance.

I am grateful to the National University of Singapore for awarding a research scholarship to pursue my studies.

Last but not least I would like to thank my parents and my sister for their support during this period, and my friends for their well wishes.

TABLE OF CONTENTS

EXECUTIVE SUMMARY

Aircraft safety on the runway is a major area of focus in the aviation industry. Runway excursions constitute a significant part of runway related accidents. Researchers have identified runway friction performance as one of the main causal factors of runway excursions. Therefore, from a safety point of view airport authorities have an important role to ensure airport pavement performance meet the standards required for safe aircraft operations.

Pavement management systems provide airport authorities with a method of establishing an effective maintenance and repair system. Most of the maintenance decision making, prioritization, and severity assessments is carried out based on subjective judgment from past experience, pavement condition determined from index method or from comparisons of measurements with pre-determined criteria etc. There is a need for an improved methodology to facilitate maintenance management decision making.

A methodology is presented to incorporate risk considerations into runway pavement maintenance management. Three main aspects namely, runway pavement management, aircraft runway safety risks, and analysis of wet pavement friction, are integrated in the development of the methodology. This research study evaluates runway distresses and surface characteristics on the basis of their impact on runway friction performance under wet pavement conditions. A finite element model has been developed to analyze tire-pavement-fluid interaction and simulate hydroplaning and skid resistance of aircraft tires on runway pavement covered with surface water. This analysis incorporates distress, runway pavement, and aircraft operating characteristics into the simulation. The results enable one to identify the relative

impacts that each of those factors have on runway friction performance and assess the risks on aircraft operations.

The first part of the thesis focuses on aircraft skid resistance in wet weather conditions. Aircraft braking distance under wet-pavement conditions is evaluated. The finite element model is used to evaluate skid resistance variation with speed. It can incorporate the effects of key factors such as water film thickness, wheel load, pressure, and surface condition into the analysis of skid resistance and braking distance. The computed braking distances, which constitute a main component of aircraft landing stopping distance, can be used to assess the overrun risk for different weather conditions and aircraft characteristics in an airport. The same approach is adopted to evaluate the beneficial effects of runway grooving in improving the skid resistance under wet pavement conditions. The results for different groove depths demonstrate the change in pavement frictional characteristics for runway with grooving, and provide a good indicator of the relative risk of aircraft overrun accidents under those conditions.

A new approach was adopted to determine the critical rut depth threshold for pavement maintenance based on its impact on aircraft safety performance. Safety risks mainly arise as a result of water accumulation which can lead to frictional losses. Therefore hydroplaning risk and increase of braking distance were identified as the main safety concern for rutting and the basis on which rut severity could be assessed. Input parameters related to aircraft, runway and ruts are used in the finite element model to evaluate hydroplaning speeds and skid resistance variation for different rut depths. These are used to identify the region where a rut of a certain depth can pose hydroplaning risk to the aircraft. Aircraft braking distances were calculated for different rut depths and analyzed to identify the rut depth at which aircraft braking distance increased to unacceptable levels. Next a probabilistic hydroplaning risk computation method for aircraft landing on a runway during wet weather is presented in this study. It considers the physical and operational characteristics of the aircraft, weather conditions, and the runway and pavement surface characteristics, for computation of hydroplaning risks for aircraft landing operations. This information is useful to determine the sensitivity of hydroplaning risk depending on other factors such as rainfall intensity, runway cross slope, surface characteristics and aircraft type.

The proposed approach allows for aircraft safety considerations to be incorporated into airport runway pavement maintenance management. Airport authorities can have a better understanding on how a distress would impact pavement performance, the relative impacts of different distress severity levels, and the safety margins involved, and enhance the decision making process in pavement maintenance management.

LIST OF TABLES

LIST OF FIGURES

CHAPTER 1 INTRODUCTION

1.1 Background

Airfield pavements are designed, constructed and maintained to support the critical loads imposed on them and to provide a smooth, skid resistant and safe riding surface (FAA, 2009a). Civil Aviation Authority (CAA) in the United Kingdom (UK) has given requirements in its standards for licensing aerodromes (CAA, 2001). The requirements for airfield pavements are as follows:

1. It must be of sufficient strength to allow aircraft to operate without risk of damage to either the pavement or to the aircraft.
2. It must provide a smooth ride. The surface profile of a new or resurfaced runway, in addition to complying with prescribed slope criteria of CAP 168, must be free of localized surface irregularities.
3. It must provide adequate friction. CAP 683 specifies minimum maintenance levels of surface friction for new and mature 'in-service' runways
4. It must be durable and free of foreign object damage (FOD).

It is vital that airfield pavements are designed and importantly maintained to meet these requirements. Pavement Management Systems (PMS) were first developed to offer a structured and comprehensive approach to pavement management. Its main functions are to improve the efficiency of decision-making, provide feedback on the consequences of decisions, and ensure the consistency of decisions made at different management levels within the same organization (Hudson et al., 1992). Pavement maintenance management is a functional phase of a pavement management system, covering all activities carried out to maintain it above the required level of service.

Pavement maintenance is essential to ensure that pavement functional performance and structural condition are maintained at the desired level.

The presence of surface distress influences both the functional performance as well as the structural integrity of a pavement. In general, maintenance work is planned based on pavement condition evaluation. Pavement condition is evaluated by two approaches: (a) functional evaluation on the pavement's ability to serve the user at the expected level of service (safety, ride comfort), and (b) secondly structural evaluation to determine effects on the pavement's strength and fatigue resistance to traffic loading and weather-related loading during its design life.

The functional performance of pavement is very important in the context of airports and particularly when considering runways. Unlike highway pavements, where a vehicle always have the option of reducing its speed when confronted with a rough pavement or low friction condition, the choice is not available for runway operations since a threshold velocity must be reached during either take-off or landing. Therefore, if a runway surface becomes too uneven or has too low a frictional capability to allow safe operations, that pavement can no longer be considered adequate, regardless of its structural capacity (Gendreau and Soriano, 1998).

Pavements can fail either structurally or functionally or both, depending on the severity and the extent of these surface distresses. Pavement system failure is a condition that develops gradually over a long period of time, and failure is determined once the pavement condition exceeds a predetermined performance criterion. Hall (2009) characterized highway safety as a driving environment free from danger or, more appropriately, one that is operated with rules and features designed to minimize crashes and the associated consequences (fatalities, injuries, economic loss). The same is applicable for airfield pavement safety, where failure refers to the occurrence of hazardous conditions which can be detrimental to safe operation of aircraft. Part of the operating environment is the pavement surface condition which should be maintained in a way to minimize the risk to aircraft safety.

Global air traffic is expected to grow at an annual rate of 5% to 6% for the next two decades (Boeing, 2011). In 2010, over 22 million departures had taken place worldwide (Boeing, 2010). As the demand for air travel increases and the capacity of airports are limited with limitations to expansion etc., it puts severe strain on both airport operators and airlines to ensure adequate safety levels are maintained. Although the expected frequency of aviation accidents is lower than for other transport modes, the consequences of accidents tend to be rather severe. It is imperative for airport authorities to maintain high safety standards. This includes implementation of a sound and well maintained airfield pavement system.

Historical accident data shows that aircraft landing/take off are the two most critical phases of a flight (Boeing, 2010). A significant part of runway related accidents are due to excursions where pavement surface plays a crucial role, especially during wet weather (Boeing, 2008; FSF, 2009; van Es, 2010). One of the main pavement related safety risks under wet pavement conditions is due to loss of friction. Considering the growth in global aircraft movements, this suggests that more aircrafts will be exposed to wet runway conditions. In view of this it is extremely relevant to address issues concerning aircraft safety during wet weather.

A main objective in airport pavement management is to ensure safe aircraft operations, this is especially critical on runway pavements. Therefore, it is the responsibility of agencies managing airport pavements to identify the risks related to pavement surface conditions and carry out pavement condition evaluation and maintenance planning accordingly to improve the overall runway safety performance.

1.2 Research Objective

The objective of the research is to develop a framework for improved runway pavement maintenance management by incorporating risk into the pavement management decision making process. As part of this objective, it is proposed that a mechanistically based approach be adopted as a tool to analyze the dynamics of distresses and evaluate how they influence pavement behavior and pavement-tire interaction. The importance of such an approach and how it alleviates some of the limitations encountered in the existing methods is the main focus of this research. The use of mechanistic analysis enables one to understand the distress and failure development mechanisms in relation to the distress characteristics, pavement behavior, and vehicle response. This can be used as a tool in airport maintenance management to improve its decision making for distress severity assessment, prioritization, and risk assessment for runway operation.

1.3 Organization of Thesis

The organization of the thesis comprises eight chapters. Chapter 1 is the introductory chapter. It gives the background to the topics discussed in the research, and describes the objective of the research.

Chapter 2 presents the literature review of the research. The literature review consists of three main areas: (i) review of airport pavement maintenance management systems, especially the maintenance strategies and distress assessment methods; (ii) a brief introduction to airport runway related safety issues; and (iii) a review of past studies on evaluation of wet pavement skid resistance and hydroplaning, and research related to tire-pavement-fluid interaction analysis. These three areas will form the basis for the methodologies developed in the research. Therefore, a basic description of them is necessary to gain a better understanding of the topics discussed later. The chapter concludes with highlighting the importance of adopting a new methodology that incorporates risk consideration in airport runway pavement maintenance management.

Chapter 3 provides the overall framework adopted in developing a methodology to incorporate risk into runway pavement maintenance management. This will be applied for the assessment of distresses or runway surface condition to evaluate the risk on aircraft safety. A major part of the methodology is concerned with evaluation of tire-pavement-fluid interaction to analyze skid resistance and hydroplaning behavior of tires. The finite element model developed for this purpose is also illustrated in the chapter.

Chapter 4 and 5 focus on aircraft tire skid resistance during landing under wet pavement conditions. The different factors that affect aircraft tire skid resistance are evaluated and a finite element model is developed to analyze the factors such as water-film thickness and wheel load effect on skid resistance. This is taken into account in computing aircraft braking distances under different wet pavement conditions. The probabilistic nature of aircraft operating characteristics is also considered.

One of the main methods used in airports to counter the loss of skid resistance is runway pavement grooving. Chapter 5 analyzes the beneficial effect of runway grooving on wet pavement skid resistance. A grooved runway pavement skid resistance is simulated using the finite element model developed in the research. Braking distances are computed for different water film thicknesses representing different wet pavement conditions. The braking distance results can be used to illustrate the beneficial effect of runway grooving.

Chapter 6 and Chapter 7 mainly focus on the risk of aircraft hydroplaning. Chapter 6 illustrates a methodology that can be used to assess rut severity based on hydroplaning consideration. The first part of the chapter is on rutting. It was established that one of the main impacts of rutting on aircraft safety was due to hydroplaning and skid resistance loss, which was used as the basis for determining rut severity. Chapter 7 analyzes another critical aspect of aircraft runway safety, i.e. hydroplaning during touchdown. A methodology is presented to evaluate aircraft hydroplaning risk for different locations in the touchdown zone under wet weather conditions.

Chapter 8 concludes and summarizes the major findings from the research and also proposes further research areas related to this theme.

CHAPTER 2 LITERATURE REVIEW

2.1 Introduction

There are differences between airfield and roadway pavements. Airfield pavements are subjected to a greater range of wheel loads, and wheel load applications are less frequent and more spatially distributed compared with roadway pavements. Aircraft speeds on the runways can be as high as 225 km/h. Therefore consideration on safety of aircraft operations is more stringent in airfield pavements, with runways as the most critical component.

The literature review consists of three main areas: (i) review of airport pavement maintenance management systems, especially the maintenance strategies and distress assessment methods; (ii) a brief introduction to airport runway related safety issues; and (iii) a review of past studies on evaluation of wet pavement skid resistance and hydroplaning, and research related to tire-pavement-fluid interaction analysis.

2.2 Airport Pavement Maintenance

Pavement maintenance is a functional phase of the pavement management system (PMS). The main activities in the maintenance process include: development of standards for pavement performance and repair methods, establishing of optimization and ranking methodologies, monitoring of pavement conditions, and scheduling of repair activities etc.

These activities are carried out in order to maintain the pavement level of service at or above the desired standards. The main challenge facing airport authorities is how to justify that maintenance treatments are necessary and to obtain funding for their implementation (Hajek et al., 2011). In other words, the first priority is to select the right pavement sections for treatment.

Maintenance activities are categorized into several types such as:

1. Routine maintenance work;
2. Time based maintenance; and
3. Condition based maintenance.

Condition based preventive maintenance is desirable for several reasons. It is considered a cost effective maintenance strategy to ensure that the pavement service levels are maintained above desirable level, and prevents premature pavement deterioration. It requires pavement condition surveys to evaluate the existing pavement condition, and expertise to understand the behavior of the pavement for formulating maintenance policies. It is also necessary to perform pavement condition prediction to identify the deterioration rate of pavement condition.

Proper maintenance and rehabilitation is necessary for maintaining functionality at a satisfactory level and also to maximize service life. Maintenance requirements can be determined based on the pavement age, types of aircraft operating, and presence of surface defects such as cracks, pavement stripping, joint disintegration, drainage issues etc.

Historically, most airport authorities have made decisions about pavement maintenance and rehabilitation based on maintenance needs rather than long-term planning or documented data (FAA, 2004). It is an "ad hoc" approach, whereby the staff applies the maintenance and repair procedure based on their experience as the best solution for the immediate problem. The drawbacks of this subjective approach are that they do not allow the decision makers to evaluate the cost effectiveness of alternative maintenance and repair strategies, and it leads to an inefficient use of funds (FAA, 2006). A systematic decision making procedure based on sound engineering analysis is preferred.

2.2.1 Pavement Condition Evaluation

Pavement condition evaluation provides one of the main inputs in the decision making process that will determine the maintenance activities to be carried out. It is therefore a key element of any PMS. Pavement condition evaluation includes the following aspects which are related to pavements structural and functional performance:

1. Pavement surface distress;
2. Pavement roughness;
3. Pavement friction;
4. Debris with FOD (Foreign Object Damage) potential; and
5. Pavement structural strength.

Airports employ pavement condition rating systems that provide a systematic method of collecting data of pavement distresses. The main pavement distresses such as cracks, potholes, rutting etc. are specified in the guidelines and priority ratings are usually defined using an aggregated index (Lim et al., 1996). It establishes a means of prioritizing all the different maintenance actions necessary to address the distresses observed, considering their characteristics such as severity, operational effect on the pavement, importance of the pavement on which it occurred and degree of deterioration (urgency of repair) etc.

At present, in most airports decision making for pavement maintenance and rehabilitation work is generally carried out based on an empirical index threshold such as Pavement Condition Index (PCI) (Green et al., 2004). The PCI method was developed in the United States, and is also adopted in European countries such as Sweden, Netherland and the UK (Barling and Fleming, 2005). Based on the PCI index maintenance strategies and priorities can be decided for each pavement section (*see* Table 2.1). It is based on observed distress characteristics such as type, severity and extent. Weighted deduct values are assigned based on these characteristics and combined to derive a single numerical value ranging from 0 to 100 (0 = Failed to 100 = Excellent) (Shahin, 1994). The detailed pavement condition surveys are carried out every 1-3 years but a survey at least once a year is recommended. PCI is essentially a surface distress index and, as such, does not constitute a comprehensive functional performance indicator. However, surface distresses have a significant influence on the functional condition of pavements and PCI can therefore be used as a means of assessing this condition, even though it is not a direct measure of it (Gendreau and Soriano, 1998).

Pavement Rehabilitation Index (PRI) is a similar index adopted in Japanese airports form the 1980s (Hachiya et al., 2008) to evaluate the surface condition of airport pavements. PRI is calculated based on physical measurements of surface conditions, and subjective opinions of pavement engineers. By comparing the calculated PRI value against appropriate criteria, the need for pavement rehabilitation work can be judged for runway, taxiway, and apron pavements. PRI for a section is calculated from three indices, namely crack ratio, maximum rut depth and roughness.

Most index methods are based on pavement distress evaluation which may not necessarily reflect pavement condition with respect to structural strength, skid resistance etc. Therefore, to obtain a more complete picture of pavement condition, airports use friction surveys, pavement non destructive test and roughness measurements in conjunction with distress based indices. The U.S. Air Force for example uses the following four factors: (i) PCI, (ii) Friction index, (iii) Structural Index, and (iv) FOD index to assess airfield pavements (Green et al., 2004) to plan maintenance and rehabilitation work.

Pavement maintenance needs can be determined based on pavement condition rating derived from subjective assessment carried out according to some guidelines such as the PASER manual (FAA, 2004). The PASER manual gives guidelines on maintenance options based on the distress types and conditions (*see* Table 2.2).

An engineered management system is necessary for the authorities to execute the complex airfield pavement maintenance tasks. Computer software is widely available today to help engineers organize and analyze pavement condition data, and formulate a pavement maintenance program. PMS software such as the PAVER system, which is based on the PCI system is widely used in the industry (Barling and Fleming, 2005). Other methods include the Integrated Airport Pavement Management System which uses both PCI and pavement residual life analysis based on expected traffic volume to estimate future pavement conditions (Gendreau and Soriano, 1998), and fuzzy logic-based systems (Fwa and Teng, 2003).

2.2.2 Pavement Distress Assessment

Distress types generally fall into one of the following broad categories according to the FAA advisory circular on Guidelines and Procedures for Maintenance of Airport Pavements (FAA, 2009a):

1. Cracking: In flexible pavements cracks are classified as longitudinal, transverse, and diagonal cracks, alligator or fatigue cracking, block cracking, slippage cracks, and reflection cracking.

2. Distortion: In flexible pavements distortion takes place in the form of rutting, corrugation and shoving, depression, swelling.
3. Disintegration: The most common type of disintegration in flexible pavements is raveling. Other forms of disintegration include potholes, jet blast erosion, and asphalt stripping.
4. Loss of skid resistance: Factors that decrease the skid resistance of a pavement surface and can also lead to hydroplaning are classified under this. Such factors include asphalt bleeding, contaminants such as rubber deposits, fuel/oil spillage, and polished aggregates etc.

The evaluation of distress characteristics can be made through direct measurements, visual condition surveys, or a combination of both. The distress identification guidelines used by inspectors specify the criteria for distress identification and severity assessment. Such criteria are based on physical parameters such as width, depth, extent measurement (Shahin, 1982). These properties of distresses are used as indicators to evaluate the condition of a pavement. For the PCI method the relative severity levels can be assessed based on the deduct value assigned for each distress severity and extent. As given in Table 2.3, for example, the relative severity of a rut defined as low, medium or high depending on the deduct values assigned based on the extent of the rut.

2.2.3 Issues in Pavement Condition Evaluation Methods

Several issues relating to the existing pavement distress condition evaluation can be identified. Subjective judgment based maintenance decision making leaves room for inconsistencies in the decision making process, which may be lead to non-optimal use of resources and budget, and could also compromise aircraft operational safety. The existing methods to prioritize distress involve assessment based on the distress physical characteristics such as length, density, width, and depth etc. It is necessary to consider the following during the assessment of pavement for distresses observed in airfield pavements:

1. Severity, extent and location of deterioration;
2. Operating characteristics of aircrafts using that pavement section;
3. Cause of deterioration and rate of deterioration; and
4. Possible maintenance and rehabilitation options.

Pavement condition index based assessment methods, used in most existing pavement management systems, incorporate most of the above mentioned aspects. However there is no reliable methodology to assess the rate of distress deterioration. Maintenance priority assignments made without considering deterioration rates may pose problems in the future. This is because pavement sections with similar index values may have different deterioration rates which could result in pavement sections conditions depreciating below the minimum acceptable levels (Baladi et al., 1992).

Another key issue is distress location. Different distress locations may receive different traffic loading, thereby affecting the rate of deterioration of structural related distresses. Similarly, due to the different levels of exposure to traffic, similar distresses formed at different locations may be assigned different levels of severity. The type of aircrafts and its operating characteristics also need to be considered in pavement condition assessment.

Another issue of artificial condition index is that they often do not have a clear physical meaning and might not have a direct relationship with the physical status of the pavement. For example, a study by McNerney (2010) revealed that certain pavement sections, though having high PCI values, had high severity map cracking and required maintenance work to be carried out. Those slabs would have a shorter service life, which was not correctly represented by their PCI values.

Distress severity classifications are generally made under three levels: low, medium, and high. These classifications include a relatively large range of distress severity levels under one category. They tend to exaggerate minute differences and in some cases conceal major differences in severity levels (Fwa and Shanmugam, 1998). Thus this procedure may not give a true representation of the actual conditions. Such methods of distress assessment do not offer an effective means for identifying the relative severity of most distresses.

PCI also does not provide a quantitative measure of the structural capacity of a pavement and it does not differentiate between different failure modes (i.e., functional or structural). To differentiate between structural or functional performance, the detailed condition survey data is required and an analytical evaluation has to be performed. This is often not carried out where the numerical condition index method is used.

With the issues highlighted in this section, it is apparent that an improved method to assess distress severities and assign maintenance priorities is necessary in airport pavement management. This is even more pertinent for distresses and pavement conditions that influence runway pavement’s functional performance with respect to safety.

2.2.4 Runway Friction Management

Pavement friction is a key attribute to ensure safety of aircrafts on the runway during landing and takeoff. The friction characteristics of the runway will vary over time as the runway is subjected to wear and tear (polishing), accumulation of rubber deposits and to effects of weather. This is evident from the runway friction report presented in Figure 2.1 which shows that the touchdown zone and sections of the runway traversed by aircrafts frequently are subjected to higher loss of friction

Some of the causes of low friction can be identified during pavement distress surveys. Identifying sections of a runway that may warrant maintenance requires a method to measure the surface friction condition. Runway friction measurements are usually made using self-wetting continuous friction measurement equipment (CFME). The FAA advisory circular recommends that friction survey scheduling frequencies be made based on aircraft traffic volume and the composition of wide body aircrafts in the traffic mix (FAA, 1997). The same circular gives the minimum friction levels allowable for runway pavements for different friction measurement equipments used for the survey (*see* Table 2.4). FAA also specifies runway friction levels and representative runway surface condition and aircraft braking action definitions (*see* Table 2.5) (FAA, 2007). This provides guidance for airport authorities as well pilots to assess suitability of runway for aircraft operations. In addition surface texture depth measurements are also conducted at areas of low friction. Similarly, guidelines for rubber deposit removal frequency are determined based on the traffic volume on the runway (FAA, 1997). However, there could be a degree of subjective judgment involved in this process since the supervisors will generally determine when to activate rubber removal (Fwa et al., 1997).

To reduce potential safety problems caused by low runway surface friction, airport authorities carry out the following activities under a pavement management program to restore the runway condition to acceptable levels.

1. Remove contaminants such as oil, dust, rubber deposits etc. based on reports from distress surveys, or runway friction measurements.

2. Overlays are constructed in the cases where the runway is structurally deficient as well.
3. Porous friction courses are used only in airports with low volume of turbojet aircrafts (FAA, 1997).
4. Saw cut grooving is implemented in many airports to improve the wet weather frictional performance of the runway.

Airport operators should develop a systematic approach to measure runway surface friction characteristics, and determine the degradation of runway surface friction in their friction management program to maintain adequate safety to the aircrafts.

2.2.5 Issues in Runway Friction Management

Airport authorities need to take measures to mitigate potential problems caused by low runway surface friction. This can be achieved by providing reliable aircraft performance data to determine the required landing or take-off distances, allowable cross wind limits etc. for different pavement friction levels. However this is not an efficient way to manage runways.

Determining aircraft performance data for take-off and landing related to available runway surface friction/aircraft braking performance has proved to be difficult. One reason is the problem of determining runway friction characteristics in operationally meaningful terms in all conditions. Another reason is the uncertainty in applying CFME measured values to assess aircraft braking performance (EASA, 2010). The operational characteristics of friction measurement devices are different from the aircraft wheel-brake-anti-skid systems that generate the braking friction during ground maneuvers. This applies in particular to aircraft operations on wet runways (CAA, 2008). Therefore, CFME measured friction values are primarily just indicative tools rather than a representation of aircraft performance. Therefore it is important to look at improved methods to plan runway pavements maintenance work related to friction.

The Engineering Science Data Unit (ESDU, 1999) formulated a model to predict the effective coefficient of friction for aircrafts based on ground vehicle measurements. However there is no comparison with actual values from aircraft tests to assess its reliability. The ESDU model is a useful step towards developing an overall analytical framework for quantifying and predicting wet runway friction. However it faces the inherent problems of empirical models that their applicability is limited to the conditions tested, and the fact that the effect of varying water depths is not included in the model also presents a limitation (Transport Canada, 2001).

The possibility of using aircraft landing data to calculate braking performance has also been investigated. This method has significant potential for the future, because it could eliminate ground friction measurements and allow the true aircraft braking action to be calculated from the aircraft instead. However, this approach is still at an early stage of development. Although a proof of concept has been developed, it is necessary to perform a number of evaluation and assessment trials to test its effectiveness, objectiveness, and comparability in different countries (EASA, 2010).

The other option to control aircraft safety risks is to ensure adequate runway surface friction at all times under all weather conditions. This involves developing and implementing appropriate standards for runway design and maintenance. This would require the determination of runway surface friction characteristics with speed during wet runway conditions. Monitoring runway surface texture/ grooving deterioration due to rubber deposits, wear and tear is also important. Surface drainage is also a critical issue in maintaining good friction conditions in wet weather. Therefore, it is necessary to identify occurrences of significant surface water depth during wet weather condition. When slippery runway conditions exist, additional measurements should be made to determine possible causes and carry out remedial work. During the pavement design phase, runway gradients, surface course with respect to its texture, provision of grooving etc. should be examined to minimize aircraft safety risks.

2.3 Evaluation of Runway Friction Performance

One of the important goals in runway maintenance is to identify and repair runway pavement conditions that affect aircraft safety. Major components of safety evaluation of runways include:

1. Friction.
2. Foreign object damage (FOD) - Aircrafts travelling at high speeds on the runway can easily get damaged due to foreign objects (e.g. tire ruptures etc.) and ingestion of foreign objects into the engines which can induce significant damage to the engine. According to the Federal Aviation Administration (FAA) Advisory Circular 150/5380-5B (FAA, 2009c), FOD costs one major airline an average of $15,000 per aircraft, which represents an industry cost of $60 million per year.
3. Roughness - Pavement roughness can impair the safe operation of the aircraft due to cockpit vibrations, excessive gravitational forces, etc. (Transport Canada, 2008; FAA, 2009b).
4. Pavement distortions such as ruts – Ruts cause water accumulation which could allow water ingestion in engines, hydroplaning, ice forming during winter

The remainder of the literature review will introduce concepts relating to runway friction since it is by far the most significant factor for aircraft safety. Analyzing runway pavement's friction performance requires the analysis of tire-pavement interaction.

2.3.1 Runway Skid Resistance

Pavement friction is the force that resists the relative motion between a vehicle tire and a pavement surface. This resistive force is generated as the tire rolls or slides over the pavement surface. The resistive force, characterized using the non-dimensional friction coefficient, μ, is the ratio of the tangential friction force (F) between the tire tread rubber and the horizontal traveled surface to the perpendicular force or vertical load (L) and is computed using Equation 2.1.

$$\mu = F / L \tag{2.1}$$

Longitudinal frictional forces occur between a rolling pneumatic tire (in the longitudinal direction) and the road surface when operating in the free rolling or constant-braked mode. In the free-rolling mode (no braking), the relative speed between the tire circumference and the pavement—referred to as the slip speed—is zero. In the constant-braked mode, the slip speed increases from zero to a potential maximum of the speed of the vehicle (Meyer, 1982). The coefficient of friction between a tire and the pavement changes with varying slip (Henry, 2000). As shown in Figure 2.2, the coefficient of friction increases rapidly with increasing slip to a peak value that usually occurs between 10 and 20 percent slip (critical slip). The friction then decreases to a value known as the coefficient of sliding friction, which occurs at

100 percent slip, and is termed as skid resistance. The difference between the peak and sliding coefficients of friction may reach up to 50 percent of the sliding value, and is much greater on wet pavements than on dry pavements (Henry, 2000).

The magnitude of the available skid resistance for an aircraft is affected by a large number of factors associated with the aircraft, aircraft tire and braking system, runway surface, and the environment (*see* Figure 2.3). It is understood that the friction level of an ordinary pavement when dry would be sufficient for safe aircraft operation in practically all cases. The main issue arises due to pavement contamination, such as oil, grease, rubber deposit and surface water. These oil and grease patches and rubber deposits must be taken care of by means of pavement maintenance operations. Surface water on rainy days presents the most common operating condition in an airport.

2.3.2 Hydroplaning

Hydroplaning is a wet weather phenomenon whereby the tires of a vehicle or aircraft are separated from the pavement surface by a thin film of fluid. Hydroplaning can be considered as the extreme case of loss of skid resistance. Three types of hydroplaning can be distinguished:

- Dynamic hydroplaning
- Viscous hydroplaning
- Reverted rubber hydroplaning

Dynamic hydroplaning is the more relevant case and will be discussed here. Hydroplaning occurs as a result of the hydrodynamic forces on a tire exerted from the trapped water between the tire foot print and the pavement. As the speed increases the magnitude of the hydrodynamic uplift forces increases and when it equals or exceeds the wheel load, the tire looses contact with the pavement and it hydroplanes. As shown in Figure 2.4, the contact area gradually decreases as the tire speed increases on the water-covered pavement. At the onset of hydroplaning, the area under Zone 3 (contact zone) completely diminishes. The speed at which this occurs is referred to as the hydroplaning speed. It is a critical safety concern since there is virtually zero friction available for braking or directional controlling of the vehicle. Factors that contribute to hydroplaning risk include water depth, high aircraft speed, low tire pressure, low wheel load on the main gear, and inadequate tire tread depth (Horne and Dreher, 1963).

2.3.3 Factors Affecting Wet Runway Friction

Aircraft performance under wet runway conditions depends on the available runway pavement friction, aircraft factors such as the braking system and pilot techniques. The magnitude of available friction will depends on (i) runway surface water film thickness, (ii) tire-pavement drainage capability, and (ii) runway pavement friction properties. Factors discussed below will influence either one or both these aspects.

1. Surface Water

The operating condition of the runway is perhaps one of the most important aspects of airport pavement management. Because of the high speed of aircraft operation during landing and takeoff, one needs to consider the braking performance and control of an aircraft during wet weather. The characteristics of the water film that affect aircraft braking performance include its thickness, viscosity, temperature, and density although water film thickness is generally considered as the most critical factor (Meyer et al., 1974; Horne, 1975). As shown in Figure 2.5, as the water depth or thickness increases on a runway surface, skid resistance decreases. More crucially it increases the rate of skid resistance reduction with speed (Trafford and Taylor, 1965).

The worst case scenario due to surface water build-up on runway is hydroplaning of tires which can lead to virtually zero level of friction (Horne and Dreher, 1963). Horne and Leland (1962) conducted a study with full-scale aircraft tires on a relatively smooth concrete test track, and reported that hydroplaning occurred on a smooth tread tire when the concrete runway was flooded with water to the extent that the fluid depth varied between 0.1 to 0.4 inches (2.54 to 10.16 mm) (Horne and Leland, 1962). Gray (1963) conducted tests with Meteor aircrafts and indicated that the minimum water depth required for hydroplaning on smooth pavements was 0.17 inches (4.32 mm).

2. Aircraft Factors

Aircraft Speed

The speed of an aircraft has a major impact on aircraft skid resistance. Skid resistance will generally decrease with an increase in speed. Several studies conducted with aircraft tires and aircraft test runs have demonstrated that the magnitude of skid resistance reduction with speed is dependent on other factors such as runway water film thickness, tire tread depth, runway grooving etc. (*see* Figures 2.5 and 2.6) (Agrawal, 1983; Horne and Leland, 1962, van Es et.al., 2001). Skid resistance will continue to decrease with speed until aircraft speed reaches hydroplaning speed.

Tire Pressure

Tire pressure has a direct positive influence on hydroplaning speed. This was first validated by experimental studies conducted by NASA (Horne and Leland, 1962). This led to the development of the following NASA hydroplaning equation which is used by many practitioners to date.

$$v_p = 9\sqrt{p} \qquad (2.2)$$

where v_p is the hydroplaning speed (in knots) and p_t is the tire inflation pressure (in psi). Hydroplaning is said to occur when the touchdown speed of a given aircraft type exceeds the NASA hydroplaning speed. The difference in the pressure within and outside (atmospheric pressure) the tire footprint creates forces which expel the water trapped in the tire-pavement contact zone. The velocity at which water is expelled increases with tire-pavement contact pressure (Horne, 1976). Thus, increasing tire inflation pressure increases the rate of flow of water drainage out of the footprint and raises the tire hydroplaning speed.

Wheel load

Tire vertical load has a relatively small effect on the tire hydroplaning speed (Horne and Dreher, 1963). However the magnitude of frictional force available at the tire pavement interface depends on the load exerted on the pavement surface (Horne and Leland, 1962). Unlike the case for road vehicles, the hydrodynamic uplift forces generated during aircraft ground roll on the runway reduces the wheel load. Lower wheel load means lower braking forces available for the aircraft, as in the case of initial phase after touchdown (Yager et al., 1970). The high speed of aircraft coupling with uplift forces compounds the problem of tire-pavement friction analysis for aircraft landing and take-off (ESDU, 1995).

Tire Properties

The mechanics of tire deformation also affects the resistance to skidding. The magnitude of tire foot print has a direct influence on the buildup of hydrodynamic forces on the tire. Other tire factors such as tread design, rubber compound, and tread depth are also important parameters that affect the braking performance of aircraft on water covered runways (Agrawal 1986, Horne and Dreher 1963, Yager and McCarty 1977).

Grooves in tire treads provide channels for drainage of water from the tire footprint area. Therefore the loss in braking traction due to partial hydroplaning effects is considerably less for ribbed tires than for smooth tires (*see* Figure 2.6). Ribbed tires with adequate tread depth increases the speed required for hydroplaning as well as increases the minimum water film thickness required to initiate hydroplaning (Horne and Leland, 1962). Results of full-scale hydroplaning tests for different aircraft tire types showed that older bias-ply tires have higher hydroplaning speeds compared to newer bias-ply tires, type-H tires and radial-belted tires (van Es, 2001). It was concluded that this is caused by the difference in tire footprint characteristics of these tires.

3. Pavement surface characteristics

Surface properties

A surface must have both macrotexture and microtexture to maintain adequate friction at the tire-pavement contact. Microtexture refers to the fine scale roughness contributed by small aggregate particles on pavement surfaces, and is related to the particle mineralogy. This irregularity in the surface texture is measured at the micron scale (1 µm – 0.5mm). The microtexture provides the harshness or grittiness needed to penetrate the thin water film formed between the tire and the surface aggregates to permit adhesion to develop. Macrotexture refers to the visible roughness of the pavement and is mainly attributed to the size, shape, angularity and the distribution of coarse aggregate. This is measured in millimeters in the range of 0.5-50mm. Macrotexture provides improved drainage from the tire-runway contact area.

Grooves are made in runways to improve pavement surface macrotexture and increase skid resistance properties. It has been established that the available friction on grooved runways covered with water are higher than on non-grooved runways under otherwise identical operational conditions (*see* Figure 2.6) (Gray, 1963; Horne and Brookes, 1967).

2.3.4 Evaluation of Tire-Pavement-Fluid Interaction

The analysis of tire-pavement interaction can provide a useful tool for runway friction management. This refers to a mechanistic approach to analyze the related factors in pavement friction, especially for wet pavement skid resistance. There have been many researchers in pavement engineering who have attempted to study this issue based on experimental methods (Horne and Dreher, 1963; Gallaway et al., 1979). A list of models developed to estimate hydroplaning speed and skid resistance is given in Tables 2.6 and 2.7.

There are several limitations associated with experimentally derived relationships. Their applications are limited to conditions similar to the original experimental test conditions. They cannot be used for different aircraft types and configurations, and different environmental and pavement conditions. The inherent complexity in the interaction of factors that influence pavement-tire friction could not be adequately explained by the experimental empirical relationship. Although the empirical models have their limitations, they are still in use today due to a lack of analytical and numerical models that can explain both the skid resistance reduction and hydroplaning.

In order to address this shortcoming several researchers adopted numerical methods, especially finite element method, to study the skid resistance and hydroplaning behavior of tires on pavement (Zmindak and Grajciar, 1997; Okano and

Koishi, 2000; Li et al., 2004; Ong and Fwa, 2007a). Ong and Fwa (2007a, 2007b, 2008) developed a finite element model for skid resistance and hydroplaning evaluation for smooth car and truck tires. They also evaluated the effects of different factors on skid resistance: sliding speed, wheel load, water-film thickness and tire inflation pressure. The results showed that loss of skid resistance is significant with increase in water-film thickness especially at high speeds and in general wheel load and tire pressure had a positive effect on skid resistance.

Finite element analysis of tire-pavement-fluid interaction offers an advanced technique to incorporate the many factors that affect wet pavement skid resistance into the analysis. Such analysis develops interactive models for tire, pavement and fluid to evaluate the hydroplaning speed and skid resistance for tires.

2.4 Analysis of Runway Safety Risks

Safety remains as one of the most important issues in the aviation industry. Critical phases of flight with respect to accidents are the landing and takeoff phase where 25% and 12% of the fatal aviation accidents take place worldwide were during aircraft landing and take-off respectively (Boeing, 2008). One of the major risks to the aircraft during landing and takeoffs is due to runway excursions. Runway excursions are the general term used to define aircraft overrun and veer-off accidents that occur during landing and take-off on the runway. An overrun occurs when an aircraft attempts to land or to abort a takeoff but fails to stop on the runway, and travels past the runway end. Veer-off accident is defined as accidents in which the aircraft could not be stopped on the runway and ran off the side of the runway edge.

In 2008, 30% of worldwide aircraft accidents were runway excursions (Boeing, 2008). Another study which analyzed the total commercial aircraft accidents (with major or substantial damage) from 1995-2008 showed that nearly 23% were landing excursion accidents (FSF 2009). Runway excursions can result in loss of life and/or damage to aircraft, buildings or other items struck by the aircraft. Excursions are estimated to cost the global industry about US$900 million every year (van Es, 2010). The Flight Safety Foundation reported that landing excursion accidents constituted nearly 80% of the total excursion accidents, and their share was steadily increasing over in the last few years (FSF, 2009). With the expected growth in international air traffic, landing excursion accidents could continue to be a major issue of aviation safety. It is imperative that the safety standards for runway overruns be improved in order to keep the number of accidents under control.

2.4.1 Runway Excursions Causal Factors

Many researchers have studied aircraft accidents to identify the causal factors for excursion accidents. These can be categorized as factors relating to flight operations, air traffic management, airport, regulatory, and aircraft manufacturer and weather (FSF, 2009). From an airport pavement management perspective this section highlights the weather and aircraft operating factors. The next section will examine pavement related factors.

Impact of wet weather

A historical analysis of aircraft runway accidents shows that the percentage related to weather is 29% (Benedetto, 2002). These include high wind, low visibility conditions, periods of high intensity rainfall, and combination of all. Kirkland et al. (2004) in their study on aircraft runway operational risk suggested that poor weather and its effect on runway condition were likely to induce overruns, particularly for landings. They showed that of the 118 overrun landings analyzed, 20% were in precipitation, and the remaining 31% suffered both precipitation and restricted visibility. The corresponding data for takeoffs were 15% and 12% respectively. For the landing overrun cases, 29% occurred on very wet, flooded, snow, ice or slush covered runways; and 14% of the takeoff overruns occurred in these conditions.

A study conducted by the Australian Transport Safety Board (ATSB) also revealed a similar relationship between runway excursion accidents and wet pavement conditions (ATSB, 2008a, b). Wet or contaminated runways were present in 77 (64%) of 120 runway excursion accidents. A Study by the Netherland Transport Safety Institute (NLR) analyzed main causal factors for overrun and veer-off accidents in Europe and worldwide (van Es, 2010). Table 2.8 presents these findings for the main factors for landing overrun accidents. Wet/contaminated runways were factors in both types of accidents during landings and takeoff (nearly 40% of all landing overrun accidents in Europe and 2/3rd worldwide), and hydroplaning was a factor in nearly 14% of the total overrun accidents.

Effect of aircraft operational characteristics

The condition of aircraft excess approach speed (fast landing) condition exists when the calibrated air speed at or near the threshold exceeds V_{ref} + 20 kts (V_{ref} is the reference landing speed). The aircraft speed flown at the threshold has a dominant influence on the landing distance (van Es et al., 2009). Under normal circumstances an aircraft is expected to touchdown within 1000 - 1400 ft (304.8m - 426.7m) from the threshold. A long landing occurs if this distance is exceeded by a considerable margin, e.g. touchdowns of more than 2000-2300 ft (609.6m to 701.04m) from the threshold or 25-33% of the runway length (van Es et al., 2009).

Kirkland et al. (2004) concluded that fast and high approaches that continued to an attempted landing are frequently a feature of landing overruns and 22% of landings are known to have been conducted with excessive approach speed. An ATSB study (ATSB, 2008a) also showed that weather-related factors were a factor in runway excursions with the presence of other contributing factors such as un-stabilized approaches, long and/or fast landings, selecting a runway that was not suitable for the aircraft type, approach type, failing to go around where potentially dangerous conditions existed, or delayed or incorrect use of braking devices. In other words, such factors can be compounded by poor environmental conditions and increase the risk of unsafe outcomes, such as a runway excursion. The Netherland Transport Safety Initiative estimated that 24% of landing overrun accidents in Europe is associated with long landing, and 14% is associated with fast landing (van Es, 2010). A list of recent runway excursions that one or more of the causal factors described above appeared is given in Table 2.9.

2.4.2 Aircraft Safety Risks due to Runway Pavement Friction

From the review in the previous sections it is clear that aircraft safety during landing and taking off is affected by runway conditions. Good runway conditions are critical for aircraft safety during landing and takeoff operations for several reasons. Firstly while vehicles on road can drastically decrease its speed during the brief periods of heavy rainstorms, aircrafts have to maintain certain high speeds for takeoff and touchdown speed (exceeding 120 knots or 222 km/h). Secondly, the drainage length of a runway is substantially longer than a road section (more than twice), resulting in thicker water films (Newell, 1991). As explained earlier, higher water film thicknesses increase the potential of hydroplaning and loss of skid resistance.

Two major forms of friction-related aircraft operational risks on runway can be identified. They are hydroplaning and loss of skid resistance, which are described in the following two sections.

Hydroplaning

Hydroplaning of aircraft tires poses the most severe hazard to safe operations on runway. Both main wheel braking effectiveness and nose wheel steering are severely affected when one or more aircraft tires hydroplane.

1. Hydroplaning of main-gear tires can cause significant loss of braking force for the aircraft. In certain cases, some of the main gear tires could hydroplane while others may not, causing the aircraft to skid to one side. This may be caused by depressions that result in pools of standing water on the runway surface, leading to a yaw movement of the aircraft from differential braking effects or from a lack of side-way friction forces if cross winds are prevalent. It also reduces the effectiveness of wheel brakes in decelerating the aircraft. (van Es et al., 2001; Bailey, 2000)
2. Nose wheel hydroplaning can occur if it is used by the pilot to steer the aircraft on a wet runway at speeds above taxiing speed. Hydroplaning results in a loss of nose wheel cornering force, and a subsequent loss of directional control. The aircraft will veer off the side of the runway if the pilot cannot regain directional control (FSF, 2000c).
3. During touchdown on flooded or slush-covered runways, wheel spin-up can be delayed due to hydroplaning. This is a very critical situation because the auto-brake system, the antiskid system and most automatic spoilers systems need wheel speed to be activated (van Es et al., 2001). Delay in activation of these will reduce the stopping force available to the aircraft.

Loss of skid resistance

Loss of tire-pavement skid resistance would result in poor braking performance for the aircraft which can lead to veer off and overrun accidents. Braking characteristics are critical to the safety of aircraft not only on landing, but more especially during an aborted take-off where the aircraft must come to a halt within the emergency stopping distance allotted.

Aircraft landing distance varies significantly depending on the aircraft operational characteristics such as touchdown speed, location, landing technique, aircraft braking type, reverse thrust usage and also the airport elevation, runway conditions, wind conditions etc. As explained earlier, pavement friction level depends on several factors such as wheel load, speed of the aircraft, tire pressure, tire type and tread design, pavement surface characteristics and surface water film thickness. On dry pavements the percentage drop in skid resistance with speed is relatively little. However when pavement has surface water, there is a considerable reduction in skid resistance. The loss of skid resistance adversely affects braking performance. The reduced braking results in a longer stopping distance than on a dry runway both during a rejected take-off and during a landing.

Flight Safety Foundation's (FSF) technical notes on aircraft braking gives the following landing distances ratios compared to dry runway conditions to demonstrate the effects of different runway conditions (FSF 2000a):

1. Wet runway 1.2-1.4
2. Water contaminated runway 2-2.3
3. Compacted snow covered runway 1.6-1.7
4. Icy runway 3.5-4.5

Regulatory authorities define the landing distance required based on the demonstrated landing distance by multiplying it by a safety factor, to account for the increase in landing distance due to variation in operating characteristics. A commonly adopted value used by many aviation regulatory authorities such as FAA, Civil Aviation Authority (UK), Joint Aviation Authority is to increase the demonstrated landing rollout length by 67%, and for water affected runways it is increased by a further 15% (FSF, 2000b). That is,

Landing distance required (dry runway) = Actual landing distance x 1.67

Landing distance required (wet runway) = Actual landing distance x 1.92

It is also worth to note that there is a certain amount of ambiguity in defining these runway conditions in practice. Terms such as wet runway, contaminated runway, slippery etc. are qualitative in nature and they do not provide clear and specific information to the pilot regarding the runway conditions (ATSB, 2008a) One quantitative definition on runway surface condition is given by Joint Aviation Authorities (JAA), where wet runway is defined as 'a runway is considered wet when there is sufficient moisture on the surface to cause it to appear reflective, but without significant areas of standing water', and contaminated runway is defined as 'a runway is considered contaminated when more than 25 per cent of the runway surface area (whether in isolated areas or not) within the required length and width being used, is covered by surface water more than 3 mm (1/8") deep….' (ATSB, 2008a)

Pavement friction is also important to maintain directional control during cross wind situations. Aircrafts are subjected to considerable aerodynamic or other forces during ground roll. This can affect its braking performance or create moments about the yaw axis. Such moments can also be induced by asymmetric engine power (e.g. engine failure on take-off), asymmetric wheel brake application or by cross-wind. The result may critically affect directional stability (ICAO, 2002). In each case, runway surface friction plays a vital role in counteracting these forces or moments. On wet and contaminated runways, the magnitudes of the side forces of tires are reduced significantly. Compared to a dry runway, the side forces can be reduced by 50-90% (van Es and van der Geest, 2001). In the case of directional control, all aircrafts are subject to specific limits regarding acceptable cross-wind components. These limits decrease as the runway surface friction decreases. For example, wet and contaminated runway conditions will limit the crosswind during ground roll. The maximum cross wind limits are specified in most aircraft manufacturers' flight manuals (*see* Table 2.10).

The use of reverse thrust in crosswind conditions on wet and contaminated runways can aggravate directional control problems during rejected take-off and landing. Whenever the aircraft is allowed to weathervane into the wind, the reverse thrust force component perpendicular to the runway centerline adds to the crosswind force component. The reverse thrust will then pull the aircraft to the downwind side of the runway (van Es et al., 2001). High-definition films taken during heavy rain conditions show clearly that the effect of the reverser flow appears to push the water in front of the wheels. While reversers are definitely a bonus for stopping on wet runways, the use of maximum reversers could result in hydroplaning (Ranganathan, 2006).

2.4.3 Remarks on Runway Safety Risk Analysis

It is evident that runway excursion, especially landing excursion accidents pose a significant threat to aviation safety. Therefore further research and study is needed to contribute towards improving the safety levels of runway operations. It is also clear that rainfall and the resulting runway contamination (surface water) creates adverse conditions for safe landing and takeoff operations. Among other aircraft operational factors such as fast landing, long landing, incorrect use of braking devices, and wet pavements have been a contributory factor in the majority of the accidents.

Occurrence of multiple risk factors related to operational and surface conditions related can have a synergizing effect, increasing the risk of excursion accidents. This was highlighted in the ATSB (2008a) study where wet/contaminated runway conditions and an operation issue such as long landing was found to be evident in many accidents. As explained earlier, wet pavement reduces the available skid resistance for aircrafts. Therefore, if cross wind is present during a landing on a contaminated runway, it can significantly impact the directional control of the aircraft. Similarly if a long landing occurs on a contaminated runway, the runway distance available may be less than the runway distance required to stop the aircraft under the reduced braking conditions.

Therefore monitoring and control of wet pavement performance is an issue of great concern in airport pavement management. The greatest challenge for airport authorities in planning pavement maintenance activities is to understand the effect wet pavement conditions have on aircraft performance (including stopping distance and directional control) and the risk of runway excursion. If there is a tool that clearly demonstrates such impacts it would be beneficial for decision making in runway pavement management.

Researchers have attempted to create models to estimate overrun risk based on statistical data (Kirkland et al.; 2004 and van Es, 2005; Manuel et al., 2011). The main obstacle is the inability to differentiate the effect of the occurrence of a factor in an overrun from the effect of the occurrence of the same factor in normal operations. This was highlighted by Kirkland et al. (2004) who concluded that due to the lack of data on normal operations, it was possible only to relate the rate of overruns to the rate of occurrence for a few of the possible driving factors where such comparable data on normal operations existed.

The model presented by Kirkland et al. (2004) is as follows,

$$p(\text{landing Overrun}) = \frac{1}{1 + e^{-(m+nD)}} \tag{2.3}$$

where D is the percent of excess landing distance available or maximum allowable weight, and m, n are regression constants to be determined. This analysis does not account for all the causal factors of overrun accidents.

One method to identify the main causal factors in overrun accidents is to use bi-variate analysis as proposed by van Es (2005). This was made possible with the use of normal operations data to calculate the risk ratio based on the number of landings with and without a particular factor. The risk ratio for a causal factor is defined as follows,

$$\text{Risk Ratio} = \frac{\left(\dfrac{\text{accidents with presence of a risk factor}}{\text{normal landings with the presence of a risk factor}}\right)}{\left(\dfrac{\text{accidents without presence of a risk factor}}{\text{normal landings without the presence of a risk factor}}\right)} \tag{2.4}$$

The risk ratio would indicate the level of risk due to the presence of one or more causal factors. However it does not give any insights into the causation mechanisms.

Another method is to develop regression models to evaluate the probability of occurrence of an overrun as a function of several causal factors. Excursion accident probability models were developed in the Airport Cooperative Research Program study by Manuel et al. (2011). The probability of runway excursion accident occurrence is given by,

$$p(\text{accident occurence}) = \frac{1}{1 + e^{\mathrm{b}_0 + \mathrm{b}_1\mathrm{x}_1 + \mathrm{b}_2\mathrm{x}_2 + \mathrm{b}_3\mathrm{x}_3 + \mathrm{b}_4\mathrm{x}_4 + \mathrm{b}_5\mathrm{x}_5 + \ldots\ldots}} \tag{2.5}$$

where, x_1, x_2 ,x_3... are the independent variables such as rain, crosswind, tailwind etc., and b_0, b_1 ,b_2… are regression coefficients. One of the independent variables used in the regression model is the runway criticality factor. It is a logarithmic ratio of the runway length available and the runway length required for a given condition. An adjustment factor of 1.4 is used in the case of wet pavement conditions to determine the runway length required. While it may be adequate to estimate the overrun risk in general, it is not possible to examine quantitatively the effects of runway characteristics, surface water depth, and other specific factors. Therefore the regression model does not offer the required information to the airport authorities for effective decision making in runway pavement management.

Fundamental engineering analysis instead of statistical method and experimental methods is required to study the detailed mechanisms involved, and generate the necessary information for sound decision making in runway pavement management. Currently, no procedures based on fundamental engineering analysis are available for this purpose.

2.5 Existing work in Pavement Management related to Risk

Risk is commonly associated in infrastructure system as well as other industries such as insurance, energy production, finance, chemical etc. However several meanings may be implied when the term ‘risk’ is used and terms such as probability and hazards are commonly used in conjunction. A hazard refers to the potential for producing an undesirable consequence or loss. In engineering analysis, risk is often associated with the likelihood of failure (Faber and Stewart, 2003), where certain failure criterions are set and the system is assessed to evaluate the likelihood of it being breeched.

While the concept of risk has been used in pavement design, its uses in pavement management are rare. It was previously used in life cycle cost analysis (Reigle and Zaniewski;, 2002, Perrone et al., 1998) and pavement remaining life analysis (Weissmann et al., 1992 and Lemer and Moavenzadeh, 1971).

Paine (2004) proposed a new approach for pavement management through risk management. In the study a risk rating for a highway section was assigned based on five parameters, i.e. road width, aquaplaning safety consideration, road user response and ride comfort, maintenance reliability, and pavement retained value. Highway section maintenance prioritization or ranking can be determined based on risk ratings for the individual components such as aquaplaning safety or with the use of combined rating for each section. A qualitative approach is adopted in the risk analysis. Risk ratings for each risk component are determined based on vulnerability and likelihood matrices. Therefore, this approach can consider only a limited number of factors in the analysis. Furthermore such techniques require subjective interpretation, they have limited number of categories to clearly differentiate between different severity levels and may also assign similar ratings to different severity levels. Therefore using this approach it will be difficult for highway management authorities to make objective decisions regarding distress severity assessments.

In highway pavement management, the concept of risk is mostly used to analyze correlations between pavement friction levels and accident rates. This provides an input in the assessment of safe friction levels in highway pavement management. A similar model developed by Rizenberg et.al. (1976) is given below,

$$AR = 31.8 - 0.55\ SN \qquad (R^2=0.09) \qquad (2.6)$$

where AR is the number of wet accidents per 100 million vehicle miles and SN is skid number at 70mph. An improved model was later proposed by Ivey and Griffin (1977) for high speed roads,

$$WAR = 21.7 + 0.0009\ ADT + 2.34\ ACC - 0.40\ SN + 286\ TW + 1.32\ LN \qquad (2.7)$$

$(R^2 = 0.46)$

where WAR is the number of wet pavement accidents per mile per year, ADT is the average daily traffic, ACC is a standardized subjective scale of roadway congestion, SN is the skid number at 40mph, TW is the proportion of time wet, and LN is the number of traffic lanes. Although these models show the relationship between accidents and the main causal factors, the regression models have poor coefficient of determination.

Accident rate is also used to evaluate accident risk resulted from roadway discontinuities such as ruts, pot holes, bumps, curbs, edge drop offs, and pavement roughness in general (Christensen and Ragnoy, 2006; and TRB, 2009). For example, Start et al. (1996) concluded that accidents rates increased with rut depth due to increase in hydroplaning potential in ruts filled with water. However it did not provide any definite relationship between distress characteristics such as rut depth and traffic accidents (Start et al., 1998; Ihs et al., 2002; Christensen and Ragnoy, 2006).

One of the common limitations of using accident data in the analysis is the scarcity of accidents. Moreover accident rate may be related to many other factors of highway and traffic operations. Performing analysis of one factor (e.g. rutting) and correlating its severity with accident rates would be difficult. As a whole, in pavement management, distress severity assessment or maintenance planning, the concept of risk is rarely adopted.

2.6 Needs for Research

The literature review has examined the basic concepts and past research in the following three main aspects related to studying of pavement maintenance to reduce aircraft operation risks on runways. The three aspects are as follows.

1. Key issues in airport pavement maintenance management;
2. Types of runway related aircraft safety risks; and
3. Efforts in tire-pavement-fluid interaction analysis.

Water film thickness on pavement surface, runway frictional characteristics, presence of pavement distresses etc., affect the safe operations of aircraft and present accident risks. Appropriate pavement maintenance activities are necessary to minimize the risks for safety. Maintaining a safe level of wet pavement skid resistance and a sufficiently high hydroplaning speed is the key to ensuring safe runway operations of aircraft.

Analysis of wet runway pavement performance, namely study of hydroplaning and skid resistance has been the subject of several experimental studies by researches of organizations such as NASA and FAA. These studies have revealed important information about the phenomena of hydroplaning and skid resistance and factors influencing them. However, to overcome the limitations of experimental studies, it is necessary to analyze tire-pavement-fluid interaction using analytical tools that are theoretically sound and mechanistically based. This can be used to evaluate skid resistance and hydroplaning for different pavement surface conditions and aircraft operating characteristics. It can be used to analyze how pavement and aircraft factors influence pavement friction performance under wet weather conditions and determine its impact on aircraft operations and risk on safety. This could lead to better understanding of pavement conditions and how it will affect aircraft operations. It will facilitate implementation of improvements in safety standards for airport pavement maintenance management.

In order to accomplish this it is necessary to understand the mechanisms of the tire-pavement-fluid interaction and allow a better evaluation of the impacts of various contributing factors.

There are several advantages of adopting a mechanistic approach:

1. The risk of failure can be defined in terms of a specified failure criterion (e.g. occurrence of hydroplaning). This gives a clear physical meaning to the development of the risk and parameters that can be controlled to reduce the risk.
2. A mechanistically based approach provides a quantitative assessment of the state of failure development, and offers the pavement engineer a good knowledge of the margin of safety involved. This enables authorities to directly assess runway pavements functional performance with respect to safety.
3. Long term runway pavement decision making can now be based on a better understanding of the aircraft operational risks involved in wet weather. Suitable strategies of runway pavement management systems can be implemented in maintenance as well as design to improve runway pavement safety performance for aircraft operations.

2.7 Scope of Proposed Research

The present research will focus on runway safety of aircraft operations related to skid resistance and hydroplaning. It will cover issues of runway frictional performance under wet pavement conditions. Risk consideration will be applied with respect to aircraft safety and maintenance management. The research endeavors to develop methodologies to incorporate risk consideration into pavement maintenance management using a mechanistic approach. The scope of research will comprise the following elements of work:

1. Identification of relevant pavement conditions/ distresses that affect aircraft safety.
2. Evaluation of the impact of pavement conditions (such as wet runway pavement) on aircraft performance and safety risks.
3. Analysis of tire-pavement-fluid interaction - The main research work will be to develop finite element model to analyze hydroplaning and skid resistance. This model will permit the impacts of various aircraft, pavement and weather factors on aircraft skid resistance and hydroplaning speed to be evaluated.
4. Risk assessment - Evaluate aircraft operational risks associated with low skid resistance and low hydroplaning speed for different aircraft types and operating conditions.

TABLE 2.1 PCI Rating Method

PCI Rating	Description	Applicable Pavement Preservation Treatments
86–100	Good—only minor distresses	Routine maintenance only
71–85	Satisfactory—low and medium distresses	Preventive maintenance
56–70	Fair, some distresses are severe	Corrective maintenance and rehabilitation
41–55	Poor—severity of some of the distresses can cause operational problems	Rehabilitation or reconstruction
26–40	Very poor—severe distresses cause operational problems	Rehabilitation and reconstruction
11–25	Serious—many severe distresses cause operational restrictions	Immediate repairs and reconstruction
0–10	Failed—pavement deterioration prevents afe aircraft operations	Reconstruction

(Shahin, 1994)

TABLE 2.2 PASER Rating System

Surface rating	Visible distress	General condition/ treatment measures
5 Excellent	None, or initial thermal cracks, all narrow (less than 1⁄8”)	New pavement less than 5 years old. No maintenance or isolated crack sealing required.
4 Good	Additional thermal cracking. Cracks generally spaced more than 50’part. Less than 10% of cracks and joints need sealing. Minimal or slight raveling. No distortion. Patches in good condition.	Recent sealcoat or pavement over 5 years old. Seal open cracks or joints and replace sealant where needed.
3 Fair	Moderate raveling. Thermal cracks and joints generally spaced less than 50’ apart. Crack sealing or repair of sealant needed on 10%-25% of cracks or joints. Edge cracks along 10% or less of pavement edges. lock crack pattern with cracks 6’-10’ apart. Isolated alligator cracking and poor patches. Minor distortion or crack settlement less than 1”.	Seal open cracks and joints. Replace failed sealant. Apply new surface treatment or thin overlay. Minor patching and joint repair.
2 Poor	Frequent thermal cracks. Wide cracks and joints with raveling in cracks. Deterioration along more than 25% of cracks. Edge cracks on up to 25% of pavement edges. Block cracks spaced 5’ apart or less. Alligator cracking or poor patches cover up to 20% of surface area. Distortion or settlement 1“-2”.	Needs significant crack sealing plus patching and repair on up to 25% of pavement surface. Overlay entire area with structural overlay.
1 Failed	Widespread, severe cracking with raveling and deterioration. Alligator cracking and potholes over 20% of the area. Distortion over 2”.	Condition may be limiting service. Needs reconstruction.

(FAA, 2004)

TABLE 2.3 Deduct Values for Airfield Rutting Based on PCI Method

Rutting	Severity (based on maximum rut depth measured)		
Extent %	Low	Medium	High
	0.25”-0.5”	0.5”-1”	1” +
0.5	12.5	20	29
1	16	25	35
5	23	37	52.5
10	29	45	62.5
20	35	52.5	75
50	45	65	95
100	52.5	77.5	100

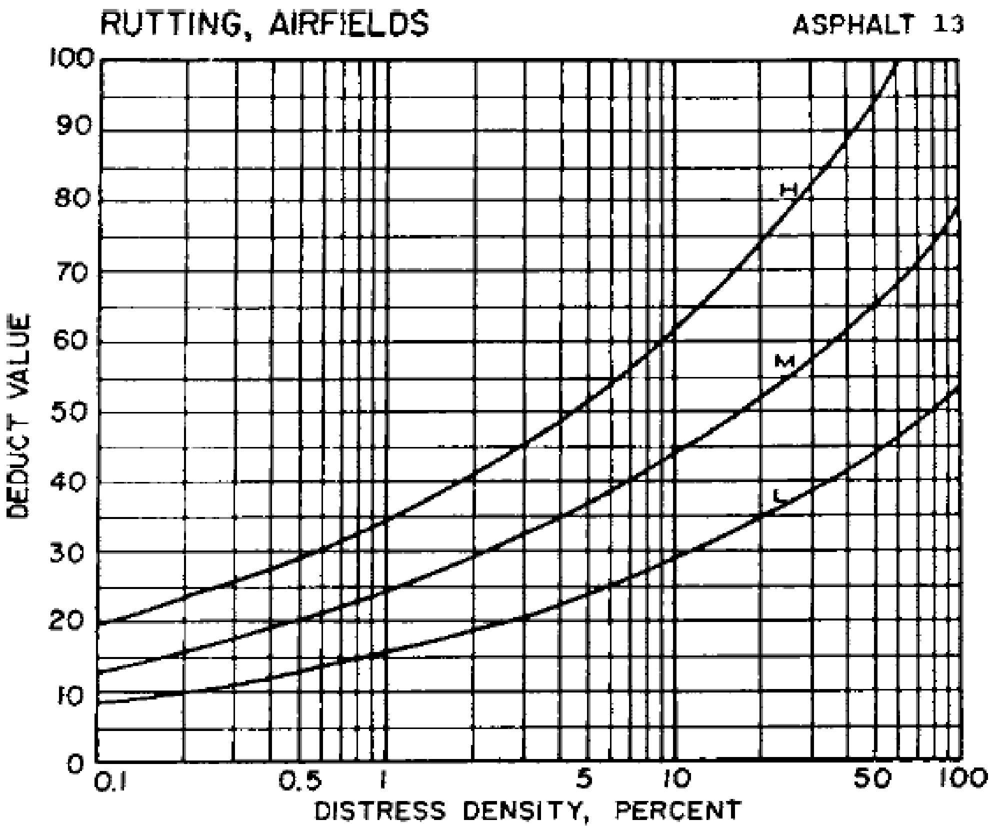

(ASTM, 2009)

TABLE 2.4 Friction Level Classification for Runway Pavement Surfaces

CFME Type Operating speed : 60 mph	Minimum	Maintenance Planning	New Design/ Construction
Mu Meter	0.26	0.38	0.66
Dynatest Consultant Inc. Runway Friction Tester	0.41	0.54	0.72
Airport Equipment Co. Skiddometer	0.34	0.47	0.74
Airport Surface Friction Tester	0.34	0.47	0.74
Airport Technology USA Safegate Friction Tester	0.34	0.47	0.74
Findlay Irvine Ltd. Griptester Friction Meter	0.24	0.36	0.64
Tatra Friction Tester	0.42	0.52	0.67

(FAA, 1997)

TABLE 2.5 FAA Braking Action Definitions

Braking Action		Estimated Correlations	
Term	**Definition**	**Runway Surface Condition**	**Mu**
Good	Braking deceleration is normal for the wheel braking effort applied. Directional control is normal.	Water depth of 1/8" or less , Dry snow less than ¾" in depth	Greater than 40
Good-Medium			36-39
Medium	Braking deceleration is noticeably reduced for the wheel braking effort applied. Directional control may be slightly reduced.	Dry snow ¾" or greater in depth , Sanded snow Sanded ice	35-30
Medium-Poor			29-26
Poor	Braking deceleration is significantly reduced for the wheel braking effort applied. Potential for hydroplaning exists. Directional control may be significantly reduced.	Wet snow, Slush Water depth more than 1/8" ,Ice (not melting)	25-21
Nil	Braking deceleration is minimal to nonexistent for the wheel braking effort applied. Directional control may be uncertain. NOTE: Taxi, takeoff, and landing operations in Nil conditions are prohibited.	Ice (melting) Wet Ice	Less than 20

(FAA, 2007)

TABLE 2.6 Hydroplaning Speed Estimation Models

Model and underlying assumptions	**Variables considered**
$v_p \text{ (knots)} = 9\sqrt{p}$ Pavement surface texture depth and tire tread depth are assumed to be zero, and runway is flooded with 7.62 mm of water (Horne Dreher, 1963)	Pressure (psi)
$v_p \text{ (mph)} = 23.3\ p^{0.21}\left(\frac{1.4}{FAR}\right)^{0.5}$ Model developed for truck tires (Horne et al., 1985)	p- Pressure (psi) FAR -tire footprint width/length
$v_p \text{ (km/h)} = 8.455\left[\left(\frac{\text{TD}}{25.4}+1\right)^{0.05} MTD^{0.01}\left(\frac{1.88}{WT^{0.01}+1}\right)\right]$ it is limited to a tire pressure of 165 kPa (24 psi) which is lower than most aircraft tires, as well as most of the ground vehicles used to measure friction at airports; it is applicable to the case where hydroplaning is defined as 10% wheel spin down (Wambold et al., 1984)	TD- tread depth (mm) WT – water film thickness (mm) MTD – mean texture depth (mm)
$v_p \text{ (mph)} = \text{SD}^{0.04} p^{0.3} (TRD+1)^{0.06} A$ $\text{A} = \max\left[\left(\frac{10.409}{t_w^{0.06}}+3.507\right), MTD^{0.04}\left(\frac{28.952}{t_w^{0.06}}-7.819\right)\right]$ (Gallaway, 1979)	p -Pressure (psi) TRD- tread depth (1/32 inch) t_w – water film thickness (inch) MTD – mean texture depth (inch) SD- spin down %
$v_p \text{ (mph)} = 33.7 + 5.28\left(t_w^{-0.5}\right)$ locked sliding tires on pavement with water film thickness less than 2.4 mm (Agrawal and Henry, 1977)	t_w – water film thickness (inch)

TABLE 2.7 Skid Resistance Estimation Model

Model	Variables considered
$SN_v = SN_0 \ e^{-\left(\frac{PNG}{100}\right)V}$, $PNG = 100\left[\frac{\left(d(SN)/dv\right)}{SN_v}\right]$ (Meyer, 1991)	SN_v is the skid number at vehicle speed *v*, zero-speed intercept (SN_0), which is an indication of friction at low speeds
$SN_v = SN_0 \ e^{-\left(\frac{v}{v_0}\right)}, v_0 = \left[\frac{v_2 - v_1}{\ln\left(SN_{v1}/SN_{v2}\right)}\right]$ (Kualkawoski and Meyer, 1991)	SN_v is the skid number at vehicle speed *v*, zero-speed intercept (SN_0), which is an indication of friction at low speeds
$\mu_{skid,wet} = \left[\frac{\mu_{ref}}{1+\left(\eta_0 + \eta_1 \frac{V^2}{2g}\right)\frac{p/p_a}{Z^{1/3}}}\right]\frac{(1-\varphi_0 q/p)}{(1+\varphi_1 q_v/p_a)}$ Empirical model was developed to estimate the coefficient of braking friction when skidding on dry surfaces is extended using the concept of the three-zone model of pressures in the footprint of the tire to incorporate the effects of a wet runway. (ESDU, 2003)	p - tire inflation pressure p_a- atmospheric pressure V- Speed q- kinetic pressure q_v - pressure in the transition zone Z -tire vertical load μ_{ref} -reference coefficient of braking friction n_0,n_1 - empirical constants for aircraft tires φ_0 ,φ_1- variables used in the process of modeling
$(\mu_{max})_A = \frac{\mu_T(\mu_{ult})_A}{(\mu_{ult})_T}$ $(\mu_{ult})_A = 0.93 - 0.0001596\ P_A$ $(\mu_{eff})_A = 0.2(\mu_{max})_A + 0.7143(\mu_{max})_A^2$ Developed to predict aircraft tire braking coefficients from ground vehicle data, based on previous research by NASA Applicable to damp, wet, and flooded pavements (Transport Canada, 2001)	P_A – Tire pressure (kPa) A- aircraft T- friction tester $(\mu_{ult})_T$ - determined from low speed (2.5 km/h)friction test on dry runway μ_T - friction value on wet runway

TABLE 2.8 Factors Affecting Landing Overruns in Europe and Worldwide

Factor	Europe	Rest of the world
Wet/Contaminated runway	38.0%	66.7%
Long landing	24.0%	44.5%
Incorrect decision to land	14.9%	16.8%
Speed too high	14.0%	22.1%
Late/incorrect use of brakes	14.0%	10.3%
Late/incorrect use of reverse thrust	14.0%	10.0%
Aquaplaning	7.4%	16.2%
Tailwind	7.4%	15.9%
Too high on approach	3.3%	7.2%

(Van Es , 2010)

TABLE 2.9 Aircraft excursion accidents related to wet runway conditions

Year	Location	Aircraft type	Fatalities/ Damages	Causal factors present
1999	Little Rock, AR, USA	McDonnell Douglas MD-82	11 fatalities, 44 serious injuries aircraft destroyed	Severe thunderstorm Long landing, hydroplaning
1999	Bangkok, Thailand	Boeing 747-400	Aircraft sustained significant damage	Heavy rain, fast approach, hydroplaning
2000	Paris, France	Boeing 747-2H7B	Severe damage to aircraft	Landing in wet weather, aircraft overran the runway
2000	Reynosa, Mexico	McDonnell Douglass DC931	Damage to houses in the vicinity, 3 fatalities	Heavy rain, hydroplaning
2002	Sligo, Ireland	Fokker F-27	-	Heavy rain, strong winds Aircraft skidded and veer-off
2002	Singapore	McDonnell Douglas DC-8-62	Aircraft sustained substantial damage	Heavy rain, long landing
2005	Ontario, Canada	Airbus A340-300	44 serious injuries, aircraft was destroyed	Severe thunderstorm, crosswind conditions, long landing
2007	Sao Paulo, Brazil	Airbus A320	187 fatalities	Runway conditions at the time of the landing were ‘wet and slippery’
2007	Phuket, Thailand	McDonnell Douglas MD-82	90 fatalities aircraft was destroyed.	Landing in heavy rain and crosswind conditions, veer- off
2008	Honduras	Airbus A320	3 fatalities	Runway was water-affected, tailwind
2009	South Africa	Embraer RJ135LR	Substantial damages to aircraft	Landing during rain, hydroplaning
2010	Ottawa, Canada	Embraer E145	-	Wet runway, pilot reported no traction on runway, overrun
2011	Sarawak, Malaysia	Airbus - A320	-	Landing in rain, skidded of the runway

TABLE 2.10 Maximum Recommended Crosswind Speeds (knots) for Different Runway Surface Conditions and Aircraft Types

	Boeing Aircraft Type				
Runway Condition	**737**	**747**	**757**	**767**	**777**
Dry	40	36	40	40	45
Wet	40	32	40	40	40
Standing Water/Slush	20	20	20	20	20
Snow (No melting)	35	25	35	35	35
Ice (No melting)	17	15	17	17	17

Note: These crosswinds are derived using piloted simulations and engineering analyses. These are not demonstrated values. (Van Es et. al., 2001)

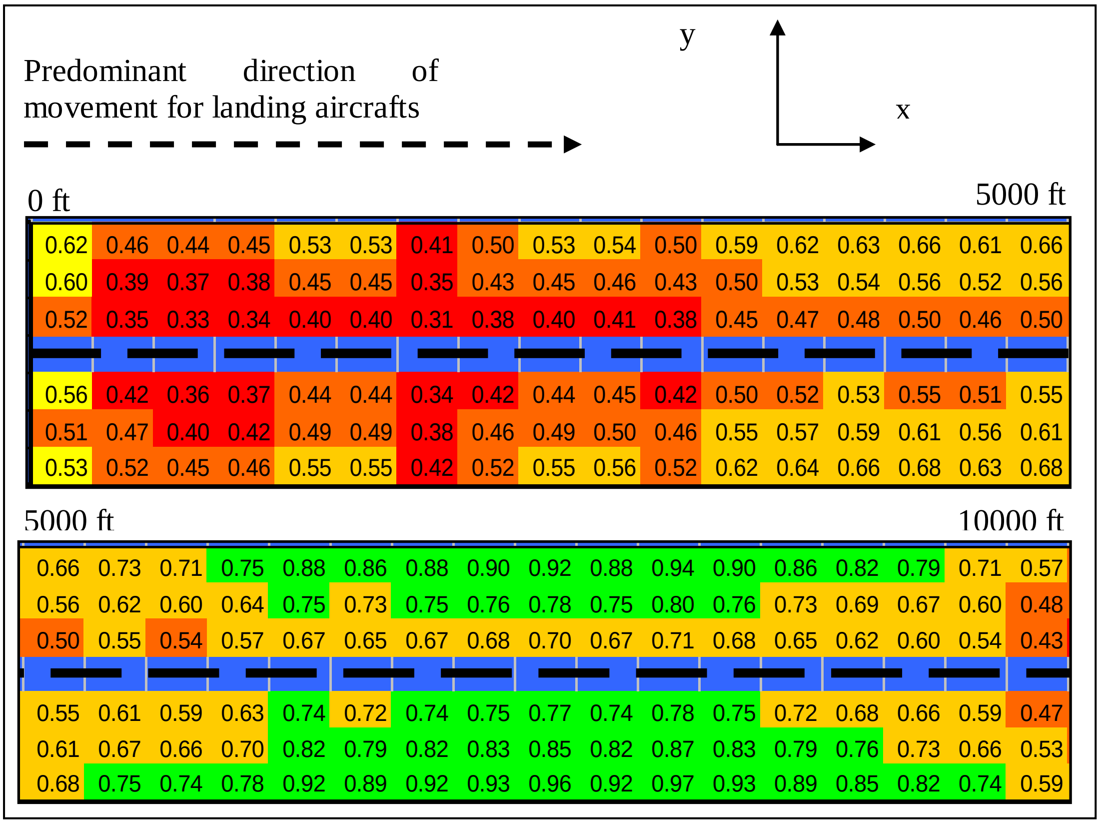

Runway width 36m

Friction Classification:	Nil	< 0.43
	Min. friction level (Poor)	0.43 - 0.53
	Maintenance planning level (Fair)	0.53 - 0.74
	Design object level (Good)	0.74 >

FIGURE 2.1 Runway friction report
(Ref: Neubert and Goff, 2006)

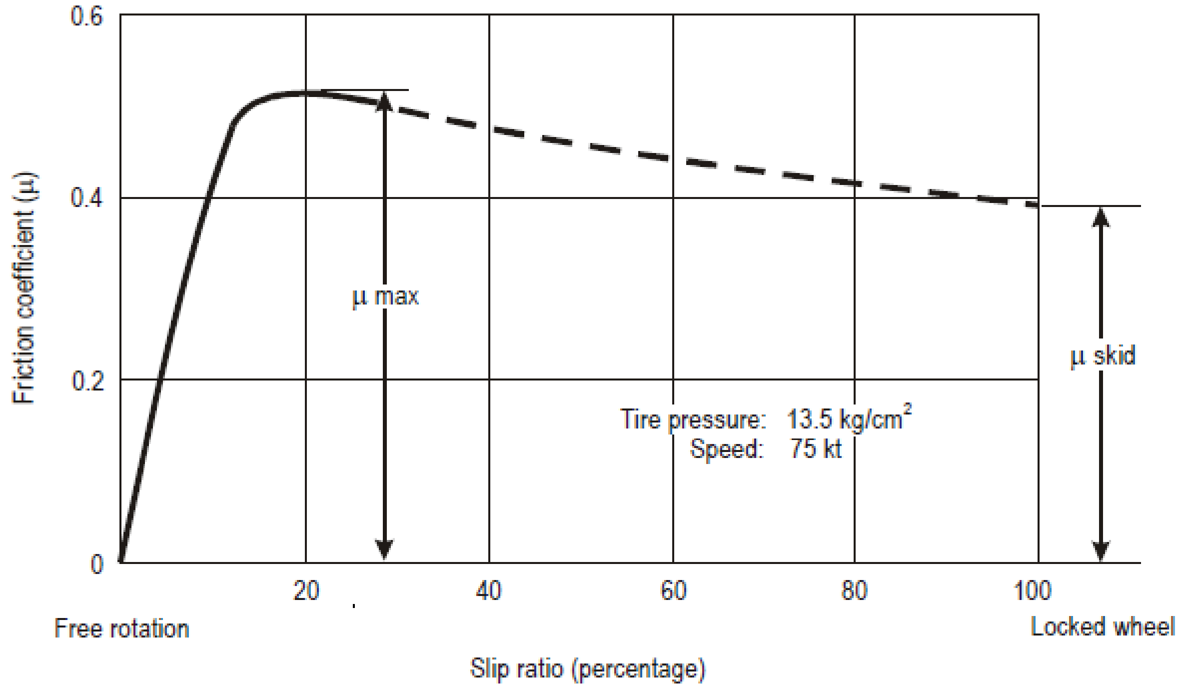

FIGURE 2.2 Relationship between percentage slip and friction coefficient on a wet runway (Ref: ICAO, 2002)

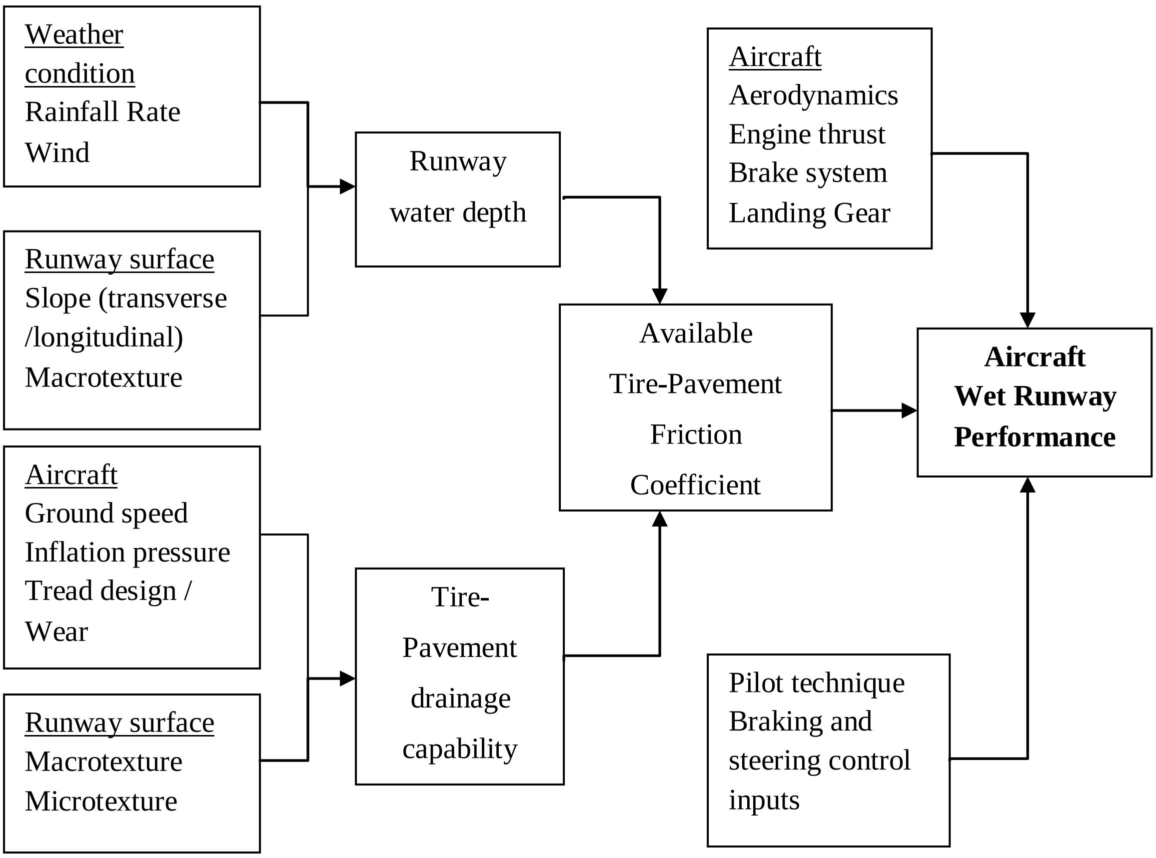

FIGURE 2.3 Factors affecting aircraft wet runway performance (Ref: Horne, 1976)

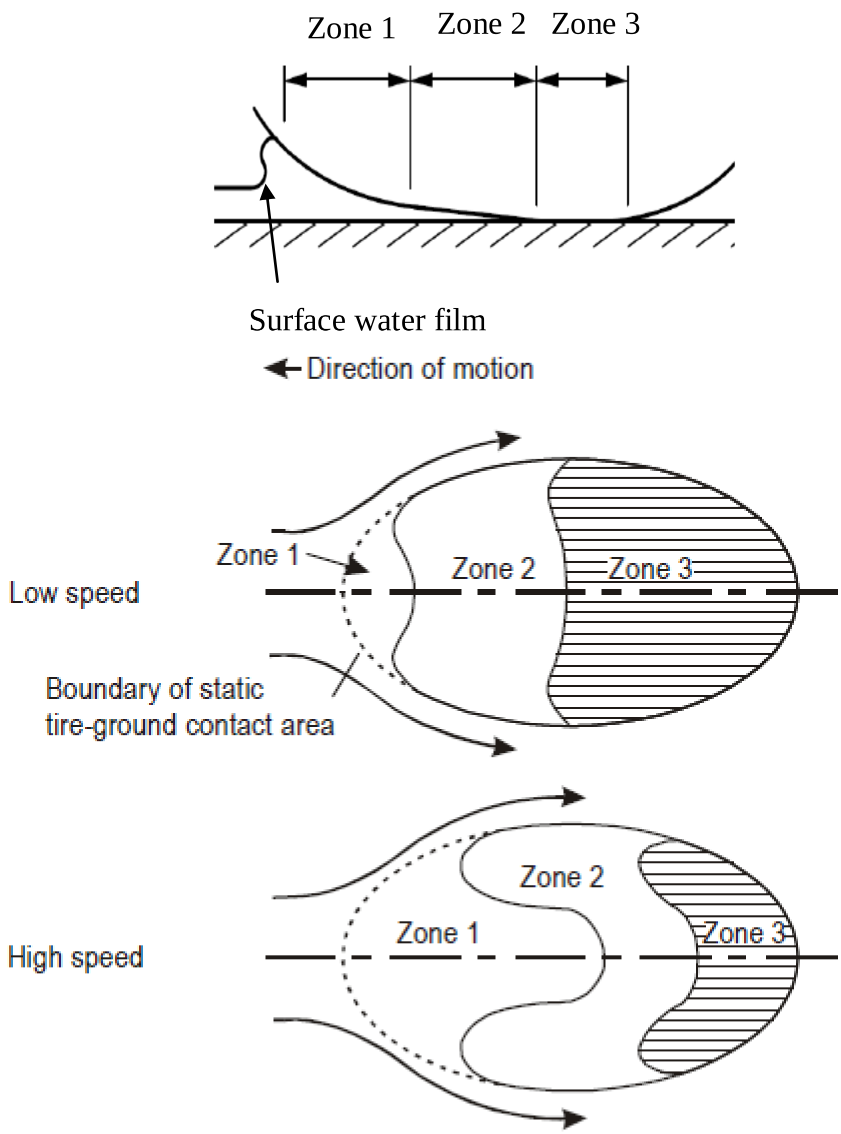

Zone 1: Sinkage zone
Zone 2: Transition zone
Zone 3: Contact zone

FIGURE 2.4 Tire Sliding on wet surface - Three zone concept
(Ref: ICAO, 2002)

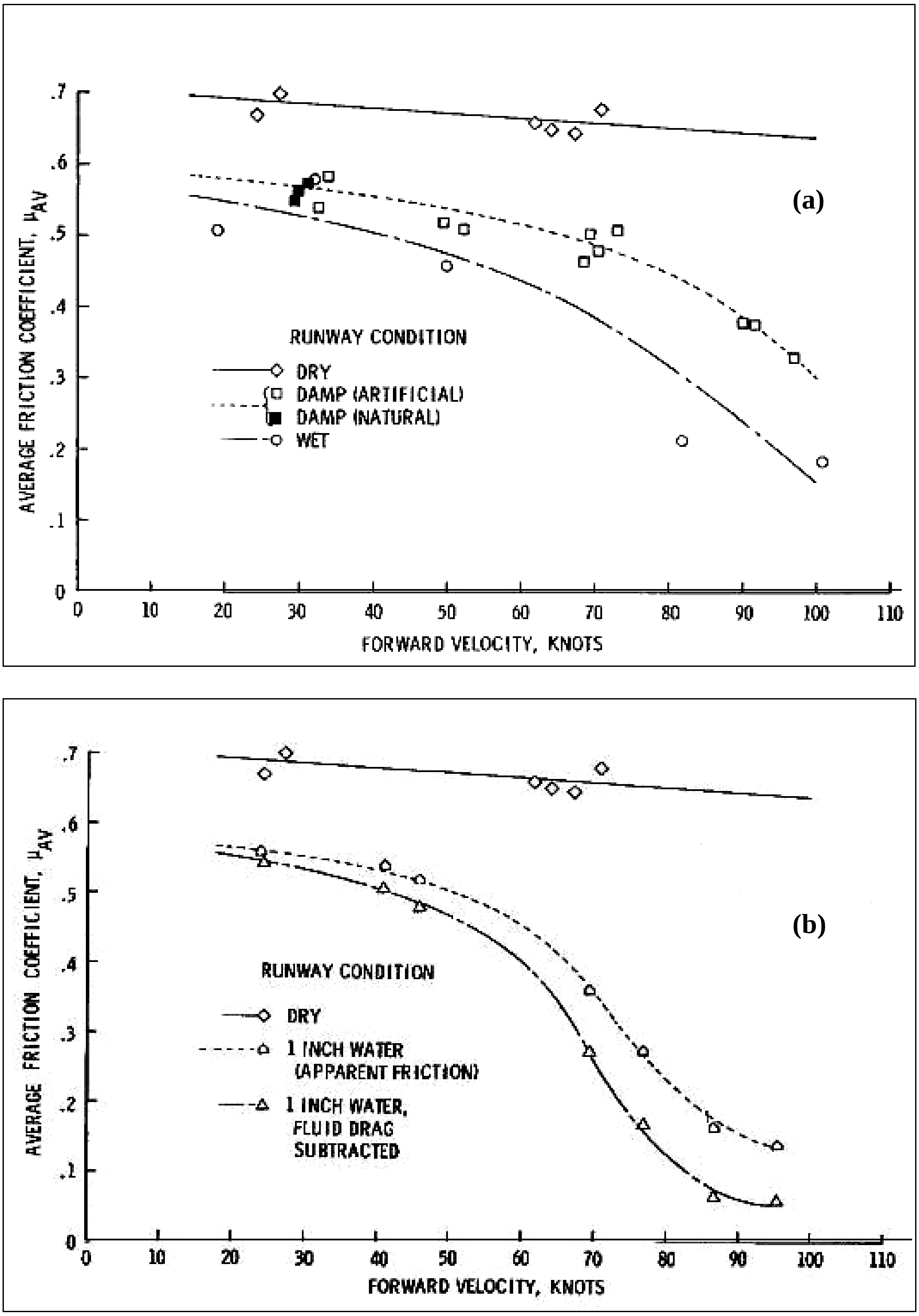

Test parameters: 30x8.8 aircraft rib tire (average tread groove depth 6mm), tire pressure 90psi, average friction coefficient measure for tire slip ratio of 0.1- 0.5, water film thickness for (a) wet condition = 6.35mm, (b) 25.4mm

FIGURE 2.5 Effect of runway water film thickness on friction (Ref: Leland and Taylor, 1965)

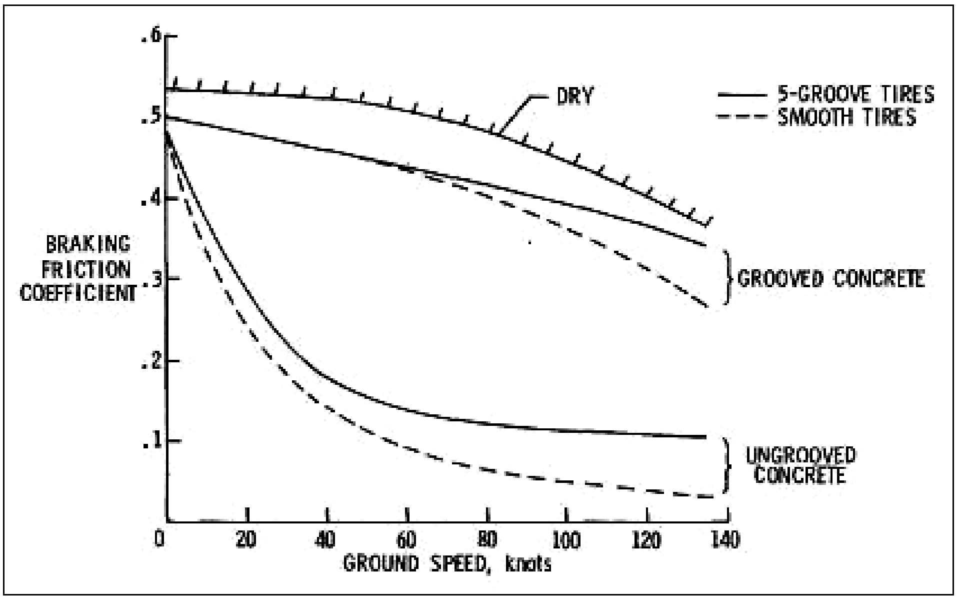

Test parameters: 41x15 Type VIII aircraft tire, tire pressure 160psi, braking friction coefficient from 990 aircraft flight test, water film thickness 2.5mm, pavement groove configuration 6.35mmx6.35mmx25.4mm

FIGURE 2.6 Effect of groove depth and tire tread design on wet runway friction (Ref: Yager, 1969)

CHAPTER 3 FRAMEWORK FOR INCORPORATING RISK CONSIDERATION FOR RUNWAY PAVEMENT MAINTENANCE MANAGEMENT

The framework for incorporating risk consideration into runway pavement management is presented in this chapter. It relates to aspects of three main areas namely, runway pavement management, aircraft runway safety risks and analysis of wet pavement friction. The concept of 'risk' adopted in this framework is introduced. Methodologies for incorporating risk consideration will be developed within this framework for different friction related runway pavement distress types or characteristics.

This framework comprises of three main sections, as follows:

1. Pavement condition evaluation: The distresses or runway pavement characteristic and their effects on runway pavement performance are identified. Based on their impact on pavement performance each distress is assigned one or more failure modes and a failure criterion is also defined under each failure mode. In the context of the research distresses that will affect runway frictional performance will be analyzed.
2. Mechanistic analysis: In order to evaluate distresses' impact on pavement performance, a mechanistic analysis involving relevant parameters of runway pavement, distress and aircraft is carried out. Since the focus of the research is on pavement friction performance, the mechanistic analysis will involve development of finite-element model to simulate aircraft tire-pavement-fluid interaction.
3. Risk assessment: The failure criterion defined earlier under each failure mode will form the basis for the risk assessment. Based on the results from the mechanistic analysis and relevant aircraft operational, runway characteristics the required

parameters defined in the failure criterion for each distress or runway characteristic is established. These analyses will be used to first evaluate effects of a distress on aircraft operations under each failure mode, establish acceptable risk levels and then to make a general assessment of pavement related risks to aircraft operational safety. This information can be used in runway maintenance management to determine maintenance thresholds.

The flow chart of the proposed framework is given in Figure 3.1.

3.1 Runway Pavement Friction Performance

Provision of adequate runway friction is essential to safe aircraft operations. Therefore from runway pavement maintenance perspective it is important to identify the distresses that are related to pavement friction performance and also evaluate how they affect it. The impacts of pavement distresses on pavement friction performance can be categorized based on:

1. Effect on drainage capacity of the runway surface and tire -pavement contact area: Surface drainage controls water buildup on the runway during wet weather conditions. The tire-pavement drainage capability must be sufficient to expel the water from the tire-pavement interface of a moving aircraft tire, in order to limit the buildup of fluid pressure and maintain adequate traction.
2. Effect on pavement friction properties (i.e. the static friction coefficient of the pavement): This is influenced by the type of aggregates used, the surface course mix properties, and construction methods etc.

These two aspects need to be considered when evaluating distresses’ effect on runway friction performance.

3.1.1 Effects of Distress on Pavement Friction Performance

Pavement Rutting

Rutting is a major form of pavement distress in asphalt pavements. It occurs due to plastic deformation of the asphalt layers and the lower layers of the pavement. On theory, it is possible for rutting deformation to continue under traffic loading up to a stage of structural failure. However, this is unlikely the case in practice because before this stage could be reached, functional service requirements of the pavement would have been violated and traffic operations would have been severely affected. In other words, long before reaching structural failure, maintenance treatment or rehabilitation of the rutted pavement would have to be performed to restore pavement surface condition for safe traffic operations.

Since the early 1970s, pavement engineering researchers have produced experimental evidence that water accumulation in pavement ruts could lead to hydroplaning and loss of skid resistance.

- Barksdale (1972) concluded from his study that in pavements with rut depths of about 0.5 in. (12.7 mm), ponding is sufficient to cause automobiles travelling at speeds of 50 mph (80.5 km/h) or more to hydroplane.
- Lister and Addis (1977) also found from their experience in the United Kingdom that pavements with ruts deeper than approximately 0.5 in. (12.7 mm) could result in ponding of water and cause hydroplaning or loss of skid resistance.
- AASHTO Joint Task Force on Rutting stated in their report that wheel path ruts greater than a third to a half an inch (8.5 to 12.7 mm) in depth are considered by many highway agencies to pose a safety hazard, due to the potential for hydroplaning, wheel spray, and vehicle handling difficulties (AASHTO 1989).

- Sousa et al. (1991) stated in a SHRP (Strategic Highway Research Program) study report that for rut depths that exceed 0.2 inches (5.1 mm), hydroplaning is a definite threat particularly to cars.

Therefore from these findings it is clear that hydroplaning due to water accumulation is one of the main impacts of rutting.

For airfield pavement rutting similar findings are available. Several runway maintenance manuals identify impact of rutting is a result of ruts impeding runway surface drainage which can lead to hydroplaning (Transport Canada, 2004). Navneet et al. (2004) indicated that rutting causes both structural and functional failure of the pavement and ruts exceeding 1 inch (25.4mm) can cause functional failure due to possible water accumulation. Moughabghab (2006) also identified ruts impact on skid resistance and surface drainage in addition to other pavement quality characteristics such as pavement strength and smoothness. United Kingdom's Civil Aviation Authority (CAA) standards on aerodrome licensing states that 'aerodrome pavements must be free of localized surface irregularities as measured by a 3 m straightedge. In addition it must not allow the accumulation of water which might affect directional control of an aircraft through aquaplaning or cause engine failure due to water ingestion' (CAA, 2001). Therefore similar to highways, runway pavement rutting also affects pavement friction performance due to water accumulation which can lead to risk of hydroplaning and loss of skid resistance.

Depressions

The impact of depressions on runway friction performance is similar to that of rutting. Depressions are caused by consolidation of the runway pavement structure after construction. They lead to unevenness in the surface profile, creating possible safety hazard in the form of "ponding". The affected areas are clearly visible after rainfall. Surface deformation may result in poor drainage, which can have a direct impact on the safety of aircraft operations (Bailey, 2000 and Transport Canada, 2010).

The FAA advisory circular on airport pavement surface skid resistance states that if the average water depth exceeds 3 mm over a longitudinal distance of 152 m, the depressed area should be corrected to the standard transverse slope (FAA, 1997). This depth corresponds to the mean critical depth for onset of hydroplaning (ICAO, 2002). Hydroplaning, once started, can be sustained on a wet runway by a much smaller depth of water. It is to be noted that this is a very vague description of a distress condition severity. In the PCI method, hydroplaning is identified as a main consideration for depression classification. PCI method classifies depression based on maximum depth into 3 categories: Low (0.125-0.5in) (3.1-12.7mm), Medium (0.5-1in) (12.7-25.4mm) and High (greater than 1in) (25.4mm). In this case a depression with a depth greater than 1 inch (25.4mm) is considered to be sufficient to cause hydroplaning (ASTM, 2009).

Other distresses that cause runway skid resistance loss

- Polished aggregates - This type of distress arises due to wear and tear of pavement surfaces. The aggregates lose their micro-texture which contributes to the reduction of pavement friction properties. A smoother surface also means that it has insufficient texture depth to provide adequate drainage between tire footprint and pavement. This can be detrimental to the frictional performance at high vehicle or aircraft speeds during wet weather.
- Asphalt bleeding creates a bituminous film on the pavement surface, and covers the texture on pavement surface. Excessive bleeding may severely reduce skid resistance.

- Contaminants such as oil spillage create a thin viscous film between the tire footprint and pavement and reduce the available friction. Rubber deposits are another major issue which causes severe runway frictional losses. The buildup of rubber on the surface covers pavement surface texture and reduces the frictional performance of the runway.

3.1.2 Effects of Runway Characteristics on Friction Performance

Runway surface profile

Adequate runway crown allows water to drain off rapidly during rainfall. Road Research Laboratory of U.K. developed the following equation to predict water film thickness along a flow path (Russam and Ross, 1968),

$$d = \frac{0.0046\, L_f^{0.5}\, I^{0.5}}{S_f^{0.2}} \tag{3.1a}$$

$$S_f = \left(S_c^{\,2} + S_l^{\,2}\right)^{0.5} \quad \text{and} \quad L_f = W \frac{S_f}{S_c} \tag{3.1b}$$

where d is the water-film thickness in mm at the end of flow path, L_f the flow length in m which is equal to the distance from the runway centerline, I the rainfall intensity in mm/h, S_f the flow path slope in m/m, S_c the cross slope, S_l the longitudinal gradient, and W is road width. An increase in cross slope results in a faster discharge of water and lower water-film thicknesses across the runway width. Typical slopes recommended by the International Civil Aviation Organization are 1.5% to 2% for the transverse cross slopes, depending on the runway type (ICAO, 2004). Excessive slopes are not recommended because aircraft load distribution would be significantly affected (Agrawal, 1986).

Runway cross slope also minimizes water accumulation due to pavement surface distortions such as ruts or depressions. For example, Balmer and Gallaway (1983) showed that for a pavement with cross slope of 2% the maximum wheel path depression (rut) allowable would be 4.5mm to ensure that water accumulation does not take place. This result is derived on the assumptions that a minimum cross slope of 0.5% is required for water to drain off the pavement and the wheel path depressions are 600mm wide. Based on this calculation even for a high cross slope of 4% the maximum permissible rut depth would be around 10.5 mm in order to prevent ponding.

Airport runways ideally should be level in the longitudinal direction. Since there can be difficulties during construction to achieve this, ICAO has specified maximum permissible longitudinal grades for runways to be within 1.25%-1.5% at airports servicing commercial jet aircrafts (ICAO, 2004). Longitudinal grades increase the flow path length for surface water. According to Equation 3.1 an increase in longitudinal gradient for any cross slope would increase pavement surface water film thickness.

Runway grooving

Pavement grooves were first studied by NASA at the landing-loads track in 1962 (Horne and Whitehurst, 1969). Several experimental studies have been conducted to evaluate the effects of runway grooves on aircraft tire braking performance (Agrawal and Daiutolo, 1981; Yager, 1969; Shilling, 1969; Williams, 1969; and Phillips, 1969). The main findings from those studies can be summarized as follows:

- Grooving increases the average texture depth in a pavement surface and as a result improves the drainage capacity for removal of surface water from tire-pavement contact area.
- Grooved pavements reduce the level of surface water accumulation compared to a smooth surface during a rainfall. It was found that a grooved pavement drains up to 10 times faster than non-grooved surfaces (Yager et al., 1970). They also limit adverse effects of surface winds on water drainage.
- Transverse runway grooves provide substantially increased aircraft braking capability and directional control. They effectively reduce landing field lengths under adverse weather conditions for a variety of runway surfaces.
- Transverse pavement grooving can significantly increase the water depth required for a vehicle or aircraft traveling at a given speed to hydroplane, thereby reducing the risk of dynamic hydroplaning.

The Federal Aviation Administration (FAA) has recommended runway grooving as a 'Proven and effective technique for providing skid resistance and prevention of hydroplaning during wet weather' (FAA, 1997). FAA AC-150/5320-12C recommends all runways servicing turbojets to be grooved. In addition, other airports should consider factors such as the history of aircraft hydroplaning incidents, frequency of rainfall, cross wind effects, runway surface profile, runway length and availability of runway end safety areas etc. when deciding on the necessity for grooving (FAA, 1997).

3.2 Mechanistic Analysis of Runway Friction Performance

The main impacts of distresses on runway friction performance identified earlier are in the form of hydroplaning and loss skid resistance. In order to understand the phenomena of hydroplaning and skid resistance, it is necessary to study the interaction between tire, pavement and fluid. This requires a mechanistic analysis involving relevant parameters of runway pavement, distress and aircraft. This section presents the theoretical formulation and development of a three-dimension finite element simulation model for skid resistance and hydroplaning.

3.2.1 Hydroplaning and Skid Resistance Analysis: Model Development

A three-dimensional finite element model was developed to simulate tire-fluid-pavement interaction based on the theories of solid mechanics and hydrodynamics. It makes use of a moving-wheel frame of reference to model the skid resistance problem as a layer of water with a given thickness moving at a given speed towards a static wheel. The finite element analysis computer software, ADINA (ADINA Inc., 2009) is used to solve the coupled tire-fluid-pavement interaction problem. A schematic diagram of the simulation process is shown in Figure 3.2. The model consists of three main components:

1. Fluid sub-model
2. Pneumatic tire sub-model
3. Pavement surface sub-model

The simulation considers interactions between these sub-models, i.e. tire-pavement contact modeling, tire-fluid interaction, and fluid-pavement interactions. The three dimensional finite element simulation model for ASTM E501 rib tire is shown in Figure 3.3.

Fluid flow modeling

The fluid domain is modeled using 4-node tetrahedral elements. This element type is known to be suitable for three-dimensional flows of both high and low

Reynolds and Peclet numbers. The complete set of Navier-Stokes equations is used to model the behavior of fluid flow near the tire pavement contact patch. The Arbitrary-Lagrangian-Eulerian (ALE) formulation is used due to the need to consider fluid-structure interaction. In a general ALE coordinate system, it is convenient to express the governing equations in integral form in an arbitrary volume *V* bounded by its boundary ∂V (ADINA Inc., 2009; Zhang et al., 2003).

$$\frac{\partial}{\partial t}\int_V \mathrm{U}\,dV + \oint_{\partial V}\left[(\mathrm{v}-\mathrm{w})\,\mathrm{U}-\mathrm{G}\right]\bullet d\mathrm{S} = \int_V \mathrm{R}\,dV \tag{3.2}$$

$$\mathrm{U}=\begin{bmatrix}\rho\\ \rho\mathrm{v}\\ \rho E\\ \rho\varphi\\ 0\end{bmatrix},\mathrm{G}=\begin{bmatrix}0\\ \tau\\ \tau\bullet\mathrm{v}+k\,\nabla\theta\\ d_\varphi\nabla\varphi\\ d_\psi\nabla\psi\end{bmatrix},\ \mathrm{R}=\begin{bmatrix}0\\ \mathrm{f}^B\\ \mathrm{f}^B\bullet\mathrm{v}+q^B\\ \mathrm{S}_\varphi\\ 0\end{bmatrix} \tag{3.3}$$

where the symbols are defined as follows:

τ - stress tensor

e - strain tensor

v - velocity vector

w - moving mesh velocity vector

p - fluid pressure

ρ - density

E - specific energy

e - internal energy

θ - effective viscosity

λ - second viscosity

f^B - body force vector of fluid medium

q^B - specific rate of heat generation

φ - other variables governed by convective-diffusive equations, with d_φ - diffusion coefficient, S_φ -source term ψ - other variables governed by the Laplace equations, with d_ψ being its diffusion coefficient.

The variables that φ might represent are the turbulence kinetic energy *K* and the turbulence dissipation rate ε for the *K*-ε turbulence model. The variables that ψ represents are the increments of fluid displacement $\Delta \boldsymbol{d}_f$ for the moving boundary condition. The fluid body force $\mathbf{f}^B$ in this case includes the gravitational forces. For incompressible flows, the density is assumed to be constant. Flow at high or near hydroplaning speeds can be modeled using the K-ε turbulence flow model given by Equation 3.4 and 3.5 (Ong and Fwa, 2007a).

$$\frac{\partial(\rho K)}{\partial t} + \nabla \bullet \left[\rho v K - \left(\mu_0 + \frac{\mu_t}{\sigma_K} \right) \nabla K \right] = 2\mu_t D^2 - \rho\varepsilon + \left(\mu_0 + \frac{\mu_t}{\sigma_\theta} \right) \beta g \bullet \nabla \theta \tag{3.4}$$

$$\frac{\partial(\rho\varepsilon)}{\partial t} + \nabla \bullet \left[\rho v \varepsilon - \left(\mu_0 + \frac{\mu_t}{\sigma_K} \right) \nabla \varepsilon \right] = \frac{\varepsilon}{K} \left[2c_1 \mu_t D^2 - c_2 \rho\varepsilon + c_1(1 - c_3) \left(\mu_0 + \frac{\mu_t}{\sigma_\theta} \right) \beta g \bullet \nabla \theta \right] \tag{3.5}$$

where K is the kinetic energy, ε is the rate of dissipation of turbulence and μ_t is the turbulent (eddy) viscosity. Here c_μ, c_1, c_2, c_3, σ_k, σ_ε, σ_θ are the model constants and have the values $c_\mu = 0.09$, $c_1 = 1.44$, $c_2 = 1.92$, $c_3 = 0.8$, $\sigma_k = 1$, $\sigma_\varepsilon = 1.3$, $\sigma_\theta = 0.9$.

Pneumatic tire modeling

A tire is modeled using 4-node iso-parametric single-layer shell elements, known as the mixed-interpolation-of-tensorial-components (MITC4 elements) in the ADINA software. In the modeling of a pneumatic tire, three structural components are considered, namely tire rim, tire sidewalls and tire tread. The tire rim can be taken to be rigid. The choice of the elastic properties of the tire tread and side walls requires a careful calibration so that the simulated footprint would be as close as possible to the actual footprint of a stationary tire on a dry pavement under the same load. Figure 3.4 illustrates the variation of tire footprint characteristics (i.e. length and width) with wheel load for the ASTM E501 rib tire. The simulation and experimental results are shown for comparison.

Pavement surface modeling

Pavement surface is modeled using the 4-node iso-parametric single layer MITC4 shell elements. Assuming that the deformations of the pavement surface are negligible in comparison with tire deformations, the plane pavement surface is represented as an analytically rigid surface that does not deform under the action of the wheel load.

Tire-pavement contact modeling

The Coulomb concept of friction is adopted for the simulation by defining a non-dimensional variable τ as follows (ADINA Inc., 2009),

$$\tau = \frac{F_T}{\mu\lambda} \tag{3.6}$$

where F_T is the contactor segment tangential force, μ is the coefficient of friction and λ is the contactor segment normal contact force.

The standard Coulomb friction condition can therefore be expressed as,

$|\tau| \leq 1$ and $|\tau| < 1$ implies $\dot{u}=0$

and $|\tau| = 1$ implies sign ($\dot{u}$) = sign (τ)

where $\dot{u}$ is the sliding velocity. For the case of standard Coulomb friction, μ is a constant given by the static coefficient of friction between the wet pavement surface and the tire tread rubber.

The contact algorithm used in the simulation is the constraint function method. In this algorithm, constraint functions are used to enforce the no-penetration and the frictional contact conditions. The pavement surface is assumed to be a contactor surface, while the tire tread face is treated to be a target surface.

The input parameters relevant to the analysis are identified from the distress evaluation, some of the parameters used in the simulation model are listed below:

1. Pavement parameters: The pavement structure is represented by elastic modulus, poisson ratio and density. The effect of pavement surface properties is represented by static friction coefficient (μ_0) which is the skid resistance at zero sliding speed. μ_0 can be measured by static friction test in the laboratory, or approximated using the measurement of the British Pendulum test.
2. Vehicle parameters: The required parameters are vehicle sliding speed, wheel load, tire inflation pressure, tire diameter and width, tire tread pattern and depth. The load deformation properties of the tire are represented by the elastic modulus and Poisson's ratio of tire rim, tire sidewalls, and tire tread.
3. Environmental factors: water-film thickness on pavement surface, temperature, and properties of water including density, dynamic viscosity, and kinematic viscosity.

Fluid-Structure Interaction Modeling

The fluid uplift forces on the tire, tire wall deformation and the resulting footprints at different sliding speeds are determined by the interaction between the pneumatic tire and the fluid and that between the pavement surface and the fluid. Since the pavement surface is modeled as a rigid surface, the interaction between the fluid and the pavement surface is comparatively straightforward. 'Two way coupling' method is used to analyze the interaction between the tire wall and the fluid. It is an iterative process to couple the responses of the fluid model and the tire model.

In the coupling analysis, the fundamental conditions applied to the fluid-structure interface are the kinematic condition or the displacement compatibility (Zhang and Bathe, 2001)

$$d_f = d_s \tag{3.7}$$

and the dynamic condition or traction equilibrium

$$\mathbf{n} \bullet \underline{\tau}_f = \mathbf{n} \bullet \underline{\tau}_s \tag{3.8}$$

where d_f and d_s are, respectively, the fluid and solid (i.e. the tire wall) displacements and τ_f and τ_s are, respectively, the fluid and solid stresses. The underlining denotes that the values are defined on the fluid-structure interface only. The stress and displacement criteria are used to check for the convergence of the iterations. The stress criterion is defined as,

$$r_\tau = \frac{\left\| \underline{\tau}_f^k - \underline{\tau}_f^{k-1} \right\|}{\max\left\{ \left\| \underline{\tau}_f^k \right\| , \ \varepsilon_0 \right\}} \leq \varepsilon_\tau \tag{3.9}$$

and the displacement criterion is defined as

$$r_d = \frac{\left\| d_s^k - d_s^{k-1} \right\|}{\max\left\{ \left\| d_s^k \right\| , \ \varepsilon_0 \right\}} \leq \varepsilon_d \tag{3.10}$$

where τ and d are tolerances for stress and displacement convergence, respectively, and ε_0 predetermined constant for the purpose of overriding the stresses and displacements in case they become too small to measure convergence. The tolerances are both set as 0.1%, and ε_0 is given a value of 10^{-8}.

The output of the simulation includes the following information: tire deformation profile, tire contact footprint, pressure distribution over the tire-pavement contact area, fluid flow pattern, hydrodynamic pressure distribution over the fluid-tire contact area, normal contact force and traction force at the tire-pavement interface, fluid uplift force and drag force at the tire-fluid interface. Results output from the finite element simulation carried out for different cases in the research study are given in Figure 3.5 and 3.6. The model is calibrated and validated with experimental results to verify its accuracy. The theoretical model developed in this research is a continuation of previous model that was developed by Ong and Fwa (2007a) for car and truck tire. The theoretical skid resistance model been validated for smooth car, truck tires on smooth pavement surface by the Ong and Fwa in their earlier works. (Ong and Fwa, 2007a, 2007b, 2008). The models developed for car and truck tires are not used to evaluate skid resistance for aircraft tires. Thus a new model is developed for aircraft tires with vastly different set of parameters. For example for car tires the load variation is limited around 4.8kN, pressure of 165kPa, but for an aircraft tire wheel loads ranging from 100kN to 150kN needs to be analyzed with tire pressures up to 1000kPa.

3.2.2 Evaluation of Hydroplaning Speed

The finite element model simulates the complete tire-fluid-pavement interaction problem. Starting from the initial state of a stationary locked wheel on a wet pavement, the sliding speed of the locked wheel is increased, until the time the fluid uplift force reaches the magnitude of the wheel load and causes hydroplaning to occur. Figure 3.7 illustrates the variation of fluid uplift forces and resulting contact forces with speed for ASTM E501 rib tire sliding on smooth pavement surface with 5mm water film thickness.

3.2.3 Evaluation of Skid Resistance

At any speed during the simulation, the vertical fluid uplift and the horizontal drag forces due to tire-fluid interaction, and the vertical tire-pavement contact forces and the horizontal traction forces developed within the tire-pavement contact area, are computed. From these results the skid resistance can be computed. At any speed v, computed as skid number SN, is given by the following equation,

$$SN_v = 100 \times \frac{F_x}{F_z} \tag{3.11}$$

$$SN_v = 100 \left[\frac{\mu_0 \, (F_z - U) + F_d}{F_z} \right] \tag{3.12}$$

where F_x is the horizontal resistance force to motion, and F_z is the vertical wheel load acting on the tire. The horizontal resistance force F_x is equal to the sum of the traction forces developed at the tire-pavement contact and the fluid drag forces (F_d) due to the tire-fluid interaction. The traction force is the product of the static friction coefficient of the pavement (μ_0) and the residual load on the pavement. Residual wheel load equates to wheel load minus the uplift force (U) generated due to hydro dynamic pressure on the fluid-tire contact area. The vertical load F_z is an input parameter and its value remains constant throughout the simulation. The skid resistance variation with speed is illustrated in Figure 3.8.

The variation in skid resistance with speed can be explained from the finite element simulation analysis. Fluid drag forces increase with the wheel sliding speed due to the higher fluid inertial forces that develop as the flow speed increases. However at the same time the uplift force increases reducing the normal contact force on the pavement. As a result there is a loss of frictional force developed between tire and pavement since frictional force is proportional to the normal load. Due to the fluid pressure on the tire-fluid interaction surface tire wall deformation takes place reducing the foot print area (reducing the tire pavement contact area). Although the drag force increase with speed, the magnitude is small comparison to the loss in normal contact force (*see* Figure 3.7), therefore there is a gradual loss in skid number with speed. The static friction coefficient depends on the pavement properties (which can be attributed to its micro texture, macro texture, paving mix design, construction techniques etc.) and tire surface characteristics. This also forms a significant component in the available skid resistance at a given speed as shown in Figure 3.8.

3.3 Evaluation of Runway Operational Risk for Aircrafts

It is important to explain as to what context 'risk' is used in this research. Risk can be defined as the probability of occurrence of a hazardous event in a given period (Janic, 2000). In engineering terms 'hazardous event' would refer to failure of infrastructure system. In this research the main focus is on aircraft operation risks related to runway friction performance. Runways are designed to provide safe operating conditions to the aircrafts and pavement friction performance is an integral part of that.

Deterioration of runway friction performance can lead to safety risks to the aircraft operations. In evaluating the risks involved, it is necessary to determine the impacts of the distresses identified in Section 3.1.1. Based on these and considering aircraft operational characteristics the failure criterion for each distress can be determined.

Runway surface distortions such as rutting and depressions cause aircraft operational risks related to hydroplaning and loss of skid resistance. Loss of skid resistance can reduce the braking capability of aircrafts which will increase the stopping distance during landing or a rejected take-off operation. Increased braking distances will increase the risk of overrun accidents. Hydroplaning can lead to loss of directional control during landing or take-off.

3.4 Summary

The chapter presents the basic framework which will be adopted in incorporating risk considerations into airport runway pavement maintenance management. It relates to aspects of three main areas namely, runway pavement management, aircraft runway safety risks and analysis of wet pavement friction. Pavement condition evaluation is required to identify distresses and runway characteristics that affect runway frictional performance and aircraft safety. Mechanistic analysis is necessary to evaluate such distresses' impact on pavement friction performance. In this study the focus will be on the frictional performance of runway pavements and the corresponding analysis of tire-pavement-fluid interaction to evaluate hydroplaning speed and skid resistance. This chapter presents the finite element model developed to determine tire hydroplaning speeds and skid resistance. The results are computed considering the pavement distresses, runway and aircraft characteristics. Risk assessment defines the failure criterion relevant to each distress or pavement characteristic analyzed. Based on the results from the mechanistic analysis the relevant parameters defined in the failure criterion for each distress or runway characteristic is established. They form the basis for airport authorities to assess the pavement-related risks to aircraft operation safety, which can be used as a tool in pavement maintenance management decision making.

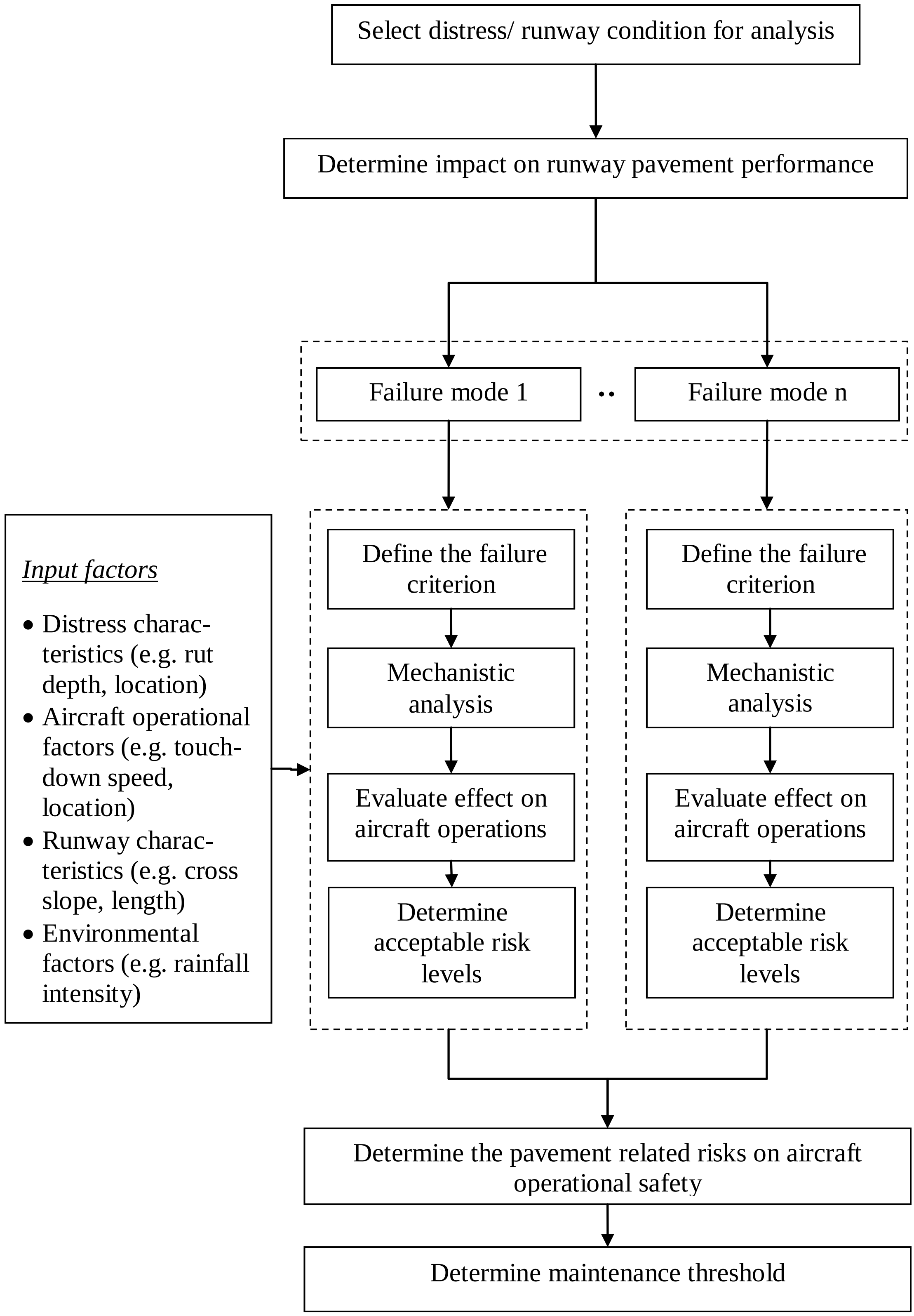

FIGURE 3.1 Framework for incorporating risk consideration in runway maintenance management

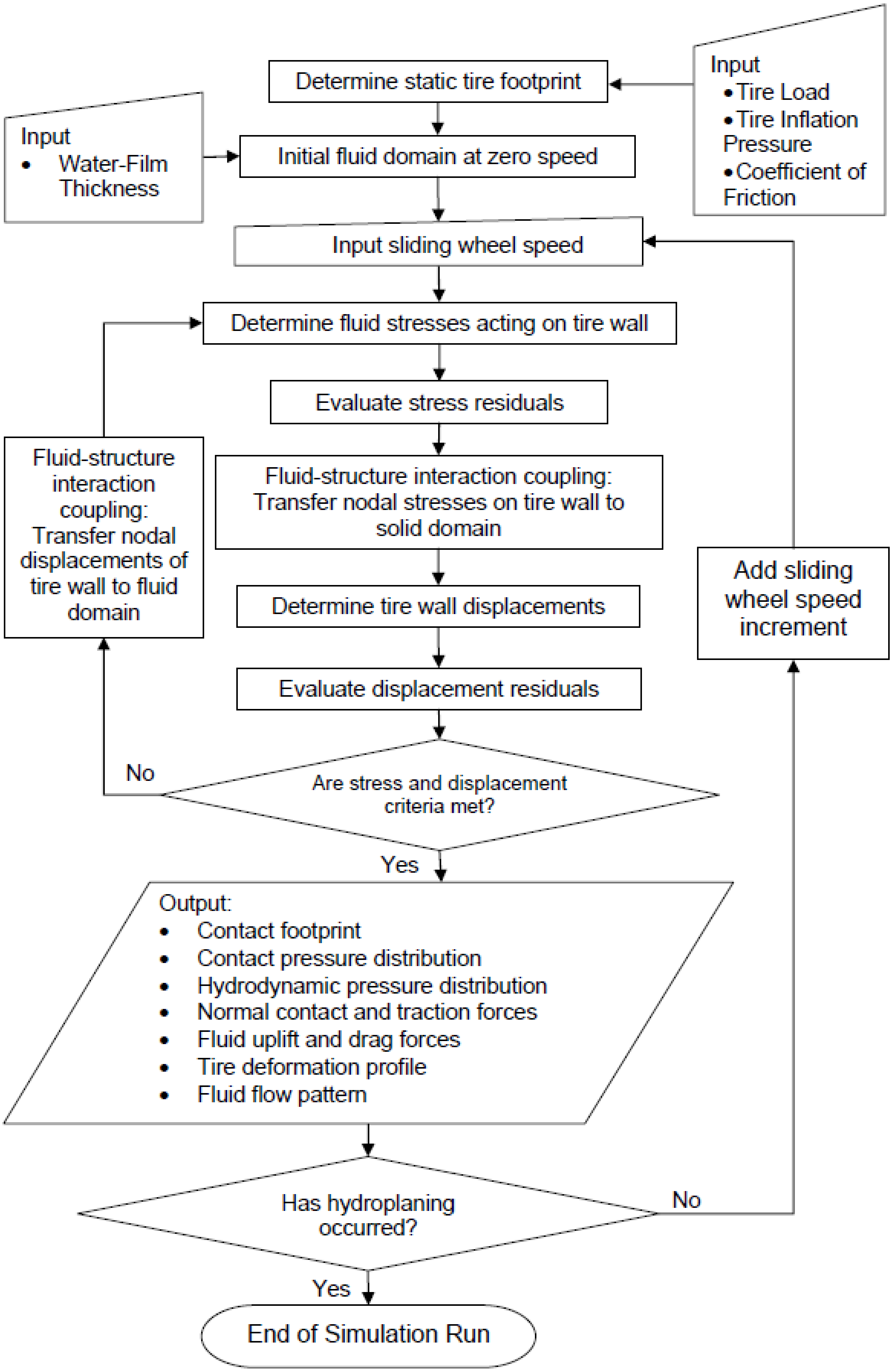

FIGURE 3.2 Simulation Procedure
(Ref: Ong and Fwa, 2007a)

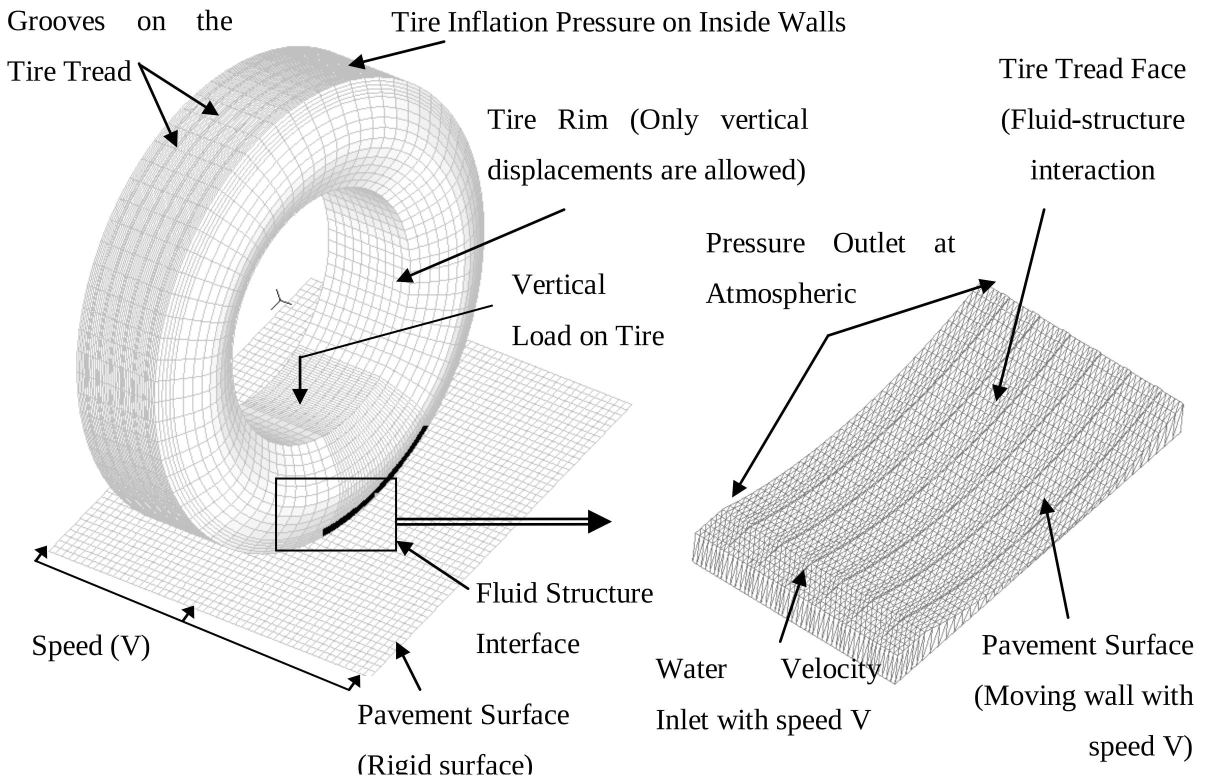

FIGURE 3.3 Three dimensional finite element model

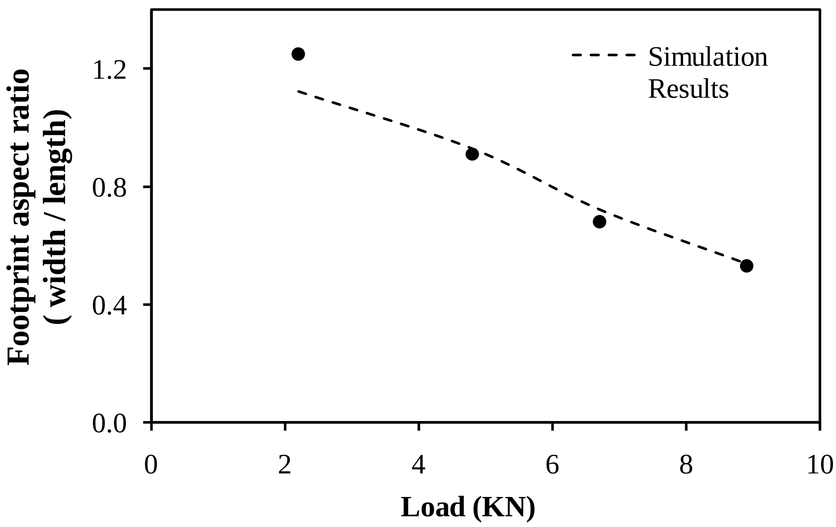

Parameters: ASTM E501 rib tire, Wheel load 4800 N, Tire pressure 165.5 kPa, Water film thickness 5mm

FIGURE 3.4 Tire foot print aspect ratio variation with wheel load

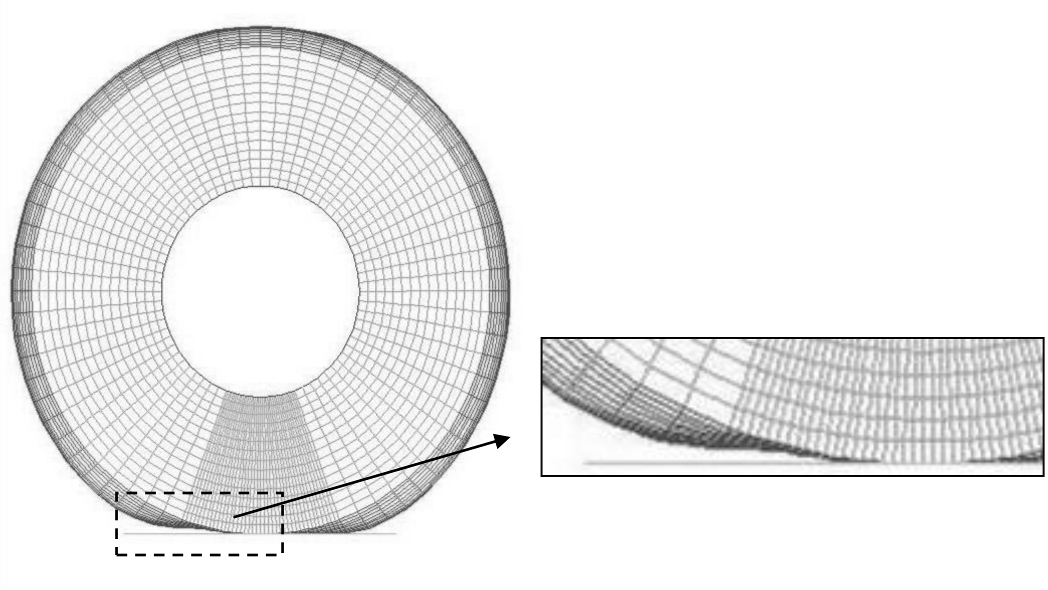

(a) Tire deformation due to fluid-structure interaction

Test parameters: 49x17 Type VII aircraft tire, wheel load = 150 kN, tire pressure = 1150 kPa, sliding speed 180 km/h

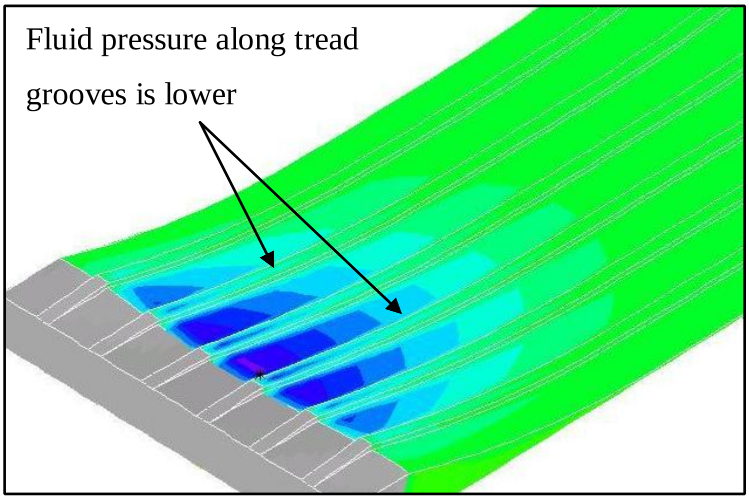

(b) Uplift force on a ribbed tire due to fluid pressure at tire - fluid interface

Test parameters: ASTM E501 rib tire, wheel load = 4.8 kN, tire pressure = 165.5 kPa, sliding speed 72 km/h

FIGURE 3.5 Finite element model simulation results - I

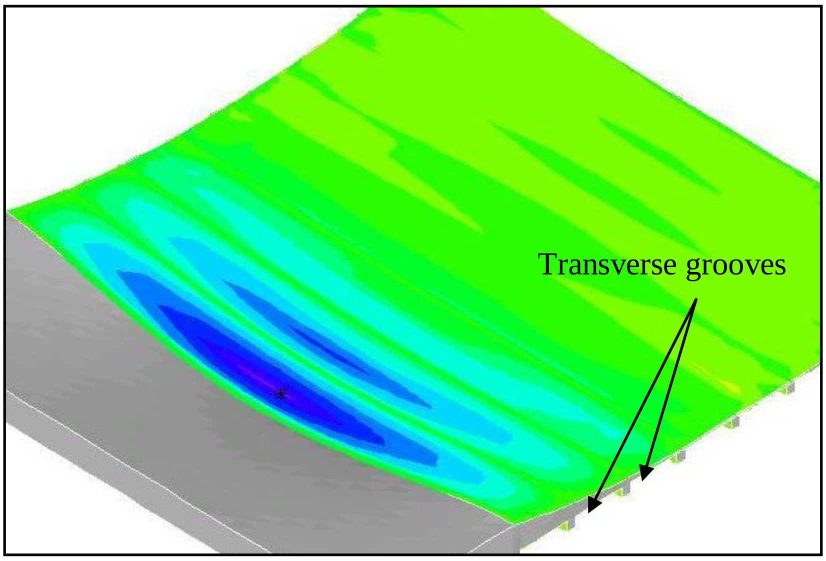

(a) Uplift force on a smooth tire on grooved pavement due to fluid pressure at fluid-tire interface

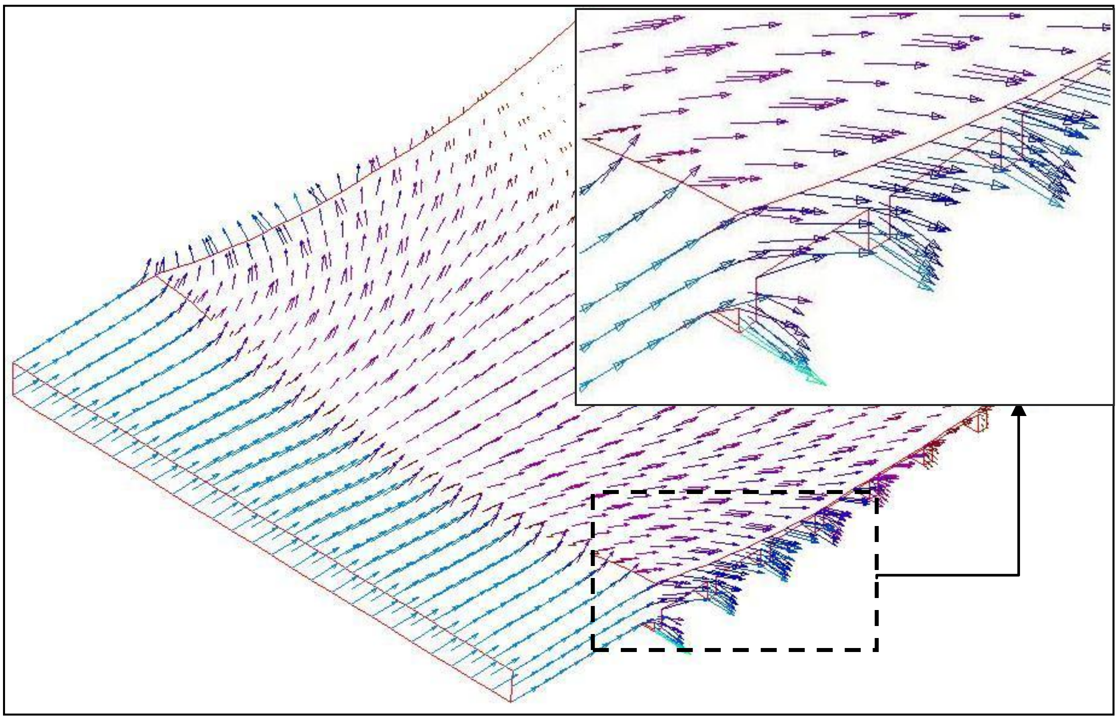

(b) Vector plot of velocity in the fluid model

Test parameters: 49x17 Type VII aircraft tire, wheel load = 125 kN, tire pressure = 1200 kPa, sliding speed 144 km/h

FIGURE 3.6 Finite element model simulation results - II

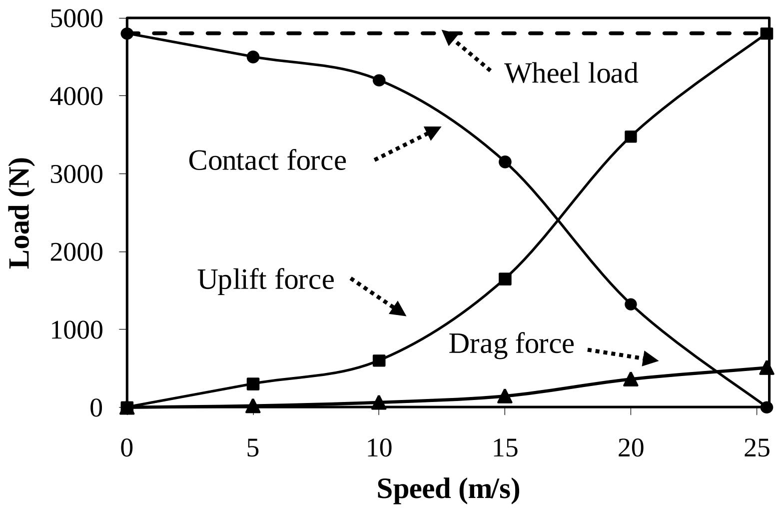

Parameters: ASTM E501 rib tire, Wheel load 4800 N, Tire pressure 165.5 kPa, Water film thickness 5mm

FIGURE 3.7 Variation of fluid uplift, contact and drag forces with speed

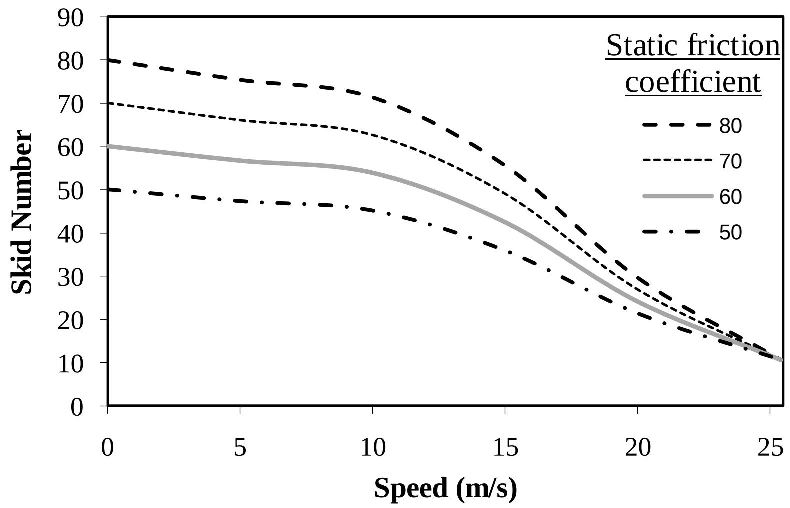

Parameters: ASTM E501 rib tire, Wheel load 4800 N, Tire pressure 165.5 kPa, Water film thickness 5mm

FIGURE 3.8 Variation of skid resistance with speed

CHAPTER 4 BRAKING DISTANCES DETERMINATION FOR OVERRUN RISK EVALUATION IN RUNWAY PAVEMENT MAINTENANCE MANAGEMENT

4.1 Introduction

Wet runway condition is known to be a major contributing factor for runway excursion accidents especially during aircraft landing (van Es et.al., 2001). Runway pavement friction is a key factor with respect to safety of landing aircrafts. Aircraft braking performance and cornering capabilities depend on the level of pavement friction available at the aircraft tire-pavement interface. Reduced skid resistance can lead to a longer braking distance and reduced directional control. This may increase the risk of runway excursion. Therefore ensuring good friction levels during all weather conditions is of great importance in airfield pavement management.

Aircraft braking distance is the main component in the calculation of the total aircraft landing distance. It is significantly affected by pavement skid resistance available to the aircraft. During wet weather, pavement skid resistance reduces substantially from its dry weather value (van Es et al., 2001; Agrawal, 1986). The magnitude of wet-pavement skid resistance is dependent on the operating conditions of the aircraft and the pavement concerned, and the relationship is a highly complex one. Research studies have shown that wet-pavement skid resistance is affected by all of the following factors: tire structural properties, pavement surface properties, aircraft speed, wheel load, tire inflation pressure, and pavement surface water-film thickness (van Es et al., 2001; Agrawal, 1986; Horne and Leland, 1962; Horne, 1976; Leland and Taylor, 1965).

Because of the relatively large number of variables involved, and the rather wide range of values possible for each variable, it is impractical to collect the required measurements and rely on statistical regression method to estimate wet-pavement aircraft braking distance. Similarly, analytical approaches that employ estimated pavement skid resistance values based on limited ground friction measurements would not be able to produce sufficiently accurate braking distance calculations to cover the wide spectrum of wet-weather aircraft operating conditions.

To overcome the difficulty and limitation encountered by the current methods of evaluating wet-pavement aircraft braking distances, this chapter presents an improved procedure for wet-pavement braking distance calculation based on engineering mechanics and fluid dynamics theory. It employs a three-dimensional finite-element skid resistance simulation model developed earlier. The adaptation of the model to simulate skid resistance of aircraft tires involved calibration and validation of the model before it was applied to perform skid resistance calculation for aircraft braking distance analysis.

4.2 Existing Methods of Aircraft Braking Distance Estimation

Aircraft braking distance is significantly affected by the available braking force which depends on the runway surface friction coefficient. Therefore a key component of any aircraft braking estimation method is the evaluation of runway friction coefficient, especially under wet pavement conditions. Researchers have generally employed two approaches to evaluate wet pavement friction behavior, one uses statistical methods derived from experimental data from aircraft test runs, and the other employs analytical techniques based on the theory of mechanics.

In a study conducted by Transport Canada (Croll and Bastian, 2004), braking distance was calculated using data from full braking runs on wet pavements using a Falcon 20 type research aircraft. Based on the test results, regression models were developed as given in Equation 4.1 to show the variation of braking coefficient μ_B *(wet)* versus ground speed V_G on a wet runway surface,

$$\mu_B(wet) = 0.237 - 0.00103\ V_G \qquad (4.1)$$

where the ground speed V_G is measured in knots. This relationship takes into account friction coefficient variation with speed during ground roll. However, since it is valid only for the aircraft type tested, its applicability in general is restricted. In addition it is defined for limited operational conditions of runway surface water film thickness, surface type, and aircraft tire properties.

A more general procedure was developed by Engineering Sciences and Data Unit (ESDU, 1995) for calculating aircraft braking distance based on estimated effective braking force G_{eff} as follows,

$$G_{eff} = Z \cdot \mu_{eff} \qquad (4.2)$$

where Z and μ_{eff} are the vertical load on the pavement and effective tire runway coefficient of friction respectively. Effective tire runway coefficient of friction is estimated from the maximum tire runway coefficient of friction (μ_{max}) and braking efficiency. A series of wet-pavement friction coefficient (μ_{max}) versus speed curves were available for the computation of aircraft braking distance. Such curves were prepared for the following specified conditions:

- Tire type: smooth and rib aircraft tires
- Tire pressure: 50 to 300 psi
- Runway surface types: five broad categories of different runway surface types are defined. They include very smooth concrete runways; lightly textured concrete or small aggregate asphalt surfaces; pavements with shallow/ or widely spaced grooving; deep grooved surfaces; and porous friction course surfaces.
- Runway surface condition: dry and wet conditions

This procedure provides a more elaborate evaluation of the wet pavement friction variation with speed compared to the regression model of Eq. 6.1. The main shortcoming is that it does not consider the effects of tire types, pavement surface water-film thickness, and the magnitude of wheel load. It is also noted that the consideration of the effect of pavement surface characteristics can be further improved quantitatively.

4.3 Finite Element Model for Skid Resistance Evaluation

As explained in the preceding section, a prerequisite to accurately evaluate wet-weather aircraft braking distance is the ability to determine the available skid resistance under the dynamic aircraft and runway operating conditions during aircraft landing operations. This requirement demands that the skid resistance computation must be able to correctly represent the complex relationship between wet-pavement skid resistance and the following factors: tire structural properties, pavement surface properties, aircraft speed, wheel load, tire inflation pressure, and pavement surface water-film thickness. The finite element simulation model elaborated in the earlier chapter is adopted in the present study through re-calibration for use in skid resistance analysis of aircraft tires (*see* Figure 4.1).

From the results the skid resistance can be computed. At any speed v, the skid number SN is given by the following equation,

$$SN_v = 100 \times \frac{F_x}{F_z} \tag{4.3}$$

where F_x is the horizontal resistance force to motion, and F_z is the vertical wheel load acting on the tire. The horizontal resistance force F_x is equal to the sum of the traction forces developed at the tire-pavement contact and the fluid drag forces due to the tire-fluid interaction. The vertical load F_z is an input parameter and its value remains constant throughout the simulation.

4.3.1 Calibration of Skid Resistance Model for Aircraft Tires

The adaptation of the aforementioned finite-element skid resistance simulation model requires calibration using measured pavement skid resistance of actual aircraft landing operations. Since the simulation model deals with the case of sliding locked wheels, it does not consider anti-skid braking systems of modern aircraft that prevent wheel locking to achieve a higher overall friction in the braking action. This means that the simulated results will represent the worst case scenario, which provides a conservative estimate of the skid resistance available as well as the braking distance.

In this chapter, the calibration of the skid resistance simulation model is demonstrated using the 32 x 8.8 Type VII smooth aircraft tire. This tire was selected for the demonstration because of the availability of experimentally measured data of its structural behavior and skid resistance. Such data are found in a study conducted by Horne and Leland (1962).

For the calibration analysis, the geometrical dimensions of the tire were found from the specifications published by the tire manufacturer (Goodyear Tire & Rubber Co., 2002). Three structural components of the tire are modeled, namely tire rim, tire sidewalls and tire tread. Tire rim is assumed to be rigid. Tire sidewall and treads are considered to be homogeneous elastic materials. The structural properties of each of the three components are characterized by the elastic moduli, Poisson's ratio and material density. These are the tire properties required for the skid resistance simulation analysis.

The calibration of these tire properties was performed where trial values were tried and adjusted until the load deformation characteristics of the tire were correctly represented. Matching of tire footprint was used as the basis for this purpose. The selected tire properties from the calibration analysis are summarized in Table 4.1, along with the selected properties for the pavement and fluid sub-models.

Table 4.2 shows the measured tire footprint dimensions from the study by Horne and Leland (1962) for the 32 x 8.8 Type VII smooth aircraft tire under a load of 10,000 lbs (4535.9 kg). The inflation pressure of the tire was 260 psi (1792.6 KPa). The percentage error between the experimental and simulation results for tire footprint length, width and area were 4.8%, 5.1% and 6.8% respectively. These magnitudes of error were considered satisfactory and acceptable for the purpose of tire calibration.

4.3.2 Validation of Skid Resistance Model for Aircraft Tires

Using the calibrated values for the various model parameters as given in Table 4.1, the validation of the model was conducted by checking the model computed skid resistance values against measured values. Measured skid resistance values are available from a study conducted by Horne et al. (1965) for the following conditions: 32 x 8.8 Type VII Smooth aircraft tire, wheel load = 22,000 lbs (9,979 kg), tire inflation pressure 290 psi (1,999.5 KPa), average water film thickness = 3.8 mm.

Two skid resistance tests were conducted in the study by Horne et al. (1965), one on a concrete pavement surface and another on an asphalt surface. The original measured skid resistance-speed data from the NASA study are reproduced in Figures 4.2(a) and 4.2(b). In applying the finite element simulation model to compute skid resistance, besides calibrating the tire properties as presented in the preceding section, it is also necessary to determine the pavement surface input parameter represented by the static frictional coefficient of the tire-pavement contact. The static friction coefficient is essentially the skid number at zero speed SN_0. This value can be determined from a field measured skid resistance value at a given sliding speed, by performing a back-analysis to derive the SN_0 value using the method proposed by Fwa and Ong (2007). For the concrete and asphalt pavement surfaces in the study by Horne et al. (1965), the SN_0 values were found to be 22.5 and 37.5 respectively.

Using the simulation model, skid resistance values were computed at sliding speeds of 10, 20, 30 and 40 m/s for the case of concrete pavement surface, and at sliding speeds of 10, 20, 30, 40 and 50 m/s for the case of asphalt pavement surface. These computed values are marked in Figures 4.2(a) and 4.2(b) for comparison with the measured data. Table 4.3 presents the measured and computed skid resistance values, as well as the percent errors of the computed values. As the magnitudes of the errors are all within +/- 9%, the agreement between the measured and computed values can be considered to be good.

4.4 Calculation of Aircraft Braking Distance

The braking distance is calculated as the distance travelled from the onset of application of brakes to aircraft stopping. The calculation of braking distance must consider the effects of the following factors: (i) runway pavement frictional level that determines the tire braking force available, (ii) aerodynamic drag forces acting on the aircraft, (iii) use of reverse thrust, and (iv) braking efficiency. For this analysis, it is assumed that no reverse thrust is used, and the case of locked wheel is considered. Since the locked wheel condition gives rise to the minimum pavement friction, the computed braking distance will represent the worst scenario and provide a conservative estimate for the actual braking distance.

From equations of motion, the general expression for calculating the braking distance is,

$$S = \int_0^T v(t)\, dt = \sum_i (\Delta x)_i \tag{4.4}$$

$$v(t) = v(t = 0) - \int_0^t a(t)\, dt \tag{4.5}$$

where *v(t)* is the aircraft speed at time *t*, *t* = 0 is the time when the brake is first applied, *t* = *T* is the time at which the aircraft comes to a complete stop, i.e. *v(T)* = 0, Δx represents the distance covered over a time period Δt, and *a(t)* is the deceleration rate of the aircraft at time t.

Applying the laws of motion to the aircraft, we can compute the deceleration rate during braking phase on a runway with zero gradient, with the assumption that both drag and lift coefficients are independent of speed.

$$D + \mu\,(Wg - L) = W\,a \tag{4.6a}$$

where W = aircraft landing weight

The forces acting on the aircraft during ground roll are defined as follows,

Uplift Force, $L = 0.5\,\rho\,v^2\,A\,C_L$ (4.6b)

Drag Force, $D = 0.5\,\rho\,v^2\,A\,C_D$ (4.6c)

The deceleration rate *a(t)* is given by,

$$a(t) = [\mu(t)]g + \frac{0.5\,\rho\,[v(t)]^2\,A\left(C_D - [\mu(t)]C_L\right)}{W} \tag{4.7}$$

where,

v = speed of aircraft
ρ = density of air
A = wing area
C_D = coefficient of drag
C_L = coefficient of lift
μ = coefficient of friction
g = gravitational acceleration

The braking distance for an aircraft is given by the following equation,

$$S = \int_0^T \left[V_b - \left([\mu(t)]g + \frac{0.5\,\rho\,[v(t)]^2\,A\left(C_D - [\mu(t)]C_L\right)}{W} \right) t \right] dt \tag{4.8}$$

where V_b is the speed at t = 0, which is the speed of the aircraft at onset of braking. Depending on the characteristics of the aircraft considered, the speed V_b is lower than the touchdown speed. This reduction in speed from the touchdown speed V_t can be estimated as follows (Kim et al., 1996),

$$V_b = V_t - k \tag{4.9}$$

where k is the speed reduction for the aircraft considered.

From previous landing survey data (Barnes et.al., 1999; Ho Sang, 1975), aircraft operational characteristics such as touchdown speed, landing weight are known to vary. This is considered in the computation of braking distance. Therefore the distribution of touchdown speed V_t can also be derived from survey data, and represented as a random variable following a probability distribution function $f(V_t)$. Similarly the landing weight of aircraft W is also represented by a probability distribution function $f(W)$.

The coefficient of friction is related to skid number by the following relationship

$$\mu = 0.01\ (SN) \tag{4.10}$$

As explained earlier, the skid number depends on the following factors

- Aircraft speed (v)
- Wheel load (w)
- Tire pressure (p)
- Surface type (static friction coefficient- SN_0)
- Water film thickness (t_w)

Unlike vehicles, for aircrafts the wheel load will vary due to the uplift forces acting on the aircraft during ground roll. Assuming 95% of the total aircraft weight is on the main gear, the wheel load *w* is calculated from the following relationship,

$$w = 0.95 \left(\frac{\mathrm{W - L}}{\mathrm{n}} \right) \tag{4.11}$$

where, n is the total number of wheels in the aircraft main gears. Similarly, the wheel load of the nose wheel can be calculated accordingly.

Hence, skid resistance (SN) can be written as a function of all the above factors,

$$\mathrm{SN} = f\,(v, W, L, p, SN_0, t_w) \tag{4.12}$$

where all the variables are as defined earlier. The procedure described above for braking distance calculation is summarized in Figure 4.3.

4.5 Aircraft Braking Distance Analysis -- Illustrative Example

To illustrate the application of the proposed procedure, a numerical example is presented to determine the wet-weather braking distance of an aircraft with the tire considered in the earlier calibration analysis (*see* Table 4.1 and Figure 4.1) under the section on "Calibration of Skid Resistance Model for Aircraft Tires".

4.5.1 Aircraft Tire Wet - Pavement Skid Resistance Evaluation

From the simulation results, skid resistance was computed for water-film thickness of 1mm, 2 mm and 5mm; different wheel load values up to 50kN; and different sliding speeds. The results of the analysis are plotted in Figure 4.4. The corresponding braking distance calculations were performed based on the computed skid resistance. It can be observed that skid resistance decreases with increase in speed as well as water film thickness.

4.5.2 Calculation of Braking Distance

A summary of the aircraft input parameters is given in Table 4.4. The values are taken from related landing survey and manufacturer's manuals (Ho Sang, 1975; Jackson, 2001). As explained earlier aircraft touchdown speed is included as a random variable. Calculation of the braking speed V_b is done by assuming a speed reduction, k equal to 2 m/s speed from the touchdown speed as given in Equation 4.9. Based on the finite element simulation results for skid resistance for the given input parameters, a relationship can be built to express the skid resistance variation with those factors identified in Equation 4.12. The computed skid number is used to estimate the coefficient of friction as given in Equation 4.10. This is incorporated into calculation of the braking distance, starting from the speed at the onset of braking to zero speed, as given in Equations 4.4 to 4.8. The braking distance was computed using a numerical step by step integration method. Considering the probabilistic nature of the input variables representing aircraft operational characteristics, the final results will also be presented in the form of a frequency distribution.

4.5.3 Results of Analysis

The results of braking distance calculation for different water film thickness are presented in Figures 4.5 and 4.6. The mean braking distance on a pavement with 5mm, 2mm and 1mm water-film thickness are 621m (2037ft), 531m (1742ft) and 489m (1604ft) respectively. As expected the computed braking distance increases with water film thickness. This is due to the decrease in wet-pavement skid resistance with the increase in water film thickness. The variation in the braking distance is due to the variance in the initial braking speed which occurs as a result of the probability distribution of touchdown speed.

It can also be observed from the results that the deceleration rate varies inversely with aircraft speed. This is due to two reasons, firstly as shown in the skid resistance evaluation results, skid resistance decreases with increase in speed. Secondly, at higher speed there is greater uplift force acting on the aircraft and the net wheel loads are lower as a result. It has also been shown that skid resistance generally reduces with a decrease in wheel load. This results in a lower skid resistance at higher speed and consequently a lower deceleration rate. The calculated results represent the worst case scenario as it has not factored in additional braking available for the aircraft by use of reverse thrust and anti-skid braking systems, etc. However, the results clearly demonstrate the impact wet-pavement conditions have in increasing aircraft braking distance.

4.6 Computation of Aircraft Landing Stopping Distance

Aircraft landing stopping distance varies significantly depending on the aircraft operational characteristics such as touchdown speed, location, landing technique, aircraft braking type, reverse thrust usage and also the airport elevation, runway conditions, wind conditions etc. Several risk factors could be acting concurrently during a landing overrun accident. The presence of multiple risk factors could significantly increase the probability of a runway overrun accident. This wet pavement conditions can compound the effects from other operational factors such as long landing and fast landing on the runway. Therefore it is important to consider operational characteristics such as touchdown speed and location in the analysis of aircraft landing performance on wet runway conditions. This allows one to assess how each factor will affect the aircraft landing distance and the potential for overrun accidents.

4.6.1 Illustrative Example

An example is presented in this section to compute the landing distance for a regional aircraft. The aircraft characteristics and other parameters used in the calculations are given in Table 4.4.

Aircraft landing distance calculation includes three main phases as shown in Figure 4.7:

1. Air distance - distance travelled from 50 feet (15.25m) above the runway to the point of touchdown.

   Landing parameter surveys conducted at several airports by FAA (Barnes et al., 1999) give data for aircraft touchdown position variation along the runway. Data from such studies can be used to model the touchdown location distribution for a given aircraft type. Therefore the air distance S_a in the calculation is represented as a random variable $f(S_a)$.

2. Transition distance - The transition distance is the distance travelled from the touchdown point to the onset of braking application. The reduction in speed (k) from the touchdown speed during this period is around 2m/s for most aircraft types and the delay is estimated to be around 2 seconds (Trani et al., 1995). This reduction in speed from the touchdown speed V_t can be estimated as follows from Equation 4.9. The aircraft touchdown speed is taken as a random variable following a probability distribution function $f(V_t)$. The delay distance can be computed as follows,

   $$S_d = 0.5\,(V_t + V_b)\,t_d \qquad (4.13)$$

   where, t_d= delay time

3. Braking distance - The braking distance is calculated as the distance travelled from the onset of application of brakes to aircraft stopping. For this analysis, the braking distance S_b computed in Sections 4.5 in the chapter will be used.

   The total stopping distance is given by the summation of results for the three phases during landing.

$$S = S_a + S_d + S_b \qquad (4.14)$$

Braking distance was computed using a numerical step by step integration method. Considering the probabilistic nature of the input variables representing aircraft operational characteristics, the final results will also be presented in the form of a frequency distribution.

4.6.2 Results of Analysis

The results of aircraft landing stopping distance for different water film thickness are presented in Figure 4.8. The mean landing distance on a pavement with 1mm and 5mm water-film thickness are 933m and 1012m respectively. As expected the computed landing stopping distance increases by 8.4% due to the increase in water film thickness. This increases of overrun risk is due to increase in braking distance as a result of decrease in wet-pavement skid resistance at higher water film thickness. The percentage increase is approximately 20% if the braking distances for the respective water film thicknesses were compared. The variation of aircraft landing distance with touchdown speed and distance shows that touchdown speed has more significant impact than touchdown distance on the overall landing distance. The calculated results represent the worst case scenario as it has not factored in additional braking available for the aircraft by use of reverse thrust and anti-skid braking systems, etc. However, the results clearly demonstrate the impact wet-pavement conditions and aircraft operational characteristics have on landing distance, and give an indication as to how overrun risk would increase from changes in them.

4.7 Summary

This chapter presents a methodology to compute aircraft braking distance under wet-pavement conditions. This approach incorporates a mechanistic based analysis and uses finite element simulation to evaluate aircraft tire wet-pavement skid resistance. The main advantage is that it can incorporate the effects of the key factors such as water film thickness, wheel load, pressure, and surface condition into the analysis of skid resistance and braking distance. Skid resistance variations with these factors such as speed, weight, water film thickness, surface condition are accounted for in the computation of braking distance. The analysis also considers the probabilistic nature of aircraft operational characteristics such as touchdown speed, location and weight. It can be easily extended to include variation of tire pressure and other related parameters if necessary. This procedure offers an improved understanding of the factors affecting runway friction which is an integral part of the aircraft braking distance computation and stopping distance estimation.

The proposed procedure can be used to evaluate the overrun risks for different runway conditions and aircraft operating characteristics in an airport. It presents a useful tool for airport authorities in assessing the runway conditions for surface friction management as well as other safety measures to improve the overall safety performance of aircraft landing and take-off operations.

TABLE 4.1 Material Properties for Calibration of Aircraft Tire

	Elastic Modulus	Poisson's Ratio	Density (kg/m^3)
Tire Properties			
Rim	100 GPa	0.3	2,700
Sidewall	50 MPa	0.45	1,200
Tread	200 MPa	0.45	1,200
Pavement Properties	30 GPa	0.15	2,200
Fluid Properties	Temperature		25°C
	Density		997.1 kg/m^3
	Dynamic Viscosity		$0.894 x 10^{-3} Ns/m^3$
	Kinematic Viscosity		$0.897 x 10^{-6}\ m^2 / s$

TABLE 4.2 Comparison of Measured and Computed Footprint Dimensions

	Experiment	Simulation	Error
Width (mm)	142.7	135.4	-5.1%
Length (mm)	201.2	191.6	-4.8%
Area (mm^2)	21,142	19,697	-6.8%

TABLE 4.3 Comparison of Measured and Computed Skid Resistance

Pavement Surface Type : Asphalt

Speed (m/s)	Simulation Computed Skid Number (SN)	Measured Skid Number (SN)	Difference	% Difference
10	36.5	39	-2.5	-6.4
20	34.9	34	0.9	2.7
30	31.2	29	2.2	7.6
40	26.2	24	2.2	9.0
50	19.9	19	0.9	4.7

Pavement Surface Type : Concrete

Speed (m/s)	Simulation Computed Skid Number (SN)	Measured Skid Number (SN)	Difference	% Difference
10	21.2	23	-1.8	-7.8
20	20.5	20	0.5	2.3
30	17.8	16.5	1.3	7.9
40	14.1	13	1.1	8.6

TABLE 4.4 Input Parameters Used for Numerical Example

Aircraft Type : Regional Jet		
Main Gear Type	Dual	
Maximum landing weight	21319 kg	
Landing weight used for analysis	20000 kg	
Wing Area	$54 m^2$	
Air density	$1.224 kg/m^3$	
Touchdown speed (m/s)	Mean = 55	Standard Deviation = 7
Touchdown location (m)	Mean = 300	Standard Deviation = 25
Dry runway friction coefficient	0.5	

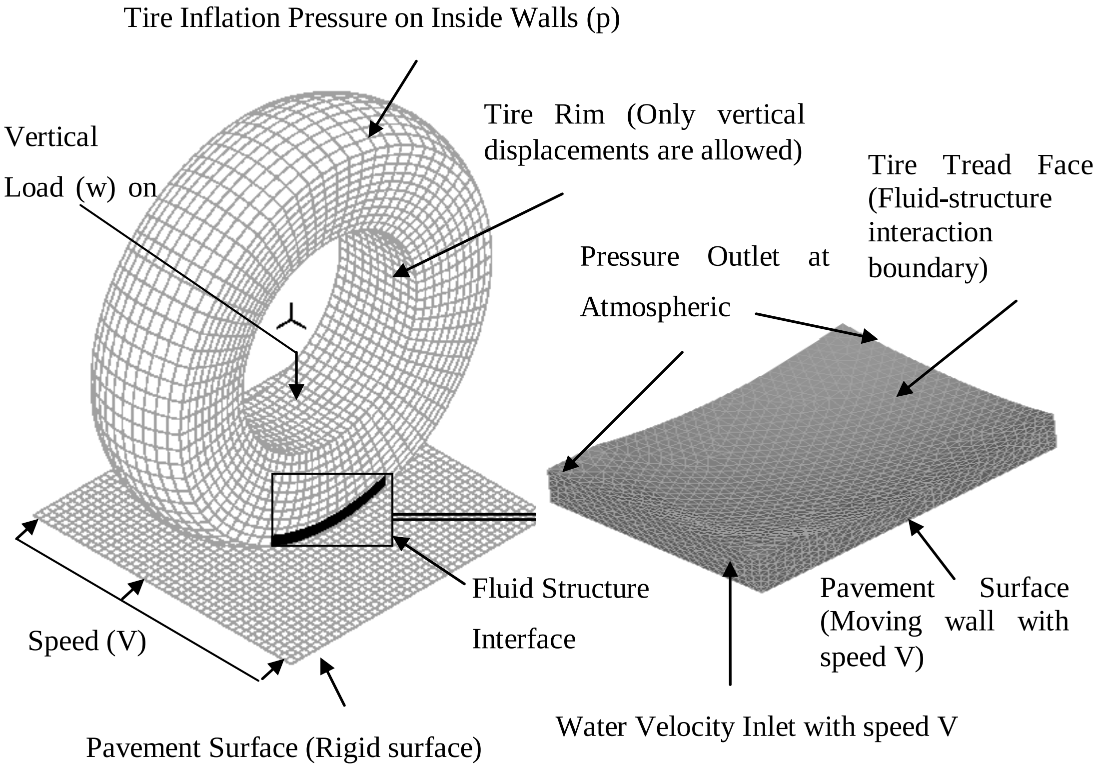

FIGURE 4.1 Finite-element model of aircraft tire and pavement surface.

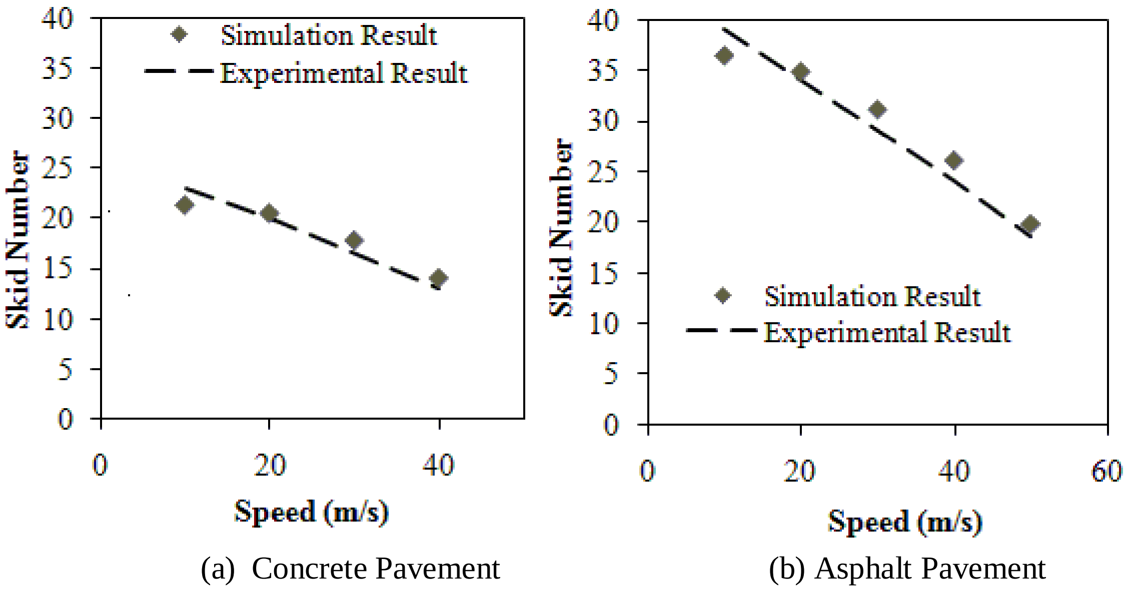

Note: 32 x 8.8 Type VII Smooth aircraft tire, Average water film thickness 3.8mm, Load 22000 lbs (9979 kg), Pressure 290 psi (1999.5 KPa)

FIGURE 4.2 Comparison of measured and computed skid resistance for (a) Concrete surface and (b) Asphalt surface

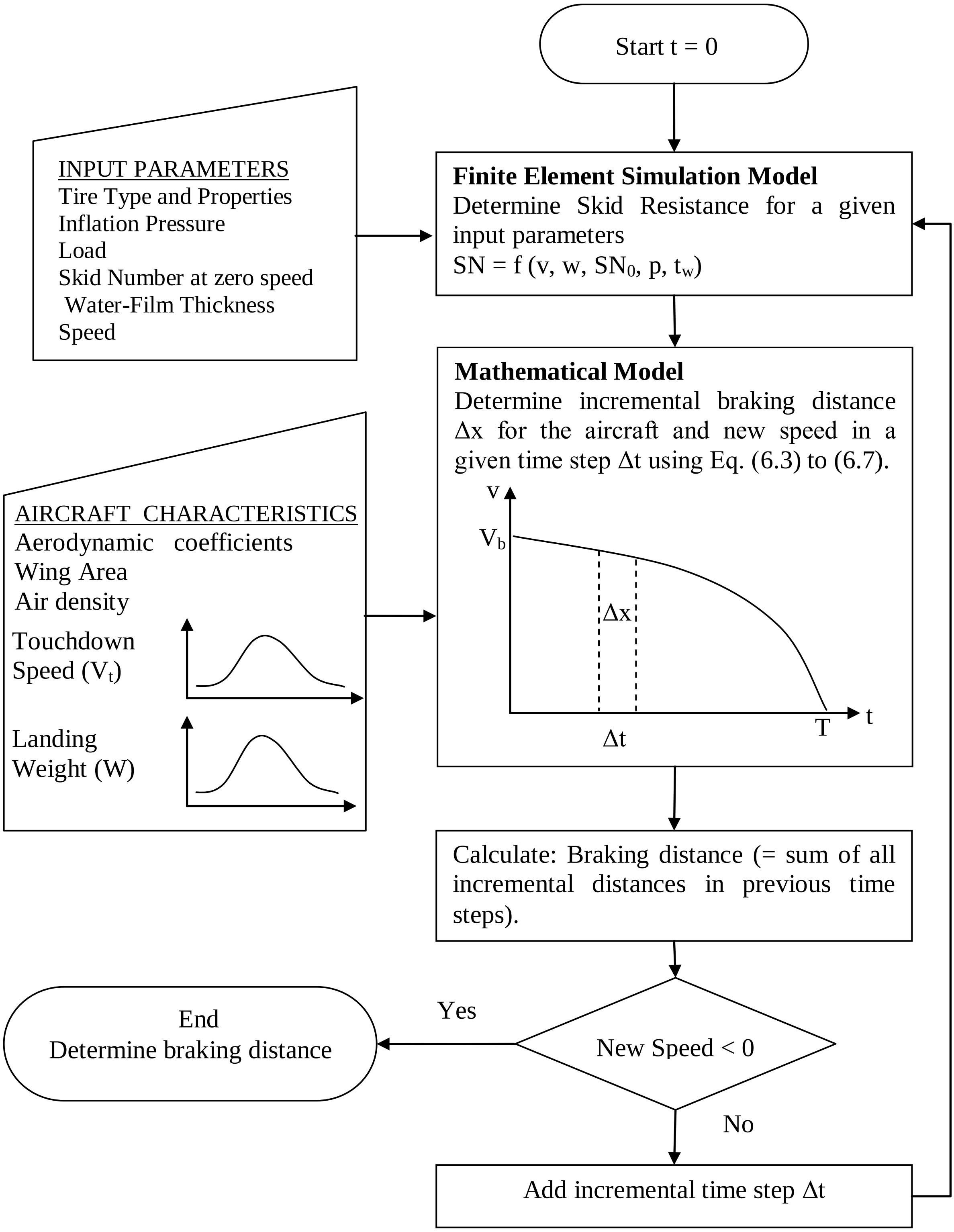

FIGURE 4.3 Procedure for aircraft braking distance computation

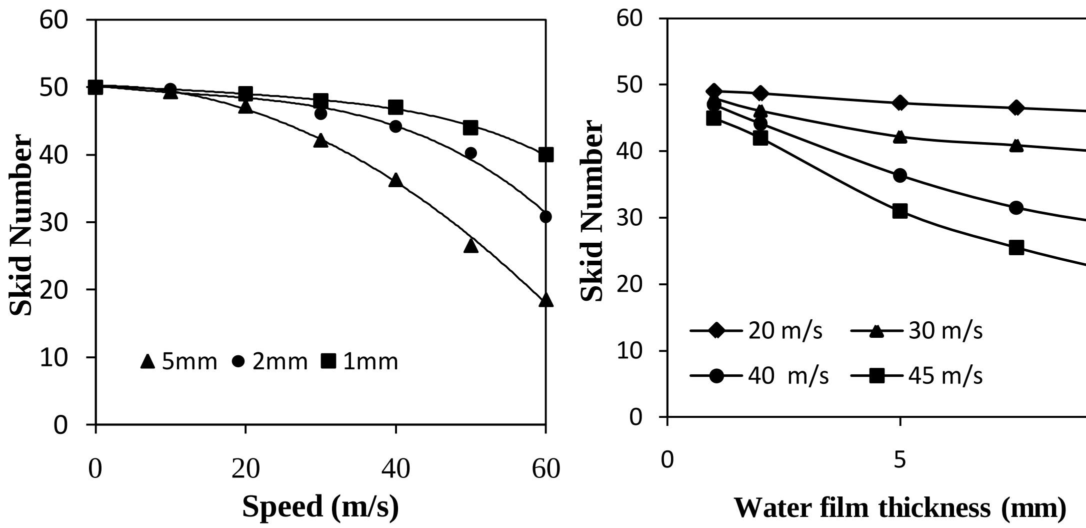

(a) Effects of water-film thickness

(b) Effect of Sliding Speed

Note: Data presented for smooth aircraft tire, 32 x 8.8 Type VII with inflation pressure of 1104 kPa, wheel load 50 kN.

FIGURE 4.4 Factors affecting skid resistance

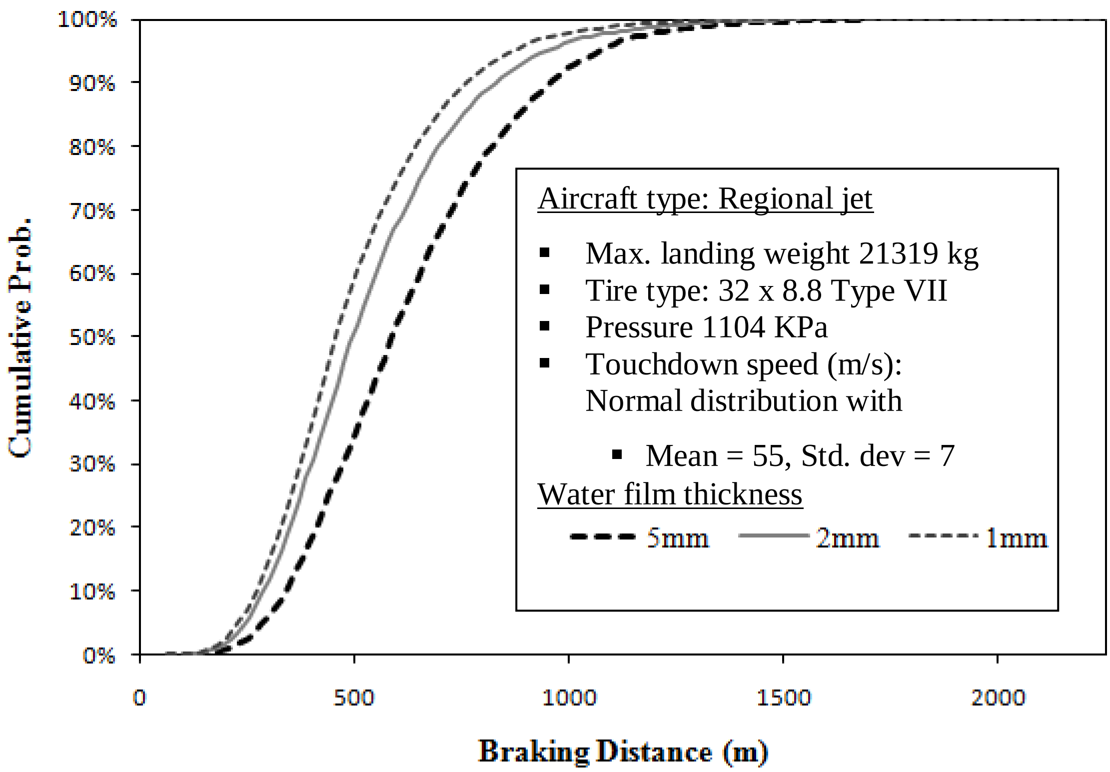

FIGURE 4.5 Comparison of computed aircraft braking distance distributions for 2mm and 5mm water-film thickness

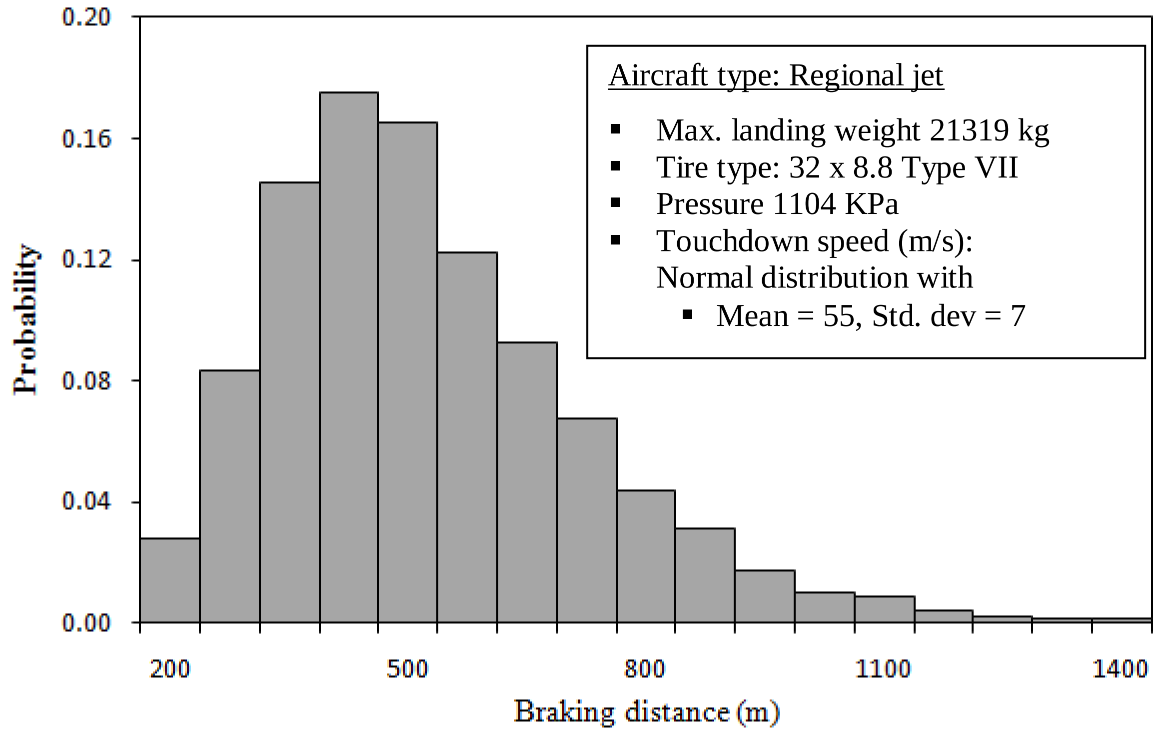

(a) 1mm water film thickness

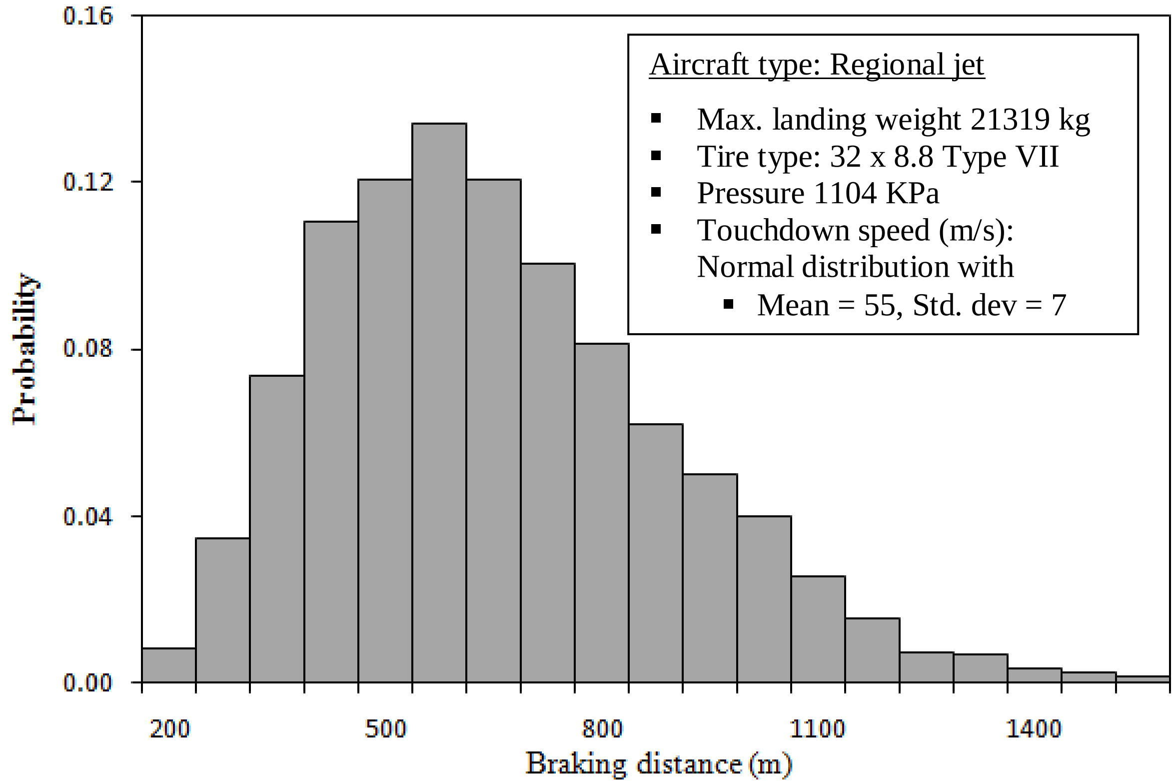

(b) 5mm water film thickness

FIGURE 4.6 Computed aircraft braking distances for example problem (a) 2mm (b) 5mm water-film thickness

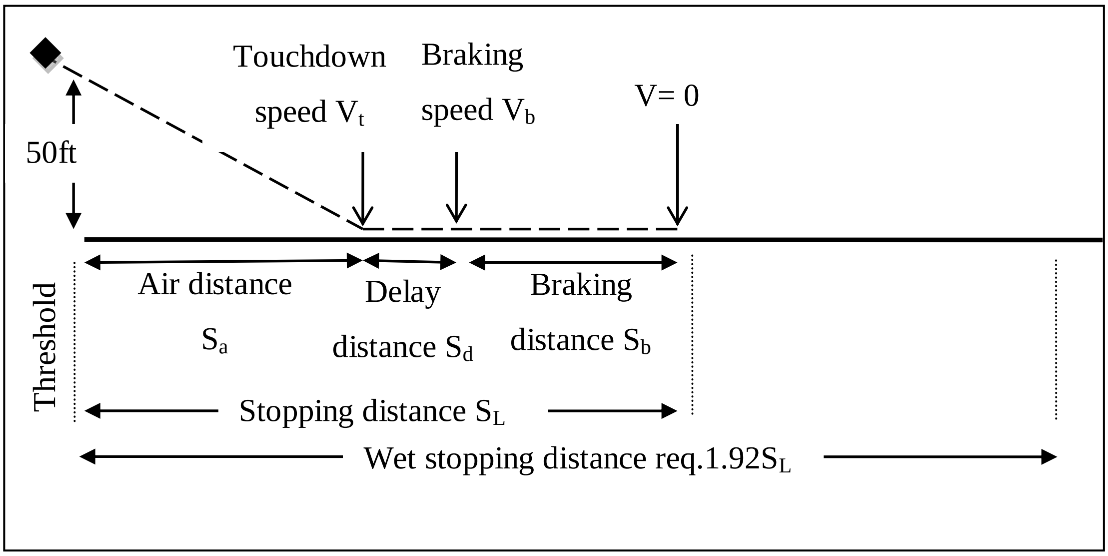

FIGURE 4.7 Aircraft landing distance phases

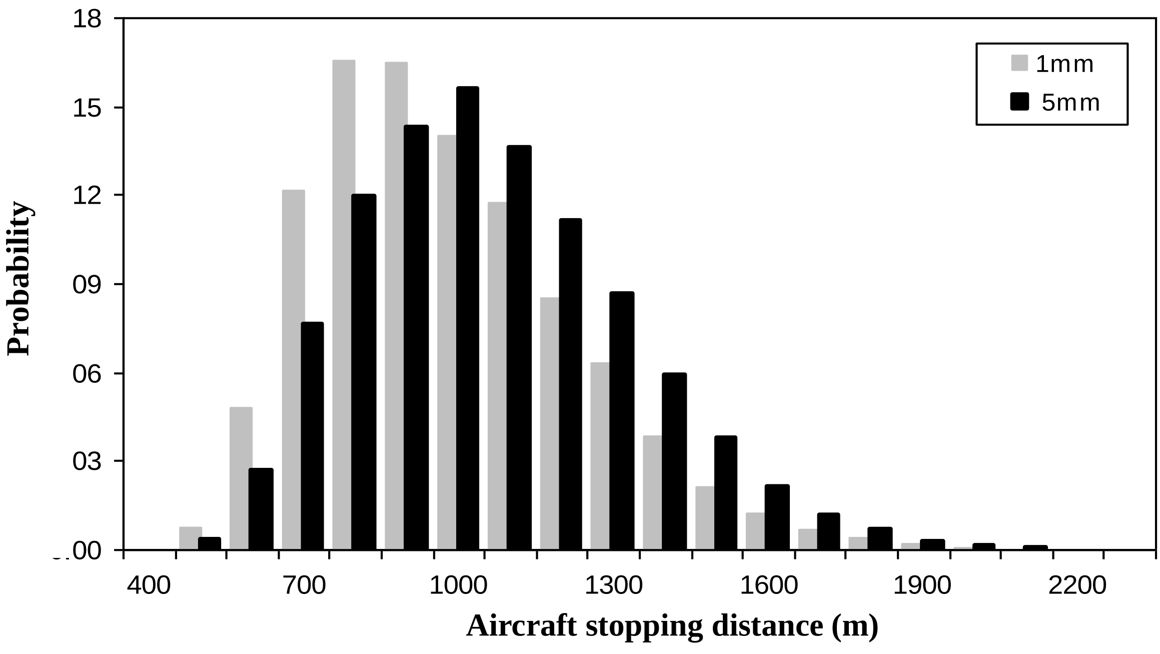

Note: Max. landing weight 21319 kg, Tire type: 32 x 8.8 Type VII, Pressure 1104 KPa, Touchdown speed (m/s): Normal distribution with Mean = 55, Std. dev = 7

FIGURE 4.8 Aircraft Landing Stopping distance distribution for water film thickness of 1mm and 5mm

CHAPTER 5 EVALUATION OF BENEFICIAL EFFECT OF RUNWAY PAVEMENT GROOVING ON AIRCRAFT BRAKING DISTANCES

5.1 Introduction

As highlighted in Chapter 4, runway skid resistance is an important factor for aircraft safety. Skid resistance reduces during wet weather conditions, and has significant effects on aircraft braking performances. This chapter will examine grooving as a runway pavement management method to counter the loss of skid resistance during wet weather conditions, and analytically evaluate its beneficial effect on aircraft braking distances.

The magnitude of wet-pavement skid resistance is dependent on the operating conditions of aircraft and the properties of pavement. Pavement surface properties refer to pavement type, its macro-texture and micro-texture which determine the frictional characteristics of the pavement. Pavement surfaces with low macrotexture provide low skid resistance during the presence of surface water, especially at high aircraft speeds. This is an important safety concern on runways since aircrafts operate at high speeds during take-off and landing ground roll. Runway surface friction management ensures that adequate friction levels are available to the aircrafts during operations. One of the methods adopted in most major airports in the United States and worldwide is to introduce transverse grooves on runway pavements to improve its frictional properties under wet pavement conditions.

This chapter presents an analytical approach to evaluate the beneficial effect of runway grooving on aircraft braking performance on wet runway pavements. A finite element simulation model developed in the research is used to simulate aircraft tire skidding on a grooved pavement with a given water film thickness. The simulation results are used to compute the skid resistance and are incorporated into the calculation of aircraft landing braking distance. The analysis can compare the computed braking distance values for grooved pavements and smooth pavements respectively for different levels of water film thickness, and assess the beneficial effect of pavement grooving on aircraft braking performance under wet pavement conditions.

5.2 Development of Simulation Model for Skid Resistance Evaluation

In the present study, the simulation model described in the preceding chapter was modified to consider aircraft tire sliding on a grooved runway pavements. Finite element simulation analysis is used to evaluate skid resistance considering aircraft tire and pavement properties. The finite-element mesh of the simulation model developed for this analysis is shown in Figure 5.1.

5.2.1 Calibration of Finite Element Simulation Model for Aircraft Tires

In this section, the calibration of the finite element simulation model is demonstrated using the 49 x 17 Type VII smooth aircraft tire. This tire is used in modern jet aircrafts such as Boeing 727. Such data are found in a study conducted by Agrawal (1981).

For the calibration analysis, the geometrical dimensions of the tire were found from the specifications published by the tire manufacturer (The Goodyear Tire & Rubber Co., 2002). Three structural components of the tire is modeled, namely tire rim, tire sidewalls and tire tread. The calibration of these tire properties was performed following the calibration procedure discussed in Chapter 3, under finite element model development. Matching of tire footprint was used as the basis for this purpose. Tire rim is assumed to be rigid have an elastic modulus of 100 GPa, a Poisson's ratio of 0.3, and a density of 2,700 kg/m^3. Tire sidewall and treads are considered to be homogeneous, isotropic elastic materials. The structural properties of each of the three components are characterized by the elastic moduli, Poisson's ratio and material density and the corresponding values for tire tread are 350 MPa, 0.45, 1200 kg/m^3 and for the sidewall 200 MPa, 0.45, 1200 kg/m^3 respectively. These are the tire properties required for the skid resistance simulation analysis. For the problems analyzed in this study, the fluid, tire and pavement sub-models with 23700, 8800, 2700 number of elements, respectively, were found to give sufficiently accurate results.

Table 5.1 shows the measured tire footprint dimensions from the study by Agrawal (1981) for the 49 x 17 Type VII smooth aircraft tire under a load of 30,000 lbs (13500 kg). The inflation pressure of the tire was 140 psi (966 kPa). The percentage error between the experimental and simulation results for tire footprint length and width were 7.2% and 3.1% respectively. These magnitudes of error were considered satisfactory and acceptable for the purpose of tire calibration.

The case of locked wheel is considered because it represents the worst case scenario that produces the longest braking distance (Williams, 1971; Yager and Dreher, 1976). The skid resistance at any speed v, computed as skid number SN_v, is given by Equation 4.3.

5.2.2 Validation Analysis of Skid Resistance Simulation

The simulation model developed to analyze the skid resistance of aircraft tire on grooved pavement with surface water is validated with experimental results. Skid resistance tests were conducted in the study by Horne and Brooks (1967*)*, on a concrete pavement surface with different groove patterns and another on an un-grooved concrete surface. The measured skid resistance values from the study conducted by them are available for the following conditions: 49 x 17 Type VII Smooth aircraft tire, wheel load = 30,000 lbs (13500 kg), tire inflation pressure 170 psi (1,173 KPa), average water film thickness = 6.35 mm, and speed of the skidding tire =100 knots (50 m/s).

The following surface types are considered in the validation:

- Case 1: concrete surface – transversely grooved 0.25" (6.35mm) wide x 0.25" (6.35mm) deep x 1" (25.4mm) spacing
- Case 2: concrete surface – transversely grooved 0.375" (0.95mm) wide x 0.25" (6.35mm) deep x 1" (25.4mm) spacing
- Case 3: concrete surface - un-grooved

In applying the finite element simulation model to compute skid resistance, besides calibrating the tire properties as presented in the preceding section, it is also necessary to determine the pavement surface input parameter represented by the static frictional coefficient of the tire-pavement contact. The static friction coefficient SN_0 value of 50 is obtained from experimental data available from a study conducted by Yager (1969).

The measured skid resistance data from the study are given in Table 5.2. The difference between the experimental results and simulated values are +2.1, +1.2 and +3.4 for the three cases analyzed. As the magnitudes of the errors are all within +/- 5, the agreement between the measured and computed values can be considered to be good. The validation in this section confirms that the skid resistance model is able to correctly simulate skid resistance behavior aircraft tire on grooved pavements.

5.3 Determination of Grooved Pavement Skid Resistance

The simulation model is used to analyze how different parameters affect the skid resistance of an aircraft under wet pavement conditions. Skid resistance of wet pavement decreases as the vehicle speed increases, and the magnitude of loss of skid resistance also increase at higher water film thickness (Horne and Leland, 1962; Horne, 1976). Past experimental studies have demonstrated that grooving significantly improves wet pavement skid resistance (Yager, 1969; Shilling, 1969). Therefore it is of interest to analytically quantify the beneficial effects of grooving runway pavements under different wet pavement conditions.

Using the finite element simulation model, the variation of skid resistance with speed will be analyzed for the following problem parameters:

- Pavement surface model: The current groove standard provided by FAA is 6 mm (±1.6 mm) in depth by 6 mm (+1.6 mm, -0 mm) in width by 38 mm (- 3 mm, + 0 mm) center to center spacing (FAA, 1997). These dimensions will be adopted for the analysis. In addition two groove depths of 3mm, 10mm will be analyzed to assess their relative effectiveness under different wet pavement conditions.
- Fluid model: Three water depths will be studied in the analysis: 1mm, 5mm, and 10mm. These represent the typical wet and flooded runway surface conditions experienced during wet weather, and the 10mm water film thickness is used to represent a very severe condition.

- Tire model: The 49x17 Type VII smooth aircraft tire is used. This type of tire is used by modern jet aircrafts such as Boeing 727. The tire inflation pressure is 1200 kPa. Wheel loads within the range expected during normal aircraft landing are considered.

Results from the simulation for the skid resistance variation with speed for the above mentioned parameters are plotted in Figures 5.2 and 5.3. The following observations of the effect of grooving on skid resistance can be made.

- In general, all other parameters being constant, the skid resistance on a wet pavement reduces with speed. Pavement grooving reduces the rate of skid resistance loss considerably compared to smooth pavement case. It is seen in Figure 5.2 that for groove depths of 6mm and 10mm the reduction is in skid number (SN) is less than 20 and 15 respectively for a speeds up to 150km/h, while there is a SN loss of 40 for smooth pavements for a water film thickness of 5mm.
- Increase in water film thickness reduces skid resistance available to the aircraft tire. Grooved pavements compared to the smooth case provide higher skid resistance at all water film thicknesses analyzed. As seen in Figure 5.3 there is an increase in skid number by approximately 10 from smooth pavement to grooved pavement with 3mm depth. There is a more gradual increase in skid numbers as the groove depth increases from 3mm to 6mm and 10mm. This effect is more significant for high water film thicknesses since groove depths of 6mm or more provide substantial improvements in skid resistance.

Thus grooved pavements are more able to retain pavement skid resistance at high speeds under wet pavement conditions. This would ensure that aircraft has adequate braking force available during landing ground roll and minimize the risk of overrun accidents.

5.4 Evaluation of Braking Distance

The proposed method calculates braking distance for the worst case represented by a locked aircraft tire. It is the distance travelled from the onset of application of brakes to aircraft stopping. For this analysis, considering the most conservative scenario, it is assumed that no reverse thrust is used, and any braking efficiency utilized is ignored. Since the locked wheel condition gives rise to the minimum pavement friction, the computed braking distance will represent the worst scenario and provide a conservative estimate for the actual braking distance.

5.4.1 Methodology for Calculation of Aircraft Braking Distance

The proposed braking distance calculation methodology follows the same approach explained in Section 4.4 of Chapter 4. This methodology is adopted in the numerical example used to compute the braking distance for a commercial jet aircraft. A summary of the aircraft input parameters is given in Table 5.3. The values are taken from related landing survey and manufacturer's manuals (Barnes et. al., 1999; Ho Sang, 1975; Jackson, 2001). Touchdown speed V_t can also be derived from survey data, and it is represented as a random variable following a normal distribution (Barnes et. al., 1999; Ho Sang, 1975). The procedure for braking distance calculation is the same as that summarized in Figure 4.3.

As explained earlier, skid number depends on the following factors: aircraft speed (v), wheel load (w), tire pressure (p), surface type (static friction coefficient-SN_0), water film thickness (t_w). In addition, for a grooved pavement the groove pattern (width, depth, and spacing) can also be considered as a factor that affects skid number. Hence for a pavement with a particular groove pattern, skid resistance (SN) can be written as a function of all the above factors,

$$SN = f\,(v, M, L, p, SN_0, t_w) \qquad (5.1)$$

where all the variables are as defined earlier. These input parameters are used in the finite element simulation model described earlier and the output will be used to compute the skid number according to Equation 5.1. The skid number is used to estimate the coefficient of friction as given in Equation 4.10. This is incorporated into the calculation of the braking distance, starting from the speed at the onset of braking to zero speed, as given in Equation 4.4 and illustrated in Figure 4.3. The braking distance was computed using a numerical integration method.

In the case of grooved pavements the FAA specified groove pattern was used, i.e. 6mm x 6mm x 38 mm (width x depth x spacing). The other groove depths considered were 0mm, 3mm and 10mm. The braking distances on these 4 types of surfaces were calculated for 3 different water film thicknesses: 1mm, 5mm and 10mm.

5.4.2 Analysis of Braking Distance Results

The beneficial effect of grooved pavement is assessed against the case of un-grooved pavement. The distribution of computed braking distances is given in Figures 5.4 and 5.5 and the mean braking distance for each scenario is given in Figure 5.6 and Table 5.4.

The following observations can be made:

(i) Based on the average braking distance computed, the effect of grooving in reducing aircraft braking distance under wet pavement conditions can be highlighted.

- As shown in Figure 5.6, for non-grooved pavement surface the braking distance increases by approximately 40% when water film thickness increases from 1mm to 5mm; whereas for grooved pavements with 3mm, 6mm and 10mm groove depths the corresponding values are 22% ,16% and 9% respectively.
- Grooving substantially reduces the braking distance for the different water film thicknesses considered: for 1 mm water film thickness, the braking distance compared to the un-grooved pavement is reduced by 18%, 23%, and 27% respectively for grooved pavements with groove depths of 3mm, 6mm, and 10mm; similarly for 5mm water film thickness the braking distances are reduced by 28%, 36%, and 43% respectively for grooved pavements with groove depths of 3mm, 6mm, and 10mm. At 10mm water film thickness the corresponding reduction improvements are 25%, 39%, and 47%.

(ii) The computed distribution of braking distances (*see* Figures 5.4 and 5.5) shows the expected variation of braking distances taking into account the probabilistic nature of aircraft operating characteristics such as touchdown speed and landing weight. This is a good representation of overrun risk for an aircraft, since braking distance forms a major component of an aircraft's stopping distance.

- Braking distance distributions for grooved pavements show less variance compared to that of un-grooved pavements for all the water film thicknesses analyzed. The variance is significantly high for smooth pavements for water film thicknesses of 5mm and 10mm, which indicates that there is more likelihood that the braking distance will exceed acceptable levels which may lead to increased stopping distances.

- The distribution of braking distances for grooved pavements have less variance due to the fact that grooved pavements exhibit relatively less changes in skid number for different speeds and water film thicknesses compared to smooth pavements as seen from the simulation results (*see* Figure 5.2).

The calculated results represent the worst case scenario as it has not factored in additional braking available for the aircraft by use of reverse thrust and anti-skid braking systems, etc. and a smooth tire is considered in the analysis. Nevertheless, the results clearly demonstrate the relative effectiveness of grooving on aircraft braking distances in wet weather operations.

5.5 Summary

This chapter presents an analytical approach to evaluate the beneficial effects of runway grooving on aircraft braking distances under wet pavement conditions. Instead of relying on experimental evidence, this chapter makes available an analytical approach to evaluate the beneficial effect of runway grooving on aircraft braking distances under wet weather operating conditions. It offers a valuable analytical tool for pavement groove designs and evaluation. The proposed method employs a mechanistic based approach and uses finite element simulation to evaluate aircraft wet-pavement skid resistance on grooved pavements. It incorporates the effects of the key factors such as water film thickness, wheel load, pressure, and surface condition into the analysis of skid resistance and braking distance.

Skid resistance variations with the various factors such as speed, weight, water film thickness, surface condition are accounted for in the analysis of braking distance.

The analysis considers the probabilistic nature of aircraft operational characteristics such as touchdown speed and landing weight. The beneficial effects of grooving are represented by comparing the braking distances on an un-grooved pavement. The comparison between the results for un-grooved and grooved pavements with different groove depths clearly demonstrates that grooving significantly reduces the braking distances. This is especially significant at high water film thicknesses where braking distances are reduced by up to 40%.

The results for different groove depths demonstrate the change in runway pavement frictional characteristics with groove depth. This can be a case in practice where groove depth reduces over time due to rubber deposits, pavement deterioration etc. The distribution of braking distances at each water film thickness provides a good indicator of the relative risks of aircraft overrun accidents under those conditions. This procedure enables one to better understand the various factors that affect runway friction and aircraft braking distance which can be useful in decision making to improve runway safety.

TABLE 5.1 Comparison of Measured and Computed Footprint Dimensions

	Experiment	Simulation	Error
Width (mm)	330.2	311.5	-3.1%
Length (mm)	558.8	518.4	-7.2%

TABLE 5.2 Comparison of Experimental and Computed Skid Resistance Values

	Experiment	Simulation	Error
Case 1: concrete surface - grooved 0.25” wide x 0.25” deep x 1” spacing	42.5	44.6	+2.1
Case 2: concrete surface - grooved 0.375” wide x 0.25” deep x 1” spacing	45.9	47.1	+1.2
Case 3: concrete surface - un-grooved	4.7	8.1	+3.4

Note: Test parameters: 49 x 17 Type VII Smooth aircraft tire, wheel load = 30,000 lbs (13620 kg), tire inflation pressure 170 psi (1,173 KPa), average water film thickness = 6.35 mm, and speed of the skidding tire =100 knots (52 m/s)

TABLE 5.3 Input Parameters Used for Numerical Example

Aircraft Type : Commercial Jet Aircraft	
Main Gear Type	Dual
Landing weight used for analysis	62000 kg
Wing Area	160m^2
Air density	1.224 kg/m^3
Tire Properties	
Tire size	49 x 17 Type VII
Pressure	1200 KPa
Touchdown speed (m/s)	Normal distribution: Mean = 61, Standard Deviation = 5.5
Dry runway friction coefficient	0.55

TABLE 5.4 Average aircraft landing braking distances

Pavement type	Water film thickness		
	1mm	**5mm**	**10mm**
Smooth	656	924	1218
Grooved -3mm	536	658	908
Grooved -6mm	507	587	741
Grooved -10mm	481	524	638

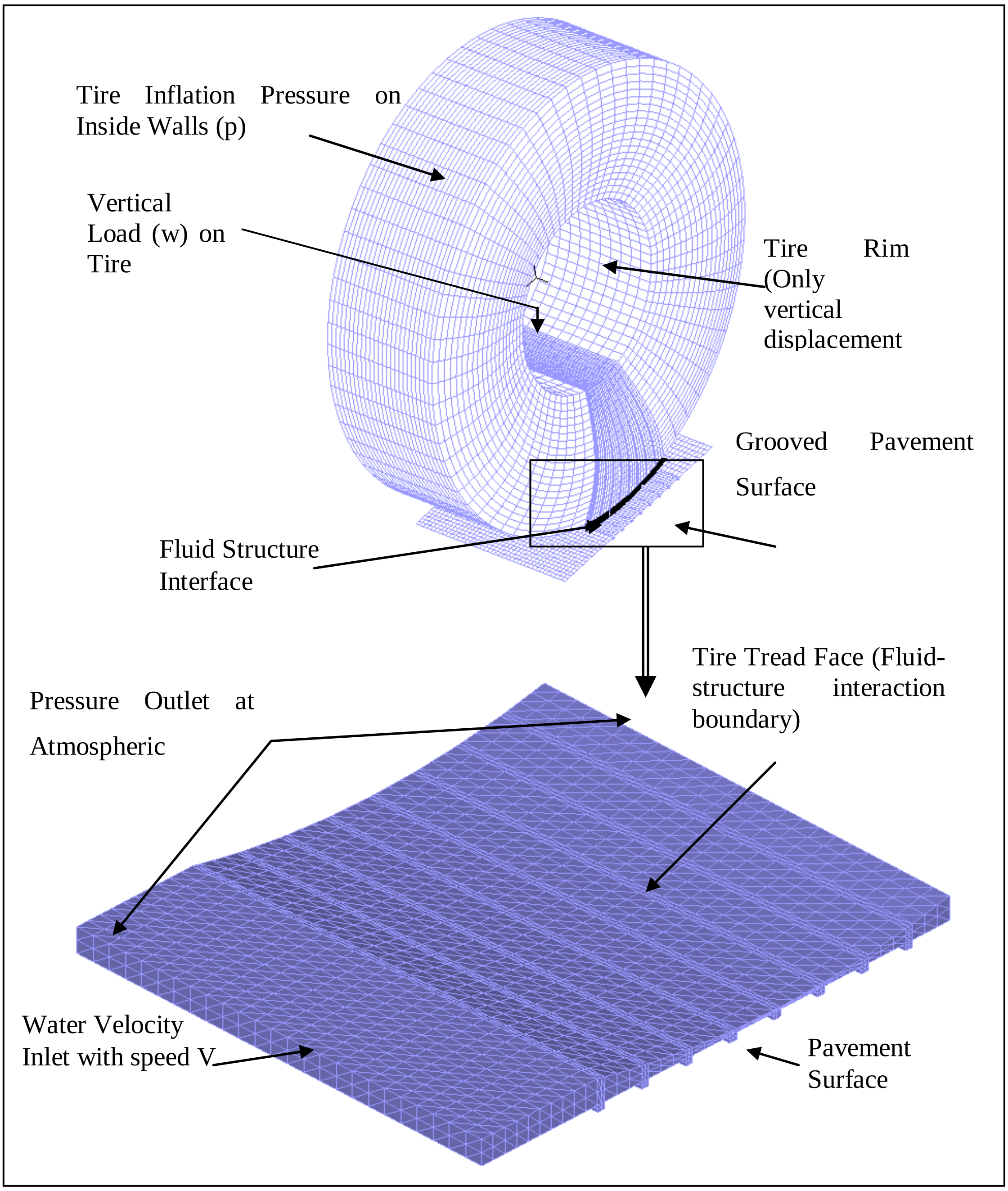

FIGURE 5.1 Finite-element model of aircraft tire and grooved pavement surface

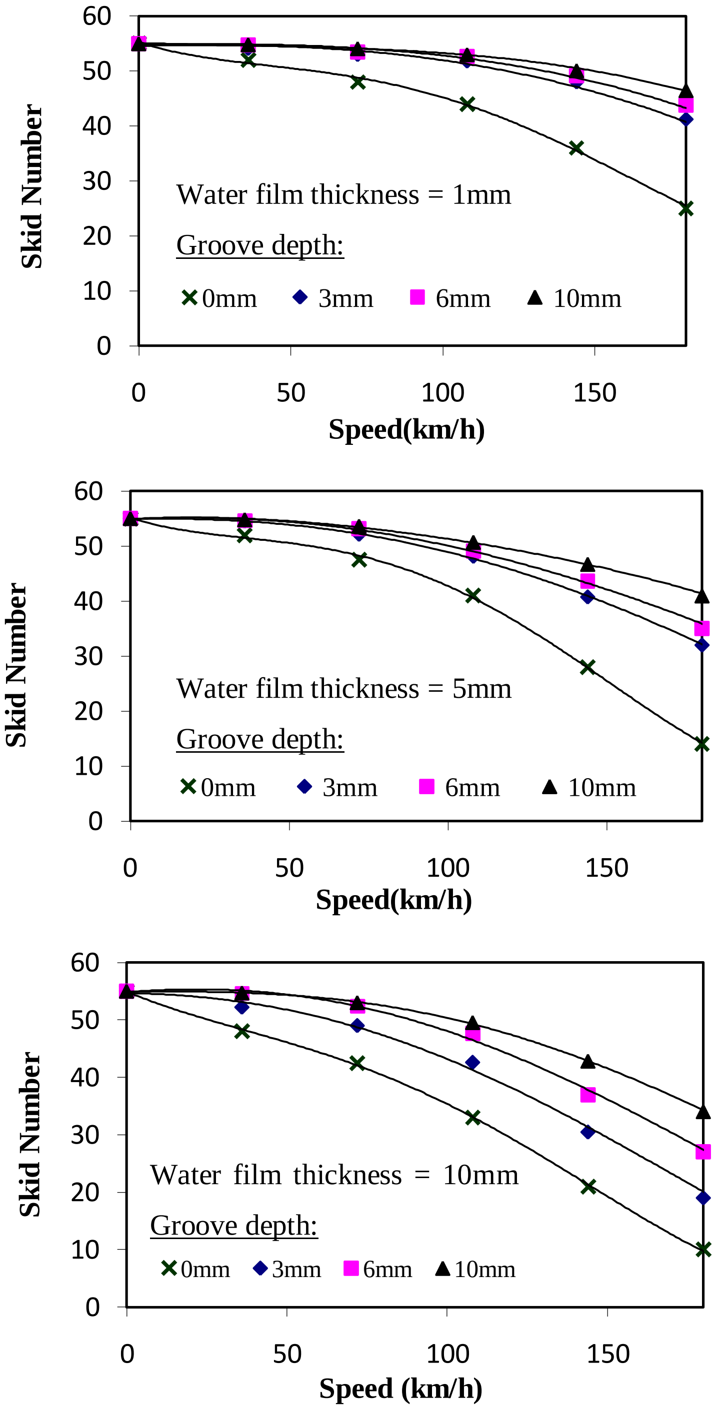

Note: Test parameters: 49 x 17 Type VII Smooth aircraft tire, tire inflation pressure 1,200 KPa, Static coefficient of friction = 0.55, Wheel load = 100kN

FIGURE 5.2 Effect of pavement grooving on skid resistance

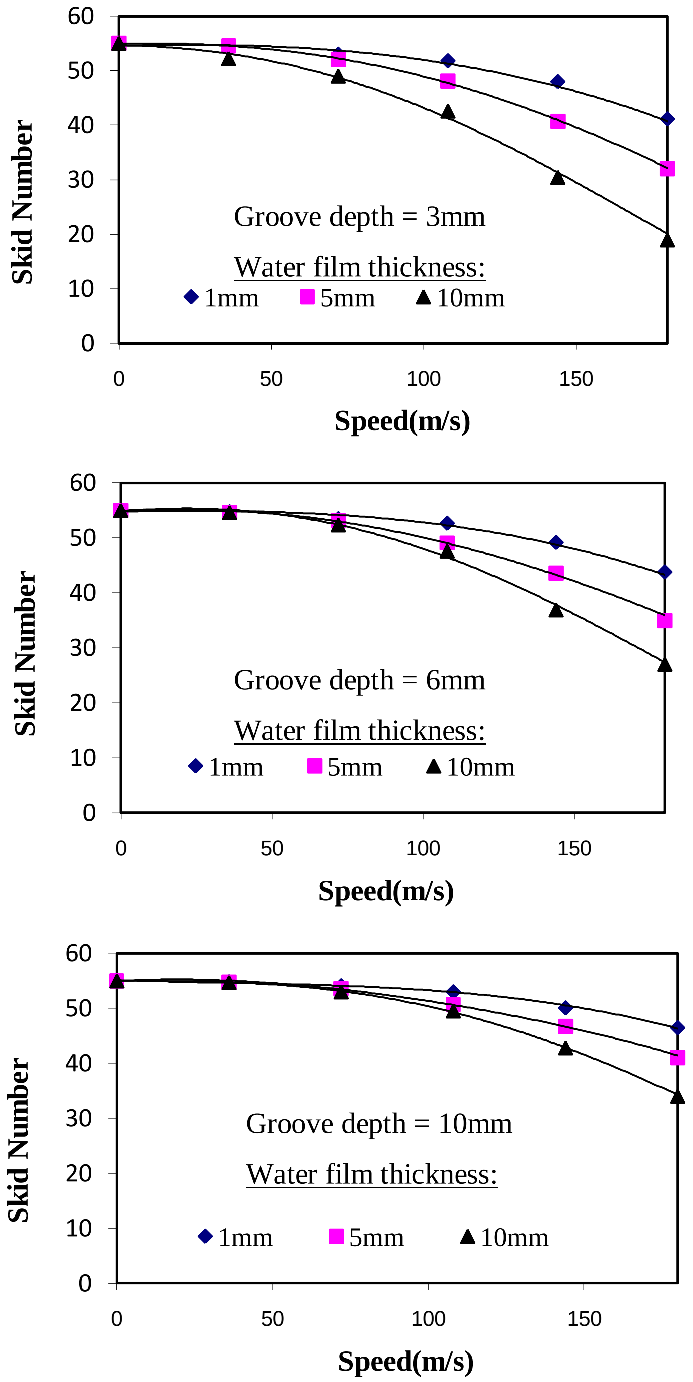

Note: Test parameters: 49 x 17 Type VII Smooth aircraft tire, tire inflation pressure 1,200 KPa, Static coefficient of friction = 0.55, Wheel load = 100 kN

FIGURE 5.3 Effect of water film thickness on grooved pavement skid resistance

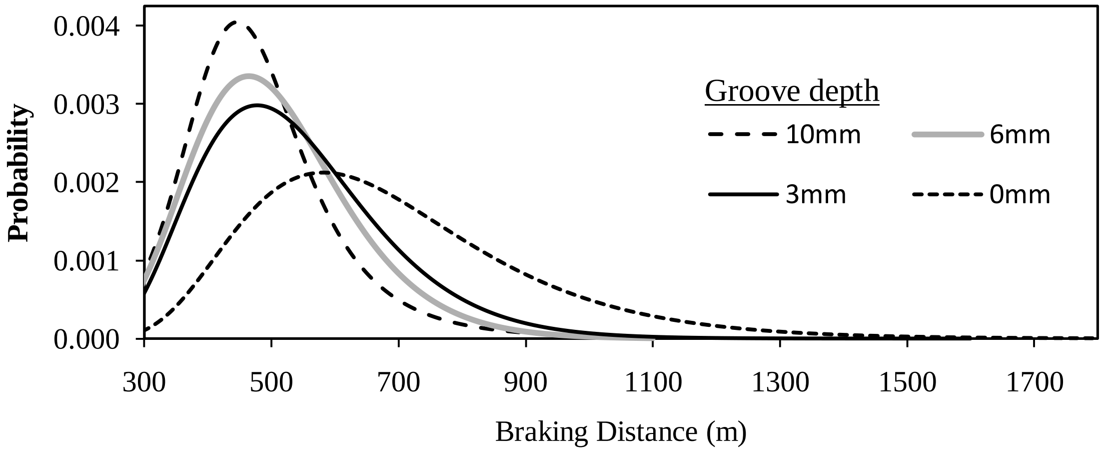

(a) 1mm water film thickness

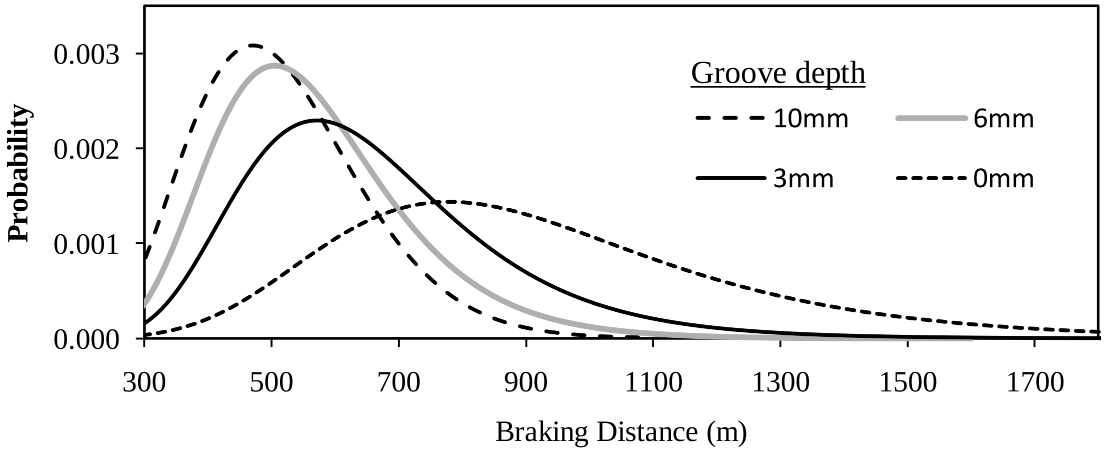

(b) 5mm water film thickness

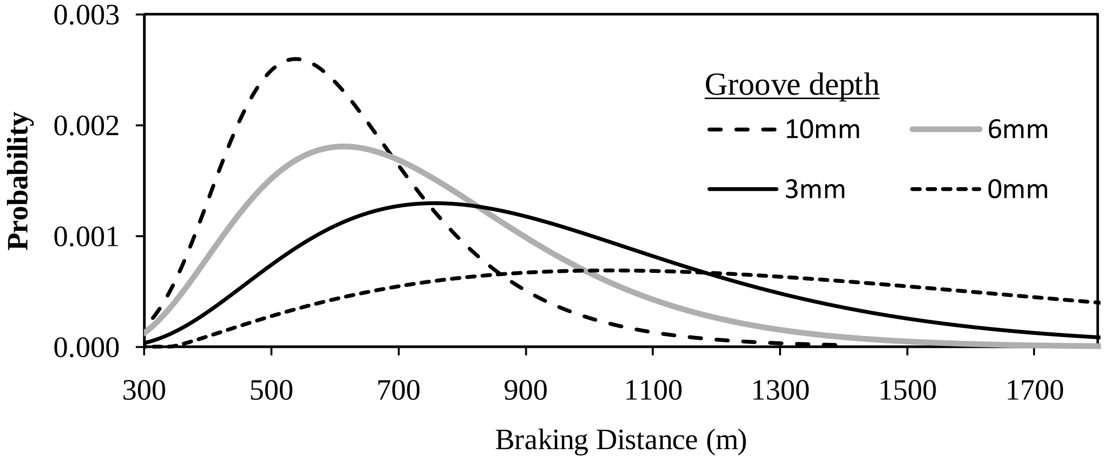

(c) 10mm water film thickness

FIGURE 5.4 Aircraft braking distances for example problem
(a) 1mm (b) 5mm and (c) 10mm water film thickness

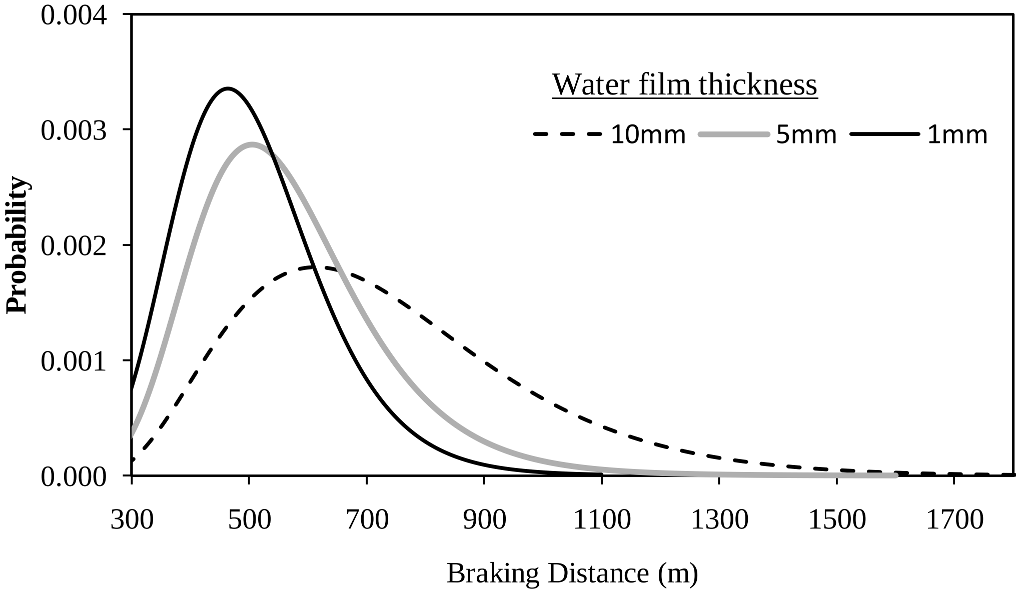

FIGURE 5.5 Comparison of aircraft braking distance distributions for grooved pavement with 6mm groove depth for different water film thicknesses

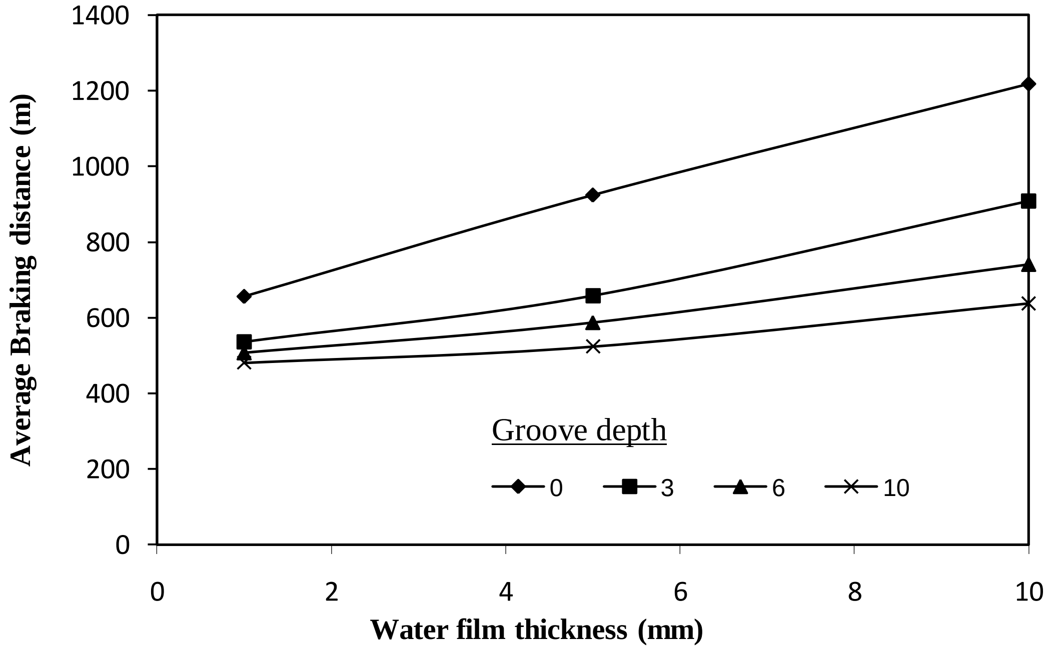

FIGURE 5.6 Average aircraft landing braking distances on grooved pavements

CHAPTER 6 RISK BASED CRITERIA FOR MAINTENANCE MANAGEMENT OF RUTTING

6.1 Introduction

This chapter aims to establish quantitative engineering criteria as a basis for determining the critical rut depth threshold for pavement maintenance and rehabilitation. It proposes an analytical approach, based on solid mechanics and hydrodynamics theories, to evaluate the hydroplaning potential and loss of skid resistance of a vehicle traveling along the flooded ruts of a road pavement. By performing this evaluation for different rut depths, an assessment of the relative severity levels of different rut depths with respect to hydroplaning as well as braking distance requirement can be made. The analysis is first applied for the case of road vehicles (as presented as Part I in Section 6.2), to establish the validity of the approach. In Section 6.3 of this chapter it is extended to assess rutting on runway pavements.

6.2 Part I: Highway Pavement Rutting

It is generally accepted that pavement rutting could lead to driving safety problems such as hydroplaning and skidding (AASHTO, 1989; Hicks et al., 2000). Unfortunately, there does not exist any quantitative engineering basis for detemining the rut depth threshold for pavement maintenance or rehabilitation. As a result, practically all highway agencies classify rut severity based on engineering judgment or past practical experience for the purpose of pavement maintenance and rehabilitation. Table 6.1 shows examples of rut depth thresholds used by different highway agencies in severity level classification of ruts for pavement maintenance management. Of special interest are the rut depth thresholds for the "high severity" classification which can be considered to be a severity level that warrants maintenance treatment. It is seen from Table 6.1 that three agencies consider rut depths exceeding 19 or 20 mm to be severe enough to justify a "high severity" classification; two agencies assign "high severity" to rut depths exceeding 25.4 mm, one agency to rut depths exceeding 38 mm, and one agency to rut depths exceeding 50.8 mm. These examples clearly suggest that there exist differences in engineering judgment among the different agencies regarding severity classification of ruts. Therefore, the establishment of a quantitative engineering basis for severity classification of ruts will be useful in offering a rational explanation and reconciling some of these differences.

The absence of a sound engineering criterion for determining the critical rut depth threshold for pavement maintenance and rehabilitation is unsatisfactory especially when driving safety is involved. It is also unsatisfactory from a pavement management perspective. By relying on engineering judgment, it presents an uncertainty as to whether the scheduled timing for pavement maintenance and rehabilitation treatments of rutting is ideal or appropriate or not for different road designs, road classes and pavement types. Therefore, it is desirable to establish an analytical engineering basis for assessing the severity of rut depth based on the consideration of driving safety.

6.2.1 Basis for Proposed Risk Based Approach

Following major experimental research efforts by pavement engineering researchers starting from the 1950s, it is now a common knowledge that the skid resistance and hydroplaning speed (i.e. the vehicle speed at which hydroplaning occurs) on a pavement are dependent on the following main factors (Horne and Dreher, 1963; Horne, 1969; Huebner et al., 1986):

- Pavement factors: pavement properties such as mix design and aggregate type, and pavement surface microtexture and macrotexture.
- Vehicle factors: vehicle speed, wheel load, tire inflation pressure, tire slip ratio, tire tread pattern and depth
- Environmental factors: water-film thickness on pavement surface, temperature.

It is thus apparent that, on a given pavement with a known rut depth filled with water, the skid resistance characteristics and hydroplaning potentials of the pavement are dependent on the operating vehicle speed and pavement surface characteristics. This means that for a given rut depth, pavement sections belonging to different highway classes (hence different prevailing operating speeds) or having different pavement micro- and macro-texture will have different skid resistance characteristics and hydroplaning potentials. In other words, based on the considerations of skid resistance (i.e. braking distance) and hydroplaning risk, the critical rut depth for different pavement sections may not be the same. That is, different road sections of a highway with either different pavement mix designs, or different design speeds or posted speeds, will have different critical rut depths. Thus, the traditional method of using the same set of critical rut depths for all pavement sections in a road network is not ideal for effective handling of rutting maintenance.

To overcome the above-mentioned limitation, an analytical procedure for evaluating the skid resistance (i.e. braking distance) and hydroplaning risk must be developed to take into consideration the various pavement, vehicle and environmental factors identified earlier. This will enable the highway maintenance agency to determine the critical rut depth threshold for each pavement section. This is the main aim of the proposed procedure presented in this chapter.

The finite element simulation model to evaluate the tire-pavement-fluid interaction presented in Chapter 3 will be adopted for this study.

6.2.2 Determination of Critical Rut Depth Threshold

For a car traveling at a given speed of the road section analyzed, the critical rut depth is considered to be reached when one of the following two events takes place: (i) hydroplaning of any of the tires of the vehicle; and (ii) the length of braking distance exceeds the design braking distance.

Critical Rut Depth Threshold based on Hydroplaning Consideration

As explained in the preceding sections, the simulation analysis produces hydroplaning speed as one of its outputs. Using the simulation model, one can vary the rut depth to obtain the hydroplaning speeds for different rut depths. The rut depth that gives a hydroplaning speed equal to the maximum allowed travel speed on the road section is the critical rut depth for that road section based on the consideration of hydroplaning.

Critical Rut Depth Threshold based on Braking Distance Consideration

In accordance with the law of motion, for a vehicle traveling at a speed of v, the braking distance required on a road with a constant friction coefficient and a highway grade is given by Equation (6.1).

$$\text{Braking Distance } D = \frac{(V_0)^2}{a} = \frac{(V_0)^2}{(\mu + G)g} \tag{6.1}$$

where V_0 is the initial vehicle speed when the brake is applied, a the rate of deceleration, μ the friction coefficient, G the highway grade, and g the acceleration due to gravity.

It is known that when a vehicle slides on a wet pavement, the skid resistance increases as the sliding speed reduces (Hayes et al., 1983; Horne and Joyner, 1965). This relationship between vehicle speed v and skid resistance μ can be obtained from the simulation analysis described in the preceding section. Hence, we have

$$\mu = h(v) \tag{6.2}$$

and $$a = (\mu + G)\, g = f(v) \tag{6.3}$$

The braking distance can then be calculated as

$$D = \int_{v=V_0}^{v=0} \frac{v}{a}\, dv = \int_{v=V_0}^{v=0} \frac{v}{f(v)}\, dv \tag{6.4}$$

In this study, the braking distance as defined in Equation 6.4 is computed by means of numerical integration method.

For a given rut depth, the simulation program described earlier can generate the skid resistance for all speeds up to the hydroplaning speed. Setting V_0 in Equation 6.4 as the maximum allowed travel speed of a road section, one can calculate the braking distance corresponding to a given rut depth. By varying the rut depth, the required braking distances for different rut depths can be calculated. The rut depth that gives a braking distance equal to the design braking distance is the critical rut depth for the road section based on the consideration of braking distance.

6.2.3 Numerical Illustration

To illustrate the application of the proposed approach to determine the critical rut depths for pavement maintenance management, a numerical illustration is presented in this section for the basic case involving the ASTM standard ASTM E501 rib tire (ASTM, 2008) with 1/16 in. (1.6mm) tread depth. This tread depth corresponds to the legal minimum allowed for passenger car tires in most states in the United States and Europe (Blythe and Seguin, 2006; Bullas, 2004). The critical rut depths thus obtained serve as a conservative reference of threshold rut depths for maintenance planning. The results of this basic case, in comparison with the common rut depth severity classifications currently adopted in practice, will also serve to demonstrate the applicability of the proposed approach for critical rut depth determination.

Problem Parameters

For illustration purposes, the analysis was performed for the following five cases of rut depths: 5mm, 10mm, 15mm, 20mm, and 25mm. This range is sufficient to cover the rut depths classified as "high severity" by practically all highway agencies. The pavement surface types considered are characterized by the following static wet-pavement friction values represented as skid number SN_0 (which is equal to $100\mu_0$): 47.5, 55, 60, 72.5 and 80. This range of pavement skid resistance values represent the surface frictional property of most in-service asphalt and concrete pavements found in practice. The values of other input parameters for the simulation analysis are as follows:

- Tire sub-model: Consider ASTM standard E501 rib tire (ASTM, 2008) with a tread depth of 1.6mm, wheel load of 4,800 N, and tire inflation pressure of 165.5 kPa; the elastic moduli and Poisson's ratios for the tire rim, tire sidewalls, and tire tread are 100 GPa and 0.3, 20 MPa and 0.45, and 100 MPa and 0.45, respectively. The density of the rim material is 2,700 kg/m^3, and that of the rubber material of the tire sidewalls and tire tread is 1,200 kg/m^3.

- Pavement sub-model: The pavement elastic modulus is 30 GPa, Poisson's ratio is 0.15, and its density is 2,200 kg/m^3.
- Fluid sub-model: The properties of water at 25°C are considered. The density, dynamic viscosity, and kinematic viscosity of water at 25°C are 997.1 kg/m^3, 0.894x10^{-3} N-s/m^3, and 0.897x10^{-6} m^2/s, respectively.

The finite element mesh of the tire and pavement surface used in the analysis is shown in Figure 3.3.

Computed Hydroplaning Speeds and Braking Distances

The computed hydroplaning speeds for different rut depth levels are presented in Table 6.2. These values are valid for different pavement surfaces since the influence of pavement surface type (i.e. the static friction μ_0) on hydroplaning speed is practically negligible. On the other hand, the influence of μ_0 on skid resistance, and hence braking distance as given in Table 6.3, is significant. Figure 6.1 plots the computed braking distances for various rut depth - pavement friction combinations at different initial vehicles speeds. A level pavement section (G = 0) is considered in the analysis. Also shown in Figure 6.1 are the AASHTO design braking distances (AASHTO, 2004). In general, all variables being equal, the results show that as rut depth increases, the hydroplaning speed reduces (i.e. hydroplaning potential increases) and the braking distance increases.

Determination of Critical Rut Depth Threshold for Severity Classification

As explained earlier, the critical rut depth of a road section considered to be reached when either hydroplaning occurs or the required braking distance exceeds the design braking distance, whichever occurring earlier. Figure 6.2 presents these two criteria graphically. The hatched area represents the range of speeds within which hydroplaning will occur, whereas the grey area represents the range of speeds within which the required braking distance exceeds the design braking distance calculated based on the guidelines of AASHTO (2004).

Figure 6.2 shows that for the range of rut depths considered, the critical rut depth is basically governed by the braking distance criterion. The hydroplaning criterion only governs when the rut depth exceeds about 20 mm and the tire-pavement static friction μ_0 is higher than about 0.72 (i.e. SN_0 exceeds 72). For instance, for a pavement section with μ_0 equal to 0.60 and has rut depth of 10 mm, hydroplaning will occur at 81 km/h, while the required braking distance exceeds the design braking distance when the speed exceeds 67 km/h. That is, the skid resistance criterion governs the critical rut depth determination for this pavement section.

Since most highway pavements will have μ_0 values exceeding 0.60, and assuming that most vehicles will be traveling at speeds not more than 70km/h on rainy days, the results of Figure 6.2 suggest that the critical rut depth threshold would be slightly higher than 20 mm. For example, for a road section with μ_0 equal to 0.725 and a maximum allowed travel speed of 70km/h, the critical rut depth threshold is 25 mm. This critical rut depth happens to be governed by both the hydroplaning and skid resistance criteria concurrently.

6.2.4 Remark on Critical Rut Depth and Rut Depth Severity Classification

The critical rut depth threshold determined in the preceding section can be taken to be a rut depth of the “high severity” classification for pavement maintenance management. Alternatively, a highway agency can set the “high severity” classification at a rut depth slightly below the critical rut depth so as to allow some lead time for maintenance planning before the rut depth reaches the critical level. Having established the rut depth of “high severity” classification, the corresponding rut depths for “medium severity” and “low severity” can be set by the highway agency concerned based on its own operational consideration.

It should be mentioned that the critical rut depth analysis requires the knowledge of the maximum allowed vehicle speed for the road section considered. This maximum speed logically refers to wet-weather vehicle operating conditions, and therefore is not equal to the roadway design speed or posted speed for fair weather conditions. Under wet-weather conditions, vehicles are known to be traveling somewhat lower than the design or posted speed (Kyte et al. 2001, Brilon and Ponzlet 1996, Ibrahim and Hall 1994). This information can be obtained from field surveys or past records of travel speed data.

For efficient practical application of the proposed approach, analyses can be made to compute the stopping distances for the full applicable range of SN_0 values and speeds, for the various types of pavement surfaces in the road network. A database of the stopping distances can be established. This numerical computer database may then be used to quickly obtain the critical threshold vehicle speeds corresponding to the point measurements of rut depth along the length of any given pavement section. By comparing this computed profile of critical threshold vehicle speeds with the corresponding design or posted speed of each section, locations of rutted pavement sections with design or posted speed exceeding the critical threshold vehicle speeds can be identified.

6.3 Part II: Runway Pavement Rutting

The preceding section evaluated the impact of rutting on highway friction performance and vehicle safety. This section extends the concept to the determination of critical rut depth for aircraft operations on runways.

A study on Japanese airports' pavement surface conditions showed that rut depth generally varies between 10mm and 30mm in airfield pavements: runways and taxiways (*see* Figure 6.3) (Hachiya et.al. 2008). The current practice of rut maintenance is carried out mainly based on its severity which is determined from the maximum rut depth measured. The PCI method defines rut severity as follows (ASTM, 2009):

- Low: less than or equal to 0.25 - 0.5 inches;
- Medium: 0.5 -1 inch; and
- High: greater than 1 inch.

In this system there are no clear causes given in the rut severity classification. Most airports follow similar criteria for rut severity classification as given in Table 6.4. The Pavement rehabilitation index (PRI) used in Japanese airports uses the maximum rut depth in a section to calculate PRI for that section (Hachiya et.al. 2008). PRI for a pavement section is defined as a function of crack ratio, maximum rut depth, and standard deviation of roughness. Similar to the PCI method this does not offer much insight into relative impact of different severities of rutting on pavement safety performance. It is also noted that airport pavement maintenance guidelines recommend surface distortions such as rutting and depressions to be repaired when there is an issue regarding surface drainage or friction is observed (Transports Quebec, 2002). Although the rut severity classifications used in most airports does not specifically provide the rationale for rut depth limits, the impact of rutting on aircraft safety due to water accumulation and the resulting hydroplaning risk is documented in several standards related to airport pavement management (Transport Canada, 2004; ICAO, 2004). 'ICAO: Aerodromes Annex 14' states that distortions with standing water (ponding) located near regions where they encounter landing aircrafts at high speeds can induce hydroplaning for water depth as low as 3mm (ICAO, 2004). In addition it highlights the need for further research on the significance of depth and length of pavement surface distortions relative to hydroplaning potential to provide further guidance on risks to aircraft operations.

Aircrafts operate at speeds up to 250 km/h on runways which are considerably higher than the normal operating speed of vehicles. Furthermore it is necessary to consider the speed profile of an aircraft during landing or take-off ground roll for hydroplaning risk analysis, unlike in highways where a constant speed can be assumed for vehicles travelling on a road section. Another difference is that aircraft wheel loads will vary during a ground roll depending on the uplift forces acting on it. Different aircraft models vary in their gear configurations, tire pressure, tire type and characteristics, and landing speeds etc. Within the same type of aircraft there will be variations in landing/takeoff weights. The analysis of aircraft operating characteristics on a runway for hydroplaning and skid resistance evaluation is more complex in comparison to vehicles on a highway.

6.3.1 Validation of Hydroplaning Results from the Simulation Model for Aircraft Tires

As explained earlier, hydroplaning is affected by several factors relating to aircraft physical and operating characteristics, pavement surface properties and geometric design, as well as environmental conditions. Figure 6.4 (a) and (b) show plots for hydroplaning speed vs. tire pressure and water film thickness respectively. Data was obtained from several experimental studies conducted under different conditions. Although it shows the general trend for hydroplaning speed with those variables, i.e. increasing with tire pressure and decreasing with water film thickness, there is a high degree of scatter in the plotted graph. This occurs as a result of other factors that influence hydroplaning, such as pavement characteristics (grooves, texture) and aircraft tire properties (tire type, tread grooves, wheel load etc.). Therefore to evaluate aircraft hydroplaning speeds on a rut filled with water, it would require a more comprehensive analysis considering all relevant parameters.

This section presents two key aspects of development of the hydroplaning simulation model for aircraft operations on runway: (i) the calibration of aircraft tire demonstrated using the 49x17 Type VII smooth aircraft tire, is described in Section 5.2.1. (ii) Hydroplaning speed results from the model is validated against experimental data obtained by past researchers.

Using the calibrated values for the various model parameters as given in Section 5.2.1, the validation of the model was conducted by checking the model computed hydroplaning speed values against experimental values. Measured hydroplaning speed values are available from a study conducted by Agrawal (1983) for the following conditions: 49 x 17 Type VII fully worn (smooth) aircraft tire, wheel load = 35,000 lbs (15890 kg), tire inflation pressure 140 psi (966 KPa), average water film thicknesses = 0.1 inch (2.54 mm). Hydroplaning test were conducted for smooth tires on different water film thicknesses on asphalt concrete surface and the results of the test are shown in Figure 6.5. Hydroplaning is considered to occur when the friction coefficient falls below the 0.05 as marked in the figure. The simulation results for the input parameters given above are also plotted on the graph. The simulation results show a good agreement with the experimental data.

6.3.2 Methodology for Incorporating Aircraft Tire Hydroplaning Risk into Runway Rut Maintenance Management

Evaluating Hydroplaning Speed

The first step in the methodology is to evaluate the hydroplaning speed for a given aircraft travelling over a rut. It is assumed in the analysis that the rut depth is filled with water, and hydroplaning speed is computed for a water depth equal to the maximum rut depth.

In the present analysis, rut depths of 5mm, 10mm, 15mm and 20mm are considered. These rut depths cover the normal range of rutting experienced in runway pavements. The values of the various parameters used in the analysis are given below:

- Tire sub-model: A commercial jet aircraft with 49x17 Type VII tire is considered. The range of wheel load is 100kN-150kN, and the tire inflation pressure is equal to 1150 kPa. The elastic moduli and Poisson’s ratios for the tire rim, tire sidewalls, and tire tread are 100 GPa and 0.3, 200 MPa and 0.45, and 350MPa and 0.45, respectively. The density of the rim material is 2,700 kg/m^3, and that of the rubber material of the tire sidewalls and tire tread is 1,200 kg/m^3.
- Pavement sub-model: The pavement elastic modulus is 30 GPa, Poisson’s ratio is 0.15, and its density is 2,200 kg/m^3. A smooth plane pavement surface is considered in the analysis
- Fluid sub-model: The properties of water at 25°C are considered. The density, dynamic viscosity, and kinematic viscosity of water at 25°C are 997.1 kg/m^3, 0.894x10^{-3} N-s/m^3, and 0.897x10^{-6} m^2/s, respectively.

The above mentioned input parameters are used in the finite element simulation analysis to compute the hydroplaning speeds for different wheel load-water film thickness combinations. Several wheel load values in the range from 100kN to 150kN are used in the computation of hydroplaning speed. These loads represent the expected range of wheel loads during an aircraft landing or takeoff operation, maximum value is approximated from the maximum takeoff weight of the aircraft.

Results of Analysis

The results from the analysis is given in Figure 6.6 for wheel loads 100kN, 125kN and 150kN and rut depths of 5mm, 10mm, 15mm and 20mm. The general trend is that hydroplaning speed increases with wheel load and decreases with rut depth. One of the main observations is that for a given water film thickness, the change in hydroplaning speed with wheel load is relatively low considering that wheel load changes amount to nearly 50kN (approximately 10 times the load on passenger car). This can be explained using the tire structural behavior at higher wheel loads. One of the factors that determine hydroplaning speed is tire foot print aspect ratio (FAR). Hydroplaning speed increases with higher FAR. The FAR of aircraft tires does not change considerably over the range of normal wheel loads (Tanner et. al., 1981). This explains the relatively small changes of hydroplaning speed with tire load.

6.3.3 Hydroplaning Risk Assessment for Rutting

Hydroplaning speeds computed in the preceding section form the basis for hydroplaning risk assessment for runway rutting. They are computed for different rut depths, considering the aircraft characteristics. It is known that wheel load of an aircraft will decrease with speed due to uplift forces on the aircraft. During a landing for example, the wheel loads will be a minimum at touchdown region and gradually increases as the aircraft decelerates as it approaches taxiway. Therefore at each location along the runway there will be a specific wheel load and speed for a particular aircraft movement. This wheel load value along with aircraft tire characteristics can be incorporated into the finite element model to compute the hydroplaning speed for rut.

Aircraft operating characteristics differ based on aircraft types (e.g. commercial jets, regional jet etc.), type of operation (landing, takeoff), and surface conditions (dry, wet etc.). This would mean hydroplaning potential of rut would also be different depending on the aircraft type and its operating characteristics. Hydroplaning potential of a rut given its depth and location relative to aircraft movement is evaluated. This is illustrated using an example in which the hydroplaning speeds computed earlier for the aircraft will be compared with its landing speed profile (*see* Fig 6.7). The probabilistic nature of aircraft operating characteristics on a runway is considered in this analysis. The aircraft landing speed profile is computed for the following conditions:

- Touchdown speed (normal distribution - mean 66m/s, standard deviation 5m/s),
- Touchdown location (normal distribution - mean 300m, standard deviation 50m),
- Deceleration rate is estimated based on the available runway length (runway length - touchdown distance - transition distance prior to braking) and
- Runway length = 2000m and single exit with exit speed (normal distribution - mean 10m/s, standard deviation 1m/s)

The dashed lines represent the 90% confidence interval for the mean aircraft speed variation with distance from the threshold. The variation is due to the probabilistic nature of operating characteristics such as touchdown speed and location. The hydroplaning speeds for wheel loads 150kN and 100kN are plotted in the same graph. Consider a case of the aircraft with a minimum wheel load of 100kN and a maximum wheel load of 150kN, the minimum speed at which hydroplaning can occur is for 100kN and the maximum is for 150kN. If the aircraft speed is above the hydroplaning speed for 150kN wheel load there is a definite risk of hydroplaning, and if it is above hydroplaning speed for 100kN wheel load, there could be hydroplaning risk during the initial phase of landing.

As seen in the Figure 6.7, for rut depth of 5mm hydroplaning risk occurs only for a short duration of landing ground roll unless in a situation where the wheel loads are very low. Compare that to a rut depth of 20mm, aircraft will be at risk for a much longer period. Although it is a simplified representation of aircraft speed profile during landing, it clearly shows how hydroplaning risk varies during landing for different rut depths, taking into consideration the based on probabilistic nature of aircraft operating characteristics.

6.3.4 Aircraft Braking Distance Evaluation for Rutting

As with the case of highway pavements, it is also necessary to evaluate the effect of runway rutting on aircraft braking distances during landing. In the analysis it is assumed that ruts exist throughout the section of the runway where the braking takes place. Braking distances are computed for the aircraft considered in the previous section for hydroplaning analysis. The analysis is done for rut depths of 5, 10, 15, and 20mm as well as braking speeds ranging from 200 to 250km/h.

Braking distance computation makes use of results from the skid resistance simulation analysis. The procedure for braking distance computation and skid resistance analysis described in detail in Chapter 4 is adopted in this analysis. The results from the braking distance analysis is compared with the braking distance computed, assuming a constant braking friction coefficient of 0.2. This value corresponds to the μ value used to define braking action on a runway as 'poor' according to the FAA circular on runway overruns (*see* Table 2.4) (FAA, 2007) and is used to estimate braking distance during aircraft landing (ATSB, 2008a).

The region where the braking distance for a given rut depth exceeds that calculated using $\mu = 0.2$ is represented by the darkened area in Figure 6.8. This indicates that at the given rut depth, the skid resistance available to the aircraft is equivalent or worse than $\mu = 0.2$. This analysis can be used to identify the rut depth equivalent to $\mu = 0.2$, for the input aircraft operating characteristics. For comparison purposes, two types of hatched areas are added in Figure 6.8. The darker and lighter hatched areas denote where the aircraft braking speeds exceed aircraft hydroplaning speed for wheel loads of 150kN and 100kN respectively. This enables to make an assessment on which rut depth would pose a risk to safe braking for aircrafts operating on the runway.

6.4 Summary

This chapter has presented an approach to determine the critical rut depth threshold for pavement maintenance based on the consideration of hydroplaning risk and safety requirement of braking distance. It offers a logical theoretical basis for setting the severity classification of rut depths. This is an improvement over the traditional approach of assigning rut severity classification based on engineering judgment and past experience. The critical rut depth analysis for highways clearly illustrates that if the frictional properties and maximum allowed vehicle speed along different pavement sections of a highway are not the same, their critical rut depths would also be different. The results for highways shows that a rut depth of around 20mm would pose risk in terms of hydroplaning as well as increase in braking distance beyond design limits; therefore could be classified as high severity. This is in agreement with the severity classification adopted by most highway agencies. In addition using this approach rut severity levels could be logically determined for all classes of roadways as well as roads with different frictional characteristics. This represents a refinement of the severity classification procedure with important road safety and pavement management implications.

Application of this approach to assess runway rut severity levels is a far more complicated process compared to highway. This is mainly due to the wide variety in aircraft operating characteristics (tire pressure, wheel loads, tire type, operating speeds etc.) on a runway as well as the complex nature of aircraft braking performance. For runway rut assessment, hydroplaning potential and braking distance were also used as the basis. Hydroplaning speeds were computed for input parameters related to the aircraft and for different rut depths. It is compared with expected speed profile on the runway to identify the region where a rut of a certain depth can pose hydroplaning risk. The results of the analysis can be used to identify hydroplaning risk for ruts based on its depth and location on the runway. Aircraft braking distances were calculated for different rut depths and compared with those calculated assuming a coefficient of friction equal to 0.2. The friction coefficient of 0.2 has been identified as a level below which the runway is said to have poor braking conditions. This comparison enables one to identify the rut depth which has frictional properties equivalent to $\mu = 0.2$. Both the hydroplaning risk and braking distance assessment will provide a useful tool to airport pavement engineers for maintenance prioritization and to assess risks posed by ruts to aircraft safety.

TABLE 6.1 Rut Severity Classification by Highway Agencies

Highway Agency	Low	Medium	High
Pavement Condition Index (PCI) *(Shahin 1994)*	0.25-0.5 in. (6.3-12.7 mm)	0.5-1 in. (12.7-25.4 mm)	>1 in. (>25.4 mm)
PASER Manual, Asphalt Roads (*Walker et al. 2002*)	0-0.5 in. (0-12.7 mm)	>1 in. (>25.4 mm)	>2 in. (>50.8 mm)
Washington State DOT *(WsDOT 1999*)	0.25-0.5 in. (6.3-12.7 mm)	0.5-0.75 in. (12.7-19.1 mm)	>0.75 in. (>19.1 mm)
Ohio DOT (*OhDOT 2006*)	0.125-0.375 in. (3.2-9.5 mm)	0.375-0.75 in. (9.5-19.1 mm)	>0.75 in. (>19.1 mm)
Massachusetts Highway Dept. (CMMPO 2006)	0.25-0.5 in. (6.3-12.7 mm)	0.5in-1.5in. (12.7-38.1 mm)	>1.5in. (>38.1 mm)
Ministry of Transportation and Infrastructure, British Columbia *(MTI BC 2009)*	3-10 mm	10-20 mm	>20 mm
California DOT (*Caltrans 2006*)	Schedule corrections when rut depth >1 in. (>25.4 mm)		

TABLE 6.2 Hydroplaning Speeds for Rut Depth Levels

Rut depth (mm)	Hydroplaning Speed (km/h)
5	91
10	87
15	83
20	76
25	72

TABLE 6.3 Braking Distance for Different Rut Depth Levels and Static Pavement Friction Values (SN_0)

Speed (km/h)	**40**	**50**	**60**	**70**	**80**
Design Braking Distance (m) (AASHTO 2004)	18	29	41	56	73
SN_0			**Rut Depth =5mm**		
47.5	13	22	34	53	85
55	12	19	30	47	76
60	11	17	27	43	72
72.5	9	14	23	36	62
80	8	13	21	33	57
SN_0			**Rut Depth =10mm**		
47.5	14	23	36	58	98
55	12	20	31	51	87
60	11	18	29	47	81
72.5	9	15	23	37	73
80	8	14	22	36	63
SN_0			**Rut Depth =15mm**		
47.5	14	24	38	60	99
55	12	20	33	54	90
60	11	19	30	50	85
72.5	9	16	25	42	74
80	8	14	23	39	70
SN_0			**Rut Depth =20mm**		
47.5	15	26	42	67	110
55	13	22	37	60	101
60	12	21	34	57	96
72.5	10	17	29	50	86
80	9	16	27	47	81
SN_0			**Rut Depth =25mm**		
47.5	15	27	45	72	108
55	13	23	41	66	100
60	12	22	38	62	95
72.5	10	18	32	56	85
80	9	17	30	51	80

TABLE 6.4 Airfield Pavement Rut Severity Classification Guidelines

Airport Authority/ Regulatory Organization	**Low**	**Medium**	**High**
ASTM D5340-04 Standard Method for PCI Surveys (ASTM, 2009) Examples: Washington State APMS: Pavement Management Manual (*WsDOT*) Aviation Pavement Maintenance Program (*Oregon DOA, 2007*) Gatwick Airport , London (*Reesaul, 2011*) Kuala Lumpur International Airport (*Malaysia Airports, 2011*) Hong Kong International Airport (*Li et al., 2008*)	0.25-0.5 in. (6.3-12.7 mm)	0.5-1 in. (12.7-25.4 mm)	>1 in. (>25.4 mm)
Airfield Inspection Reference Manual (*Florida DOT, 2006*)	0.25-0.5 in. (6.3-12.7 mm)	0.5-1 in. (12.7-25.4 mm)	>1 in. (>25.4 mm)
Airfield Pavement Rehabilitation Index, Japan (*Hachiya et al., 2009*)	Runway rutting classification criteria for rehabilitation A-Rehabilitation is not necessary : less than 10mm B-Rehabilitation will be necessary in the near future unnecessary: 10mm - 38 mm C-Rehabilitation is necessary immediately : greater than 38mm		
PASER Manual (*FAA, 2004*)	Pavements Ratings descriptions provide the following information on distortions (rutting): Failed - Greater than 2inches (50.8mm) Poor - 1-2inches (25.4-50.5mm) Fair - Less than 1inch (25.4mm) Good/Excellent - No distortions present		
International Civil Aviation Organization (*ICAO,2004*)	Isolated irregularities in the range of 25-30mm over a distance of 45m is tolerable It is noted that ponding with water depth of 3mm can induce aquaplaning		

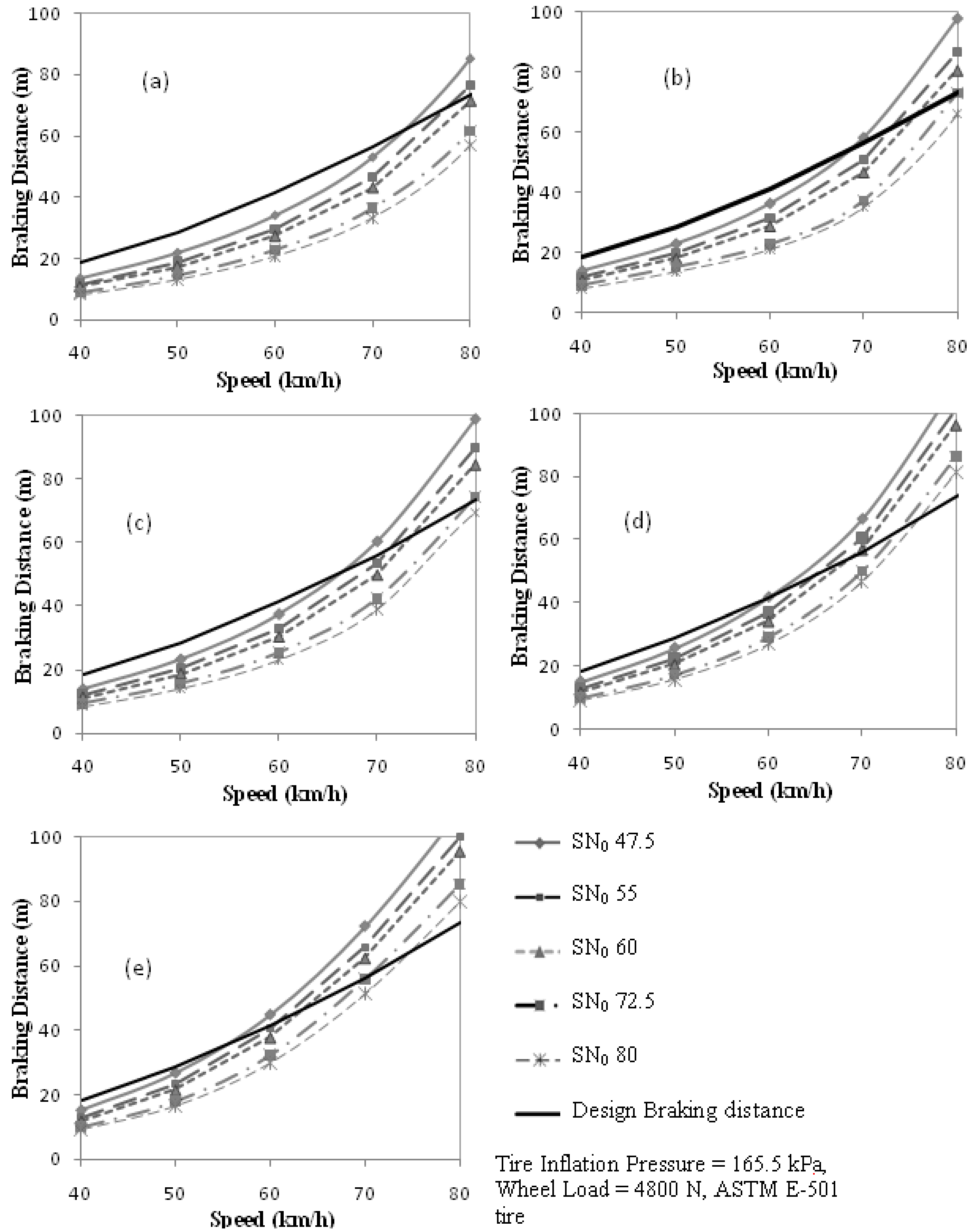

FIGURE 6.1 Braking distance variation with speed at different skid numbers for rut depths: (a) 5 mm (b) 10mm (c) 15mm (d) 20mm (e) 25mm

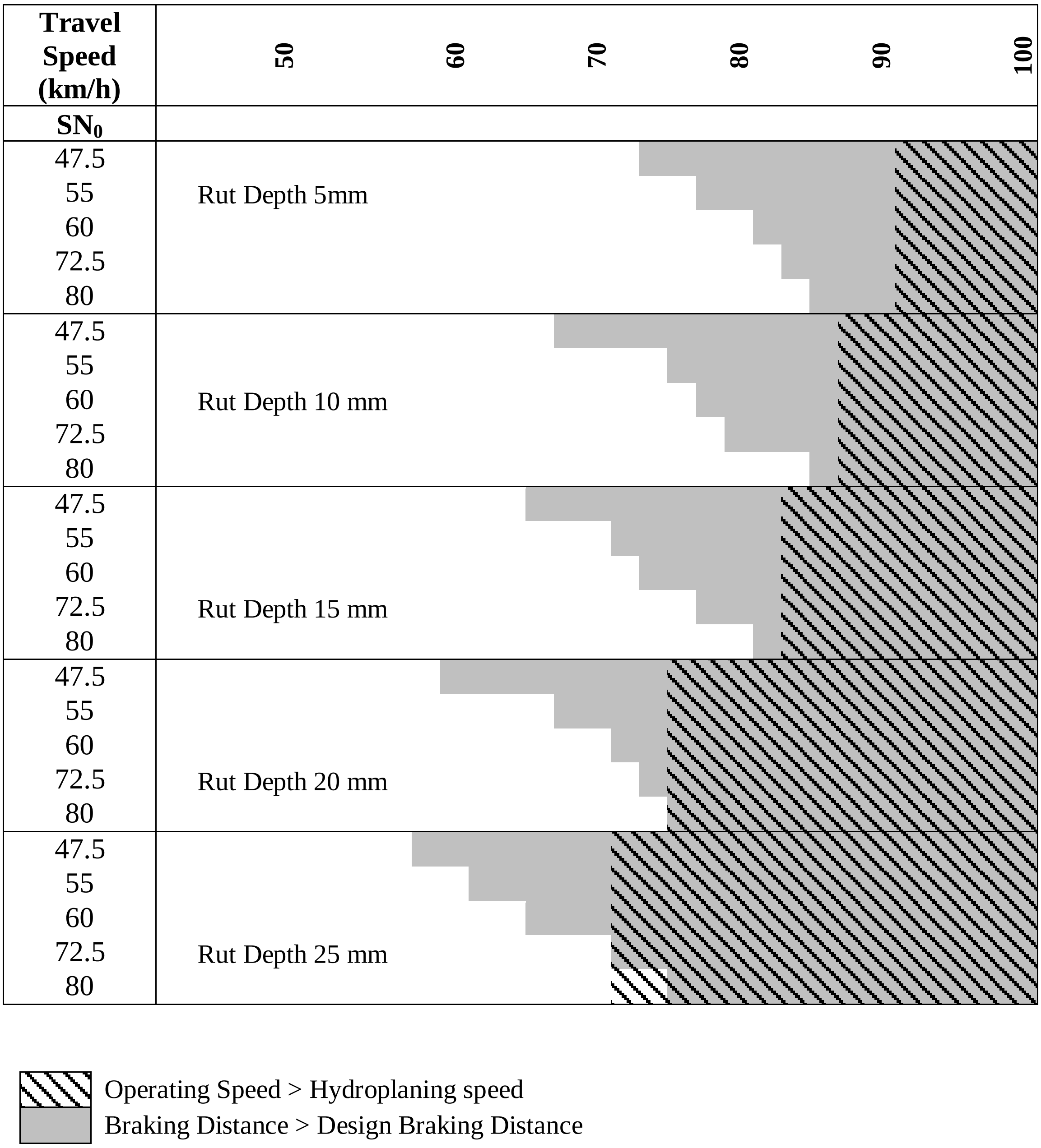

FIGURE 6.2 Governing criterion for safety assessment at different rut depths

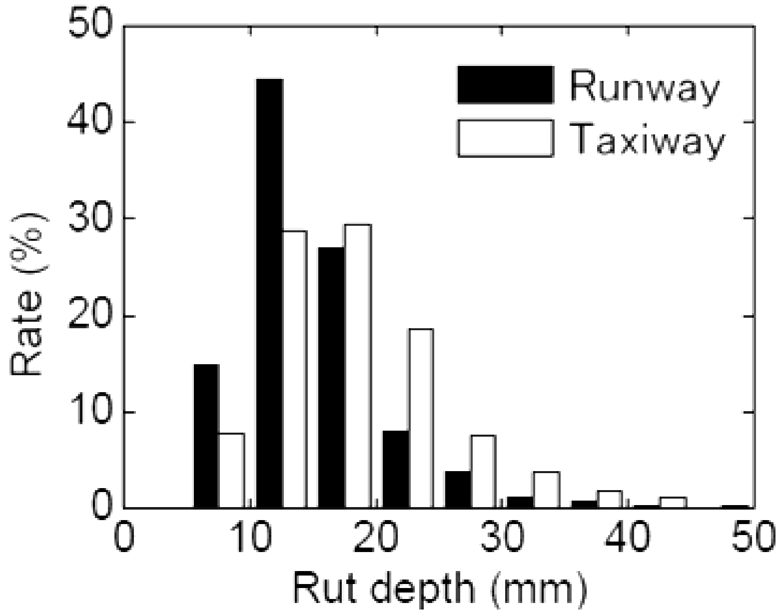

FIGURE 6.3 Distribution of rut depths in Japanese airfield pavements (Ref: Hachiya et.al. 2008)

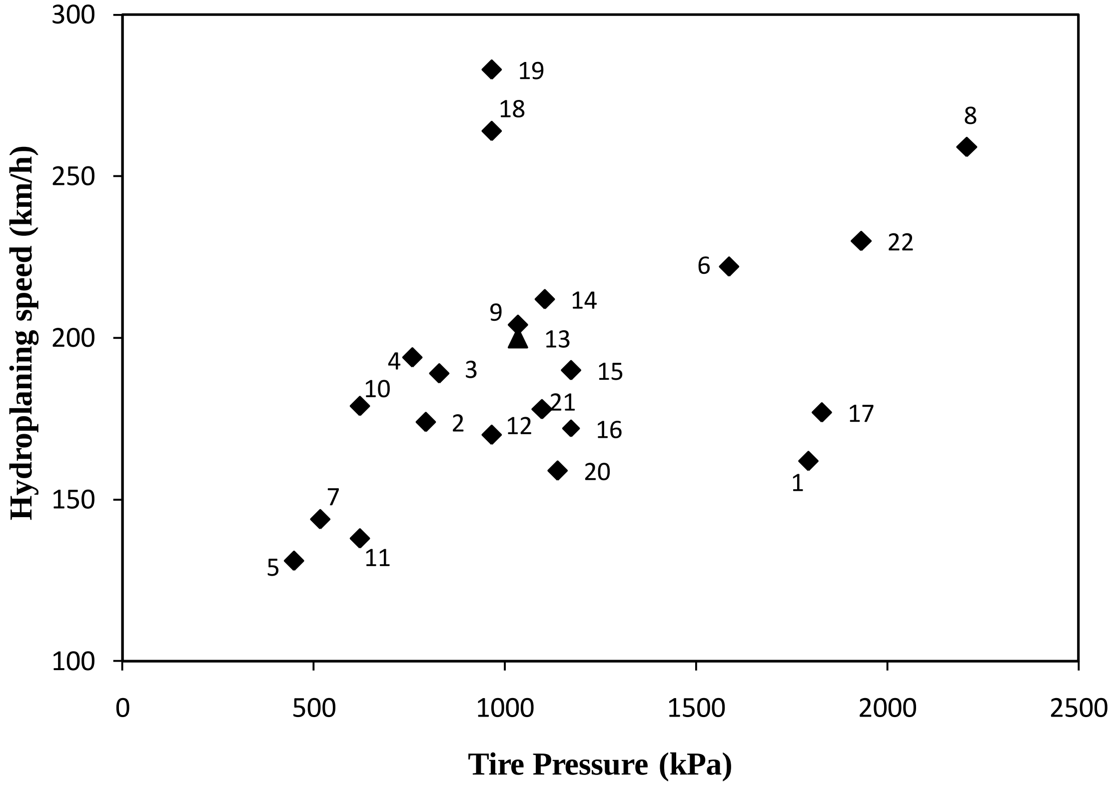

FIGURE 6.4 (a) Aircraft hydroplaning speed variation with tire pressure

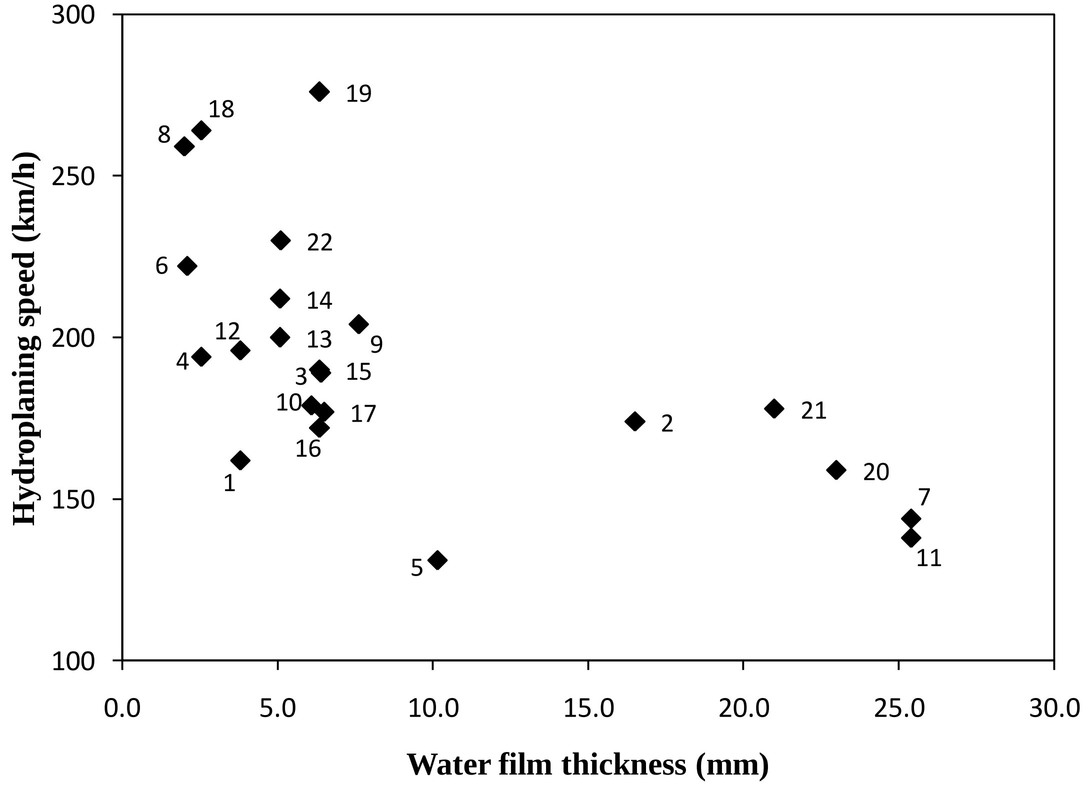

FIGURE 6.4 (b) Aircraft hydroplaning speed variation with water film thickness

FIGURE 6.4 Aircraft hydroplaning speed variation with tire pressure and water film thickness

Legend for Figure 6.4

Data Point No. in Fig. 6.4	Tire Properties	Wheel load (kN)	Tire Pressure (kPa)	Water film thickness (mm)	Hydroplaning speed (km/h)	Ref:
1	32x8.8 rib tire	44	1794	3.8	162	1
2	32x8.8 rib tire	41	794	16.5	174	1
3	32x8.8 rib tire- 5 grooves	44	828	6.4	189	1
4	44x13 Type VII rib	88	759	2.5	194	1
5	17x20 Type VII rib	44	449	10.2	131	1
6	Fighter Aircraft tires	n/a	1587	2.1	222	2
7	Dual tandem 12.5-16 Type III	98	518	25.4	144	3
8	Swift Fighter tire, rib	71	2208	2.0	259	3
9	32x8.8 rib tire	46	1035	7.6	204	3
10	32x8.8 rib tire, 5-grooves	46	621	6.1	179	4
11	32x8.8 smooth	46	621	25.4	138	4
12	32x8.8 smooth	53	966	3.8	196	5
13	32x8.8 rib tire-5 grooves	46	1035	5.1	200	5
14	41x15 TypeVIII- 5 grooves	n/a	1104	5.1	212	5
15	49x17 Type VII- 5 grooves	66	1173	6.4	190	6
16	49x17 Type VII- 3 grooves	66	1173	6.4	172	6
17	30x11.5 Type VIII- 3 grooves	66	1829	6.4	177	7
18	49x17 Type VII smooth	155	966	2.5	263	8
19	49x17 Type VII- 6 grooves	155	966	6.4	283	8
20	H36x12-18 tire	n/a	1139	23.0	159	9
21	H26.5x8-14 tire	n/a	1097	21.0	178	9
22	30x11.5 Type VIII - 3grooves	n/a	1932	5.1	230	10

References: (1) Horne and Leland, 1962; (2) Keyes, 1962; (3) Horne and Dreher, 1963; (4) Leland and Taylor, 1965; (5) Horne et.al, 1968; (6) Yager and Byrdsong, 1973; (7) Yager and Dreher, 1976; (8) Agrawal, 1983; (9) Cepic, 2004; (10) Dreher and Tanner, 1974

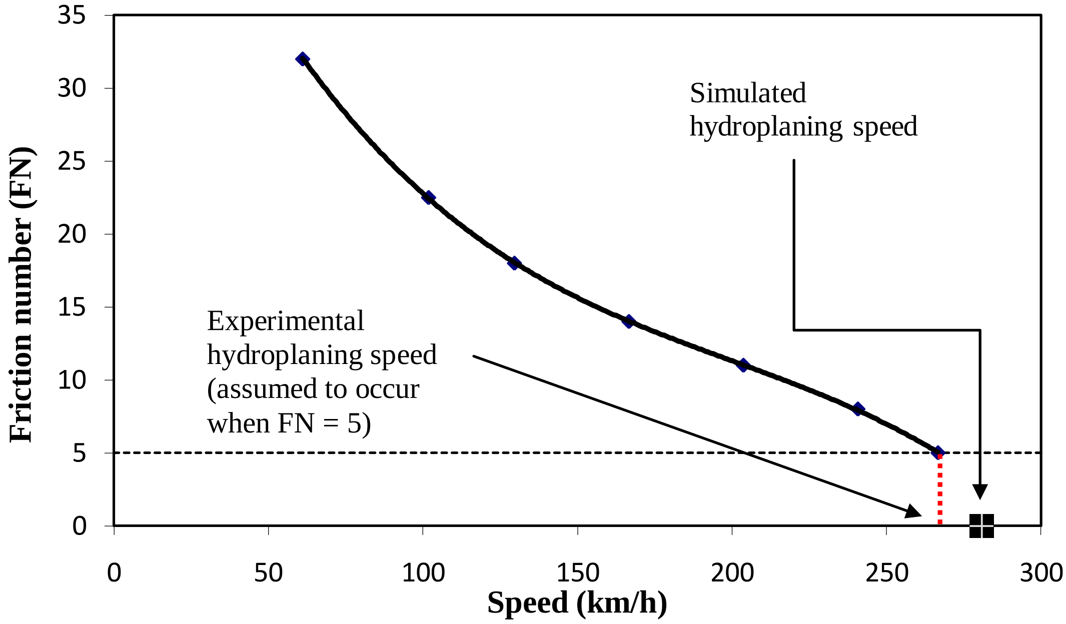

Note: Experimental results are for the following parameters: 49 x 17 Type VII fully worn (smooth) aircraft tire, wheel load = 35,000 lbs (15890 kg), tire inflation pressure 140 psi (966 KPa), average water film thicknesses = 2.54 mm

FIGURE 6.5 Hydroplaning speed results validation

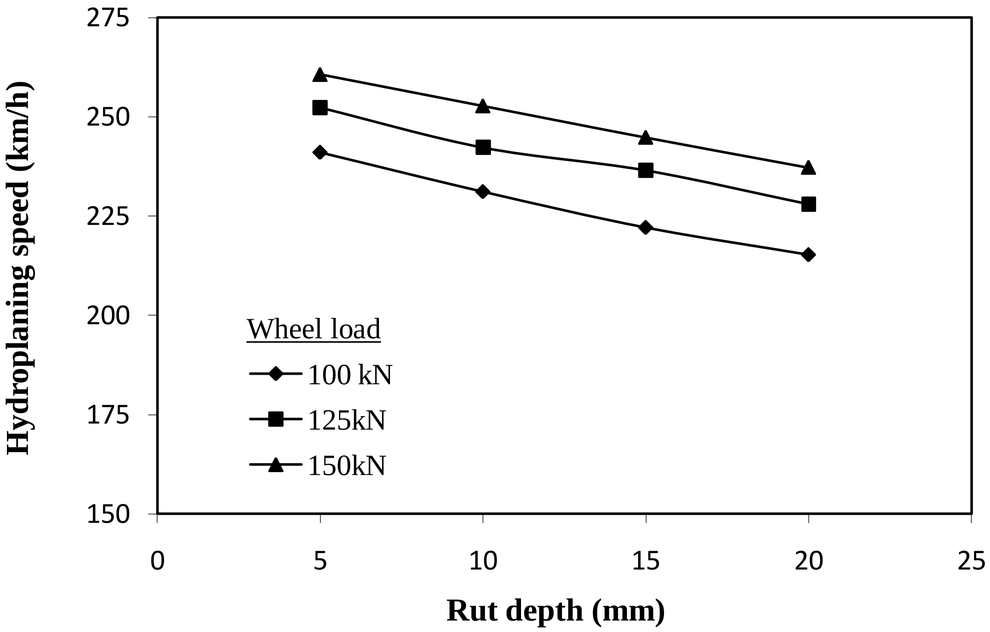

Note: Parameters used in the model - Tire type 49x17 Type VII, tire inflation pressure 1150 kPa, smooth pavement

FIGURE 6.6 Hydroplaning speed results from finite element simulation

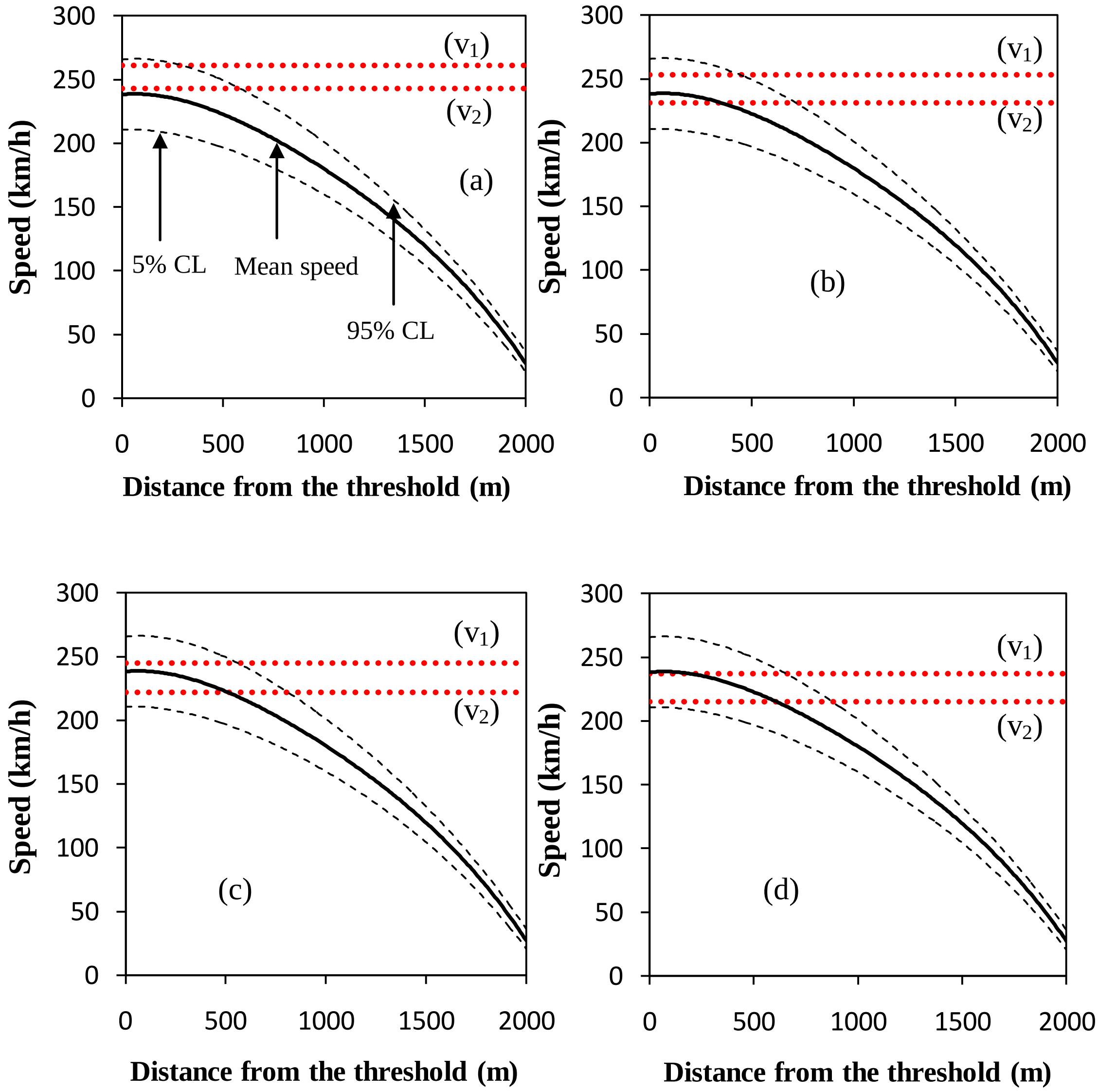

	Hydroplaning speed (km/h)	
Rut Depth (mm)	Wheel load100 kN (v_2)	Wheel load150 kN (v_1)
5	241	261
10	231	253
15	222	245
20	215	237

Note: Aircraft speed profile is computed for following parameters: touchdown speed: mean 66m/s std. dev. 5m/s; touchdown location: mean 300m std. dev. 50m; runway length 2000m with single exit, exit speed: mean 10m/s std dev 3m/s.
CL -confidence limit

FIGURE 6.7 Comparison of hydroplaning speed and aircraft speed profile for rut depths (a) 5mm, (b) 10mm, (c) 15mm and (d) 20mm.

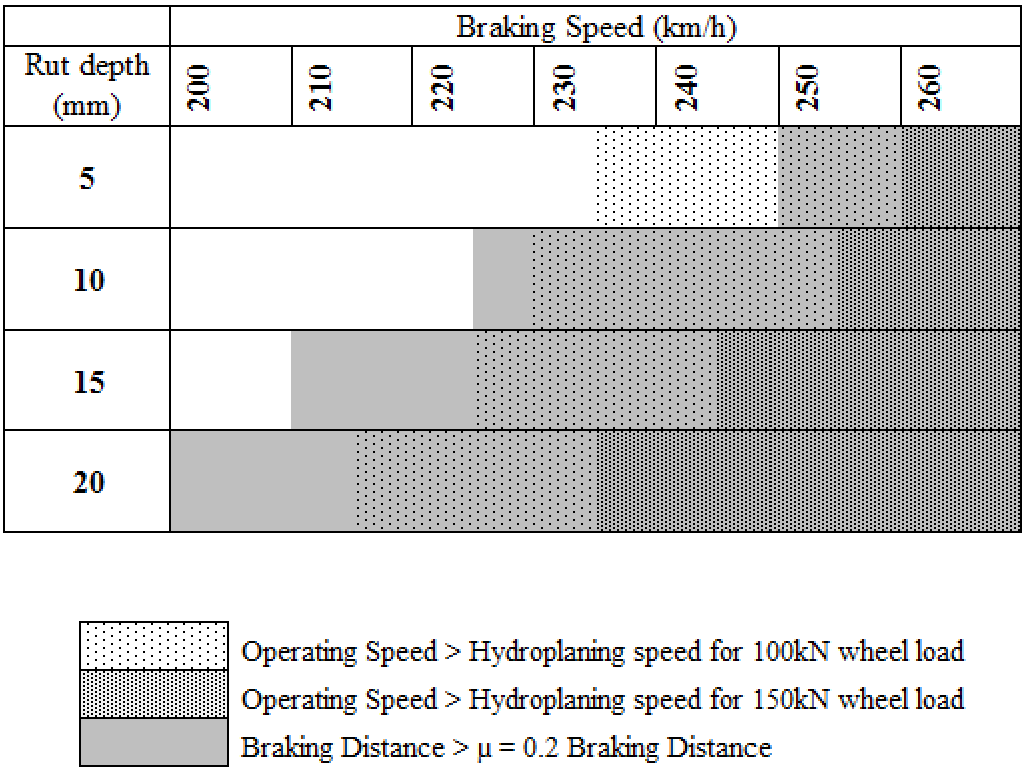

FIGURE 6.8 Braking distance evaluation for rut depths

CHAPTER 7 AIRCRAFT LANDING HYDROPLANING RISK CONSIDERATION FOR RUNWAY PAVEMENT MAINTENANCE MANAGEMENT

7.1 Introduction

Over the last decade, about 25% of the fatal accidents involving commercial jet aircrafts take place during the landing phase (Boeing, 2008). Considering that the exposure time for landing relative to the total flight time is only around 1%, aircraft landing can be considered as a highly critical phase of flight operations in terms of safety. Overruns of aircraft in landing are the 4th-largest cause of airliner fatalities worldwide from 1997-2006 (Wall Street Journal, 2007). The rate of landing overrun accidents for turbo jet aircrafts is estimated to be around 0.25 per million landings (van Es, 2005).

A major hazard aircrafts encounter during the landing maneuver is hydroplaning. As highlighted in Chapter 3, hydroplaning is a critical aviation safety issue since it results in near-zero friction between the aircraft tire and the runway pavement. It causes a loss of steering control of the aircraft, and can potentially lead to runway overruns and veer-offs. Hydroplaning of aircraft tires is known to be a contributing factor in take-off and landing overrun and veer-off accidents (van Es, 2001), and has been documented as a causal factor in 13.8% of the landing overrun accidents worldwide (van Es, 2010) .

Recognizing the importance of ascertaining the risk of hydroplaning during wet-weather landing and the serious consequences involved in the event of an overrun or veer-off, this chapter presents a methodology to calculate hydroplaning risk for an aircraft landing on a runway during wet weather. Considering the factors affecting aircraft hydroplaning risks a probabilistic approach is the proposed to incorporate these factors in the computation of aircraft landing hydroplaning risks. A numerical example is then presented to demonstrate the application of the proposed methodology.

7.2 Factors Affecting Aircraft Hydroplaning Risk

7.2.1 Wet Weather Conditions

Rainfall intensity affects the water film thickness accumulated on runway pavements, while rainfall duration influences the exposure period towards hydroplaning risk. van Es et al. (2001) analyzed aircraft landing and takeoff operations and their corresponding weather conditions at selected European airports and found that about 24% of the runway operations took place under wet or contaminated conditions. In other words, there is a significant exposure to wet weather conditions that could contribute to poor pavement surface friction and possibly hydroplaning, should the runway be inadequately designed. The rainfall intensity and duration have a major effect on hydroplaning risk during aircraft landing. The local intensity-duration-frequency (IDF) curves should be used to predict the probability of rainfall duration and intensity in the risk assessment process.

For a given rainfall intensity, the water-film thickness at any point along the runway width can be determined using the empirical model developed by Gallaway et al. (1971) as follows:

$$t_x = \left(\frac{0.01485\ MTD^{0.11} L_x^{0.43} I^{0.59}}{S^{0.42}} \right) - MTD \qquad (7.1)$$

where t_x is the water-film thickness in mm at point x, L_x the flow length in m which is equal to the distance of point x from the runway centerline, I the rainfall intensity in mm/h, S the flow path slope in m/m, and MTD the mean texture depth of the pavement in mm.

7.2.2 Runway Geometry and Pavement Surface Characteristics

Runway geometry factors and pavement surface characteristics known to affect hydroplaning occurrence include: runway width, cross slope and longitudinal slope of pavement, pavement surface macro-texture, and presence of grooving etc.

The width of runway affects the length of drainage path of surface water. An increase in runway width increases the drainage path length and results in higher water film thicknesses across the runway cross section. Similarly, pavement cross-slope plays an important factor in the discharge of rainfall off the runway. An increase in cross slope results in a faster discharge of water and lower water-film thicknesses across the runway width. Typical slopes recommended by the International Civil Aviation Organization are 1.5% to 2% for the transverse cross slopes and 1% to 2% for the longitudinal slopes, depending on the runway type (ICAO, 2004).

Besides the geometric design of the runway, pavement surface texture also plays an important role in runway drainage. Pavement macro-texture improves the drainage capacity of the pavement and reduces the risk of hydroplaning by providing enhanced drainage paths for water trapped between tire foot print and pavement surface. It is known from previous research studies that pavements with a larger mean texture depth has a higher hydroplaning speed and a lower hydroplaning risk (Gallaway et al., 1971). Pavement surface course can be designed with paving mixtures that produce macro-texture with a good texture depth. In addition, runway pavement can be grooved as is practiced in many airports in the United States and worldwide to improve drainage capacity.

7.2.3 Aircraft Physical and Operational Characteristics

Due to differences in aircraft physical and operational characteristics different aircraft types can have different hydroplaning speeds on a given runway. Aircraft physical characteristics include the type of aircraft, gear design and configuration, tire type and tire tread design (Agrawal, 1986). Aircraft operational characteristics refer to its touchdown speed, landing wander characteristics, landing weight, tire inflation pressure and tire tread depth. It is noted that in practice, variability exists in the aircraft operational characteristics whereas the physical characteristics (such as gear configuration and tire type of the given aircraft type) tend to remain constant. As such, this chapter assumes that hydroplaning risk is largely dependent on the aircraft operational characteristics such as variations in touchdown position, landing speed and landing weight during the aircraft landing operation for a given aircraft type.

Touchdown position variation can be defined in terms of the wander across the runway width and the longitudinal variation along the runway touchdown zone upon touchdown. Statistical distributions can be fitted to represent this variation for different aircraft types. The distribution can be used to determine the position of the main gears of a particular aircraft type during touchdown and the water film thicknesses at the corresponding locations.

Another important aircraft operational characteristic that can directly affect hydroplaning risk during landing is the touchdown speed of the aircraft. This varies for aircraft types as well as within the same aircraft type (Barnes et al., 1999). A higher touchdown speed will invariably increase the risk of hydroplaning. Similarly the landing weight also varies between aircraft types as well as within each type (Barnes et al., 1999) due to different fuel, passenger and cargo loading requirements.

7.3 Probabilistic Approach for Computing Aircraft Hydroplaning Risk

Noting that hydroplaning of aircraft tires during landing can lead to a significant loss of steering control and serious consequences of an aircraft accident, there is a need to evaluate the hydroplaning potential of an aircraft landing on a given runway. Traditionally, a deterministic computation of hydroplaning speeds for common commercial aircraft types is performed and a hydroplaning check is made to test if hydroplaning will occur. Equation (7.2) shows the hydroplaning equation developed in a series of experiments performed by the NASA Langley Research Center in the 1960s (Horne and Dreher, 1963):

$$v_p = 6.36\sqrt{p_t} \tag{7.2}$$

where v_p is the hydroplaning speed (in km/h) and p_t is the tire inflation pressure (in kPa). Hydroplaning is said to occur when the touchdown speed of a given aircraft type exceeds the NASA hydroplaning speed.

To illustrate the deterministic procedure, hydroplaning speeds for common commercial aircraft types can be computed and a test for hydroplaning occurrence can be made using typical touchdown speeds. Table 7.1 shows the computed hydroplaning speed for different commercial aircraft types using Equation 7.1 and compares them against the aircrafts' typical touchdown speeds. A deterministic interpretation of hydroplaning occurrence can be made, as shown in Table 7.1. It can be noted from Table 7.1 that the deterministic approach can only give a binary response (i.e. “hydroplane” or “no hydroplane”). This is very much due to the following limitations:

- The lack of consideration of the probabilistic nature of the many operational factors described in the previous sub-sections, and
- The lack of capability of the NASA hydroplaning equation to consider the effects of different water film thicknesses, tire and pavement surface characteristics.

In other words, the aforementioned procedure does not allow airport planners and engineers to have an idea of how much hydroplaning risk is associated with the landing of a given aircraft type on a given runway.

Recognizing the need for pavement maintenance engineers to estimate the hydroplaning risk associated with landing operations in an airport, this chapter adopted a probabilistic approach to compute aircraft hydroplaning risk analogous to that described by Ong and Fwa (2009). Noting the limitations of the NASA hydroplaning equation in evaluating hydroplaning speeds associated with different water-film thicknesses, landing weights and pavement surface characteristics, this chapter adopted the finite element hydroplaning simulation model described earlier in Chapter 3 to determine the hydroplaning speed of an aircraft. The simulation model is then incorporated within a probabilistic framework to determine the associated hydroplaning risk.

Since the occurrence of aircraft hydroplaning is probabilistic in nature, the concept of hydroplaning risk is proposed in this chapter to evaluate the probability of hydroplaning occurrence. When applied to runway operations, the hydroplaning risk of an aircraft operating under a known set of conditions on a given runway can be computed as the probability that the operating speed of the aircraft will reach or exceed its hydroplaning speed. Assuming that the probability density function $f(v)$ of the aircraft landing or taking off speed is known, the risk of hydroplaning is defined as:

$$\alpha = P\left(v > v_p\right) = 1 - F\left(v_p\right) = 1 - \int_0^{v_p} f\left(v\right)dv \qquad (7.3)$$

where v is the spot speed of the vehicle, v_p is the hydroplaning speed, $P(v > v_p)$ is the probability that the aircraft speed is higher than the hydroplaning speed, and $F(v_p)$ is the cumulative probability of a vehicle with speeds smaller than the design hydroplaning speed.

7.4 Methodology for Computation of Aircraft Hydroplaning Risk

For every aircraft type analyzed, the information on aircraft tire, aircraft load, water depth on the pavement and the pavement characteristics are required as inputs to the hydroplaning simulation model. The steps performed to determine the hydroplaning risk of each individual aircraft are described as follows.

i. Determine the landing weight probability distribution of each aircraft type i, $g_i(a)$ where a is the landing weight of the aircraft.

ii. Given the water depth distribution along the runway width $t_w(x,y)$ and the landing weight probability distribution of aircraft type i, $g_i(a)$, determine the hydroplaning speed probability distribution in the runway touchdown zone $v_p(x,y)$ by finite element simulation analysis.

iii. Determine the landing speed distribution of the aircraft type i, $f_i(v)$.

iv. Given the hydroplaning speed variation along the runway width and the landing speed distribution of the aircraft type i, determine the hydroplaning risk distribution $\alpha_i(x,y)$ associated with the aircraft type i across the runway touchdown zone.

$$\alpha_i\left(x,y\right)=P\left(v>v_p\right)\Big|_{(x,y),i}=\left[1-F\left(v\right)\right]\Big|_{(x,y),i}=\left[1-\int_0^{v_p} f\left(v\right)dv\right]\Bigg|_{(x,y),i} \tag{7.4}$$

v. Determine the wander distribution of the aircraft type $w_i(x)$ and the wander distribution for each tire j for the aircraft type i along the runway width $w_{ij}(x)$.

vi. Given the wander distribution associated with the tires of an aircraft type $w_{ij}(x)$ and the corresponding longitudinal variation along the runway during touchdown $w_{ij}(y)$, the probability distribution of the tires in the touchdown zone can be determined.

$$w_{ij}(x,y)=\left(\int_x^{x+\Delta x} w_{ij}(x)\ \mathrm{dx}\right)\left(\int_y^{y+\Delta y} w_{ij}(y)\ \mathrm{dy}\right) \tag{7.5}$$

vii. The hydroplaning risk of each tire j of a particular aircraft type i for an area Δx by Δy in the runway touchdown zone can be determined. Δx and Δy can be taken to be the width and length of the tire imprint respectively. Let $\beta_{ij}(x)$ be the total hydroplaning risk distribution of the tire j of a particular aircraft type i along the runway.

Hydroplaning risk of tire j of aircraft type i for a strip Δx along runway width

= Probability of tire j at the finite area × Hydroplaning risk of tire j at the finite area =

$$\left[\int_{x}^{x+\Delta x}\int_{y}^{y+\Delta y} w_{ij}\left(x,y\right)dxdy\right]\left[\int_{x}^{x+\Delta x}\int_{y}^{y+\Delta y} \alpha_{i}\left(x,y\right)dxdy\right] \tag{7.6}$$

viii. Determine the total hydroplaning risk associated with each tire *j* for the aircraft type *i*. The total hydroplaning risk of each tire *j* of a particular aircraft type *i*, R_{ij} is computed as follows,

R_{ij} = Sum of hydroplaning risks of all finite areas in the runway touchdown zone

$$\sum_{x,y}\left\{\left[\int_{x}^{x+\Delta x}\int_{y}^{y+\Delta y} w_{ij}\left(x,y\right)dxdy\right]\left[\int_{x}^{x+\Delta x}\int_{y}^{y+\Delta y} \alpha_{i}\left(x,y\right)dxdy\right]\right\} \tag{7.7}$$

ix. Determine the total hydroplaning risk for the aircraft type. In this chapter, hydroplaning is assumed to occur when any tire of the aircraft hydroplanes. Hence the total hydroplaning risk of aircraft type *i*, R_i is defined as:

$$R_i = \max\left\{R_{ij}\right\} \tag{7.8}$$

7.5 Computing Hydroplaning Risk - Numerical Example

This section demonstrates the application of the methodology described in the earlier section to evaluate hydroplaning risk of the commercial jet aircraft. Physical characteristics of aircrafts and landing characteristics are based on data in aircraft manufacturer's manuals and aircraft landing surveys (Boeing, 1985; Barnes et al., 1999). Table 7.2 describes the input parameters used in the study. Pavement mean surface texture depth is assumed to be zero to provide a conservative estimate of hydroplaning risks.

Based on the information provided in Table 7.2, the landing weight distribution of the aircraft and the touchdown location of the centerline of the aircraft can be determined. Figure 7.1 shows the cumulative probability density distribution of the landing weights of the aircraft considered in the probabilistic hydroplaning speed computations.

The finite element model presented in Chapter 6 is used for evaluation of hydroplaning speed. The input parameters for analysis are given in sections 6.3.1 and 6.3.2 of Chapter 6. Figure 7.2 shows the variation in hydroplaning speed along the runway width for the mean landing weight of aircraft used. It can be observed that hydroplaning speed decreases with increasing distance from the centerline of the runway. This is due to increasing water film thicknesses associated with a distance further from the runway centerline. Figure 7.2 also shows the probability distribution of $v_p(x,y)$ at x = 1 m, x =15 m and x = 30 m due to the possible variations in aircraft landing weights (Figure 7.1).

The next step in the analysis involves the determination of the touchdown location and variation in the runway touchdown zone. Figure 7.3 illustrates the probability distribution of the touchdown location of the centerline of the aircraft in the runway touchdown zone, using the information shown in Table 7.2. Based on the information given in Figure 7.3 and the gear configuration shown in Table 7.2, the probability distribution of each tire can be obtained. The water-film distribution in the runway touchdown zone can also be determined using Equation 7.1, given the runway parameters shown in Table 7.2 (*see* Figure 7.4).

The critical tire for aircraft hydroplaning (i.e. the tire most susceptible to hydroplaning) is the outermost tire in the main gear. This is because it is the tire that is most likely to be subjected to higher water film thickness. Therefore, hydroplaning risks (in steps (vi) to (viii) shown in the previous section) computations for the aircraft are computed using only the critical tire.

Hydroplaning risks for the critical tire are presented in form of risk contours. Figure 7.5 shows the hydroplaning risk contour for the critical tire in the runway touchdown zone. It can be observed that the highest hydroplaning risk remains closer to the centerline of the runway within the touchdown zone, despite higher hydroplaning potentials nearer to the runway edges. This is largely due to the higher touchdown concentration nearer to the centerline of the runway as compared to the unlikely scenario of an aircraft landing way off the runway centerline. It is to be noted that risk values presented in Figure 7.5 are conservative since pavement surface texture depths and tire tread depths are considered to be zero.

7.6 Remarks on Methodology

The methodology described in this chapter can be applied to all types of aircraft operating on the runway in the analysis period to compute the hydroplaning risk. This will enable the authorities to identify which types of aircraft are more susceptible to hydroplaning risk and how to mitigate it if necessary.

As highlighted above, the hydroplaning risk value depends on aircraft, pavement and weather factors. For each airport runway the relevant parameters for hydroplaning risk calculation may differ based on the types of aircraft operating, the climatic conditions, and runway surface characteristics. In the design of runway pavement such information will be useful. The design rainfall intensity will depend on the climatic conditions of the location and the choice of return period. The design rainfall intensity, runway cross slope, runway surface type will determine the water film thickness on the runway. Depending on the expected aircraft types in operation, the hydroplaning risks can be computed and its sensitivity to these influencing parameters (cross slope, texture depth, and rainfall intensity) can be identified.

The design selection of paving mix for construction of runway pavement wearing course has a major influence on its friction performance. The frictional properties of the aggregate and the surface texture of the pavement are key parameters to the hydroplaning and skid resistance analysis. The computed hydroplaning and skidding or overrun risk values can be used as a tool to determine the effectiveness of runway friction improvement treatments such as grooving and other surface texture improvements, rubber deposit removal etc.

7.7 Summary

This chapter has described a probabilistic-based hydroplaning risk computation aircrafts landing or takeoff on a runway during wet weathers. By considering the physical and operational characteristics of the aircraft, weather conditions, and the runway and pavement surface characteristics, hydroplaning risks for aircraft landing operations can be computed. This is an improvement over the conventional deterministic approach where only binary responses ("hydroplane" or "no hydroplane") are obtained. Through the numerical example presented in the chapter, useful information such as hydroplaning and skidding or overrun risk values and risk contours within the runway touchdown zones can be obtained. This information is useful for airport managers in runway friction maintenance management planning and the identification of appropriate preventive or mitigation measures to improve runway safety.

TABLE 7.1. Comparison of Typical Touchdown Speeds and NASA Hydroplaning Speeds for Different Aircraft Types

Aircraft Type	**Typical Touchdown Speed (knots)**	**NASA Hydroplaning Speed* (knots)**
A310	138	121
A320	135	119
A330	137	124
A340	142	123
B727	137	116
B737	133	119
B747	153	127
B757	132	117
B767	136	124
B777	138	124
MD-11	148	129
MD-87	133	122
F28	125	90
F100	130	107
ATR42	106	94
BAe748	95	83
F50	99	81
Saab340	110	97

Note : * For NASA hydroplaning speeds, pavement surface texture depth and tire tread depth are assumed to be zero, and runway is flooded with 7.62 mm of water. Hydroplaning speed values shown are conservative estimates.

TABLE 7.2 Input Parameters for Hydroplaning Risk Analysis

Aircraft Parameters		
Aircraft Type : Commercial jet aircraft		
Gear type - Dual, Percent Weight on Main Gear = 95%		
Tire Width = 17 in., Tire inflation pressure = 1165 kPa, Tire tread depth = 0 mm		
Distance to the centre of the outer wheel from aircraft centerline = 3.29m		
Distance to the centre of the inner wheel from aircraft centerline = 2.43m		
Landing Operations		
	Mean	Standard Deviation
Touchdown speed (km/h)	206	20
Touchdown location (m)	360	90
Lateral Wander (m)	0	1.7
Landing Weight (kg) Min:45359.24kg/Max:73028.37kg	63000	4125
Runway Parameters		
Runway Width = 60m		
Transverse Slope = 1.5%		
Mean Texture Depth = 0 mm		
Rainfall Intensity = 150mm		

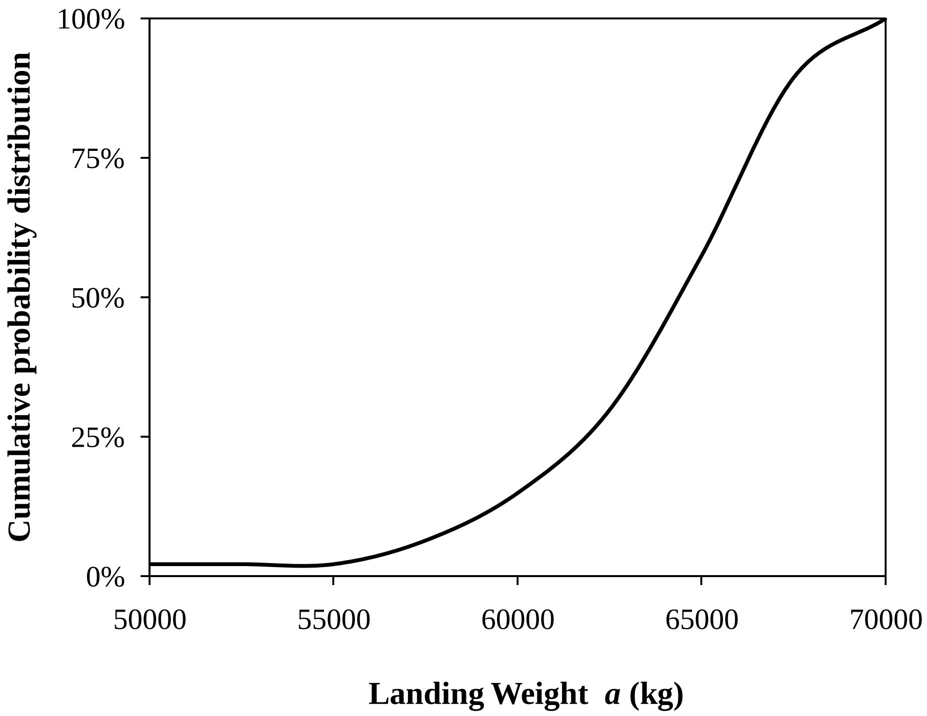

FIGURE 7.1 Cumulative density distribution of landing weight of Boeing 727-200

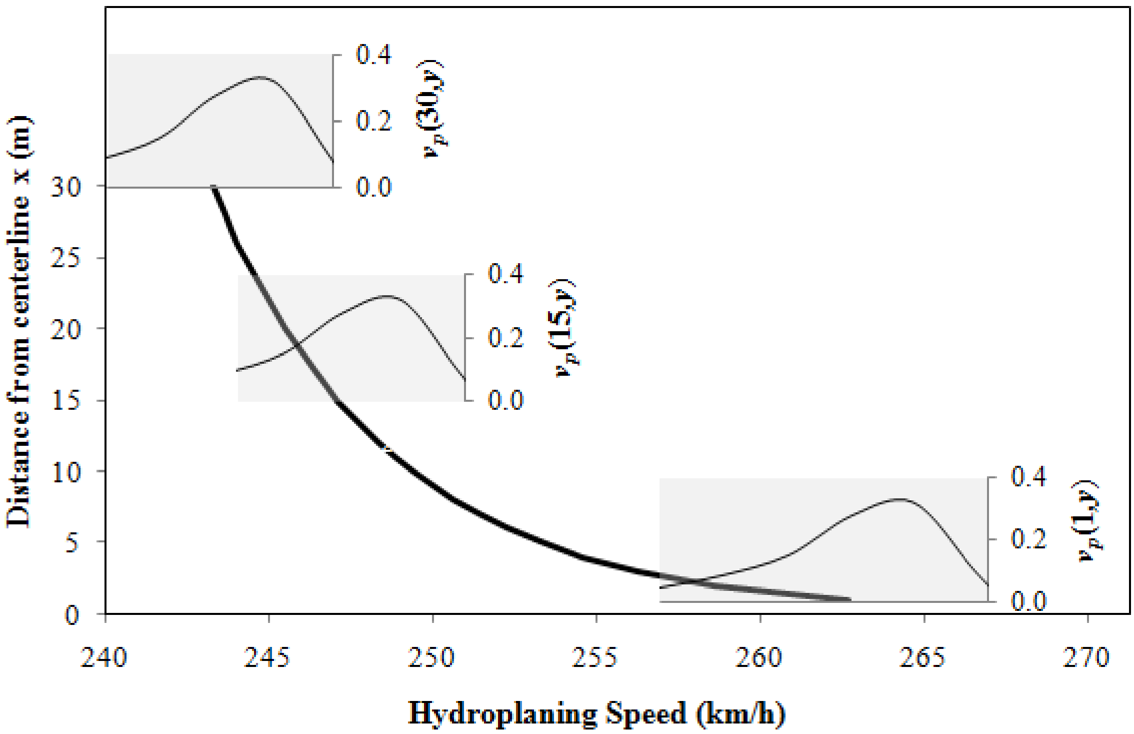

FIGURE 7.2 Hydroplaning speed variation along the runway width

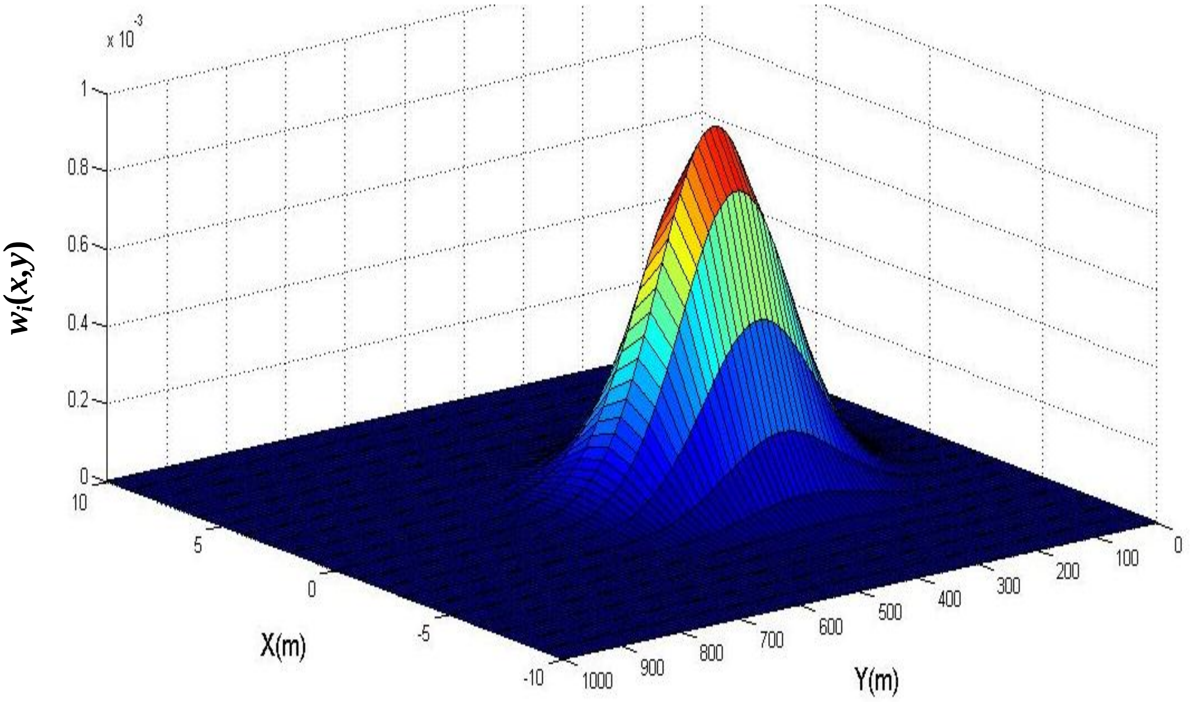

FIGURE 7.3 Probability distribution of the landing location of centerline of B727-200 aircraft

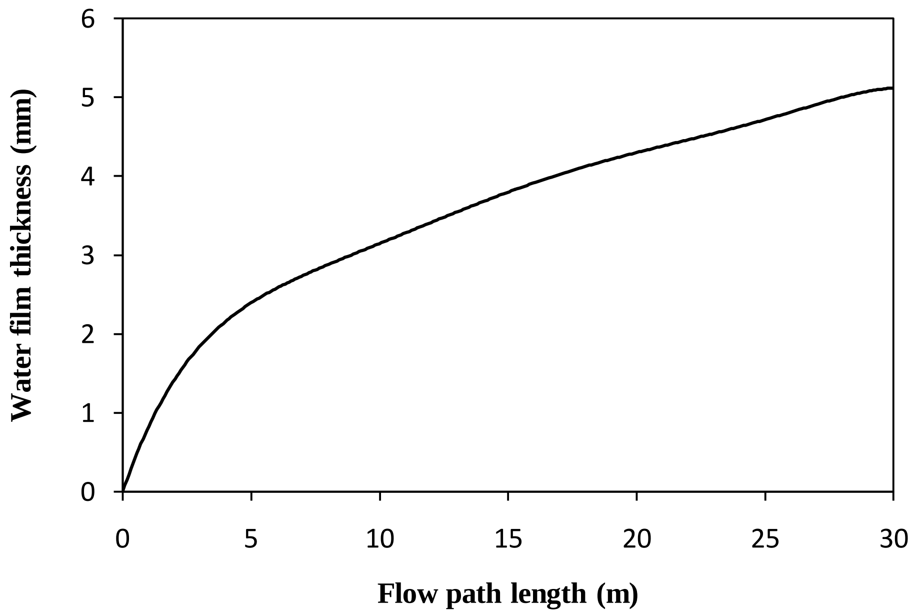

FIGURE 7.4 Water film thickness variation along the runway width

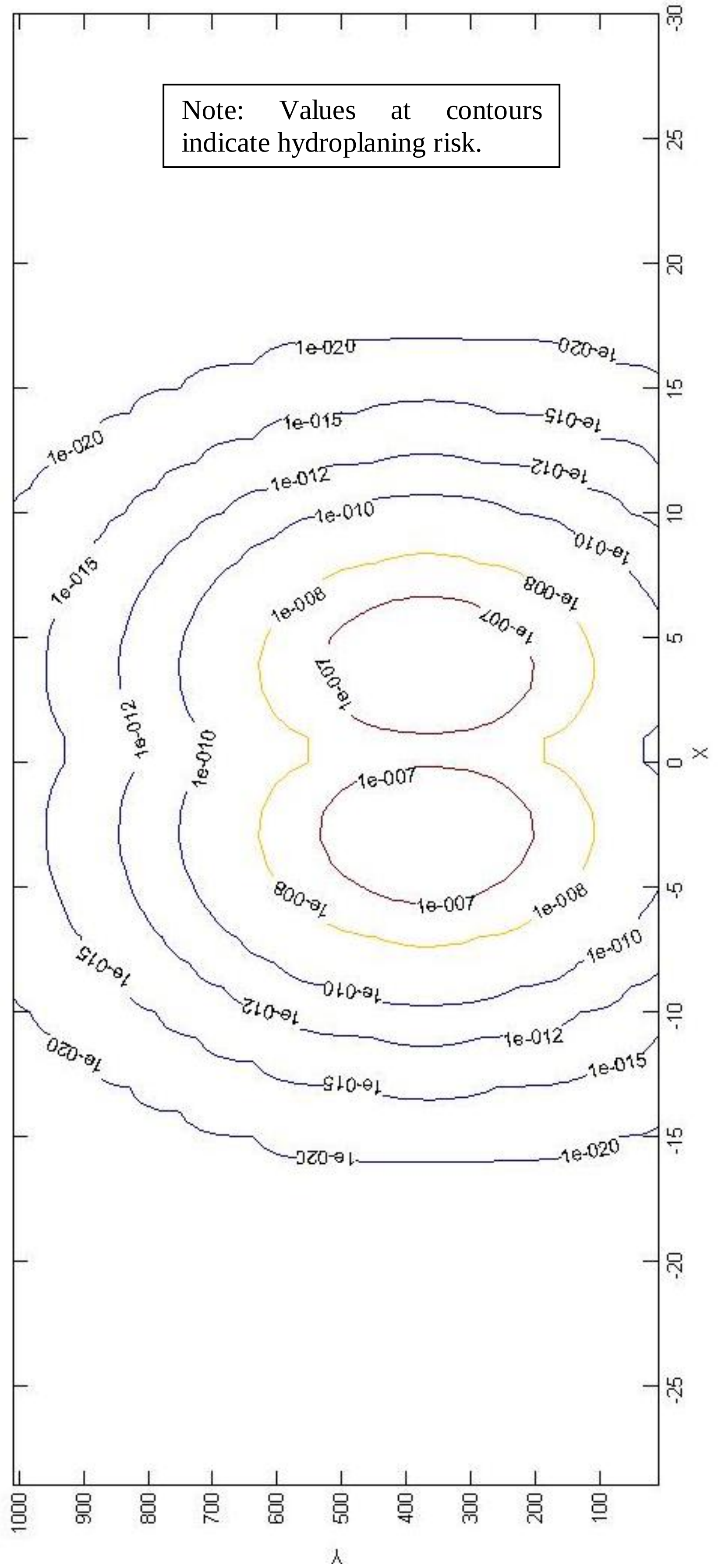

FIGURE 7.5 Hydroplaning risk contours for the touchdown zone

CHAPTER 8 CONCLUSION

8.1 Summary and Conclusions

Airfield pavement performance has a vital role in ensuring safe aircraft operations during landing and takeoff. It is the responsibility of the airport authority to design and maintain airfield pavements to meet these required performance levels as stipulated in standards issued by regulatory organizations such as the Federal Aviation Administration, the Civil Aviation Authority (UK), and ICAO etc. Pavement management systems provide airport authorities with a method of establishing an effective pavement maintenance and rehabilitation system. Among the various pavement areas in an airfield, safety is of great importance especially on runway pavement where aircraft operate at rather high speeds leaving low margins for error.

Landing and takeoff are perhaps the most critical phase of flight with respect to safety. More than one third of all accidents occur during these two phases, although they only constitute about two percent of the total flight duration. Therefore a great deal of attention is given to aircraft safety on runways. Studies on runway safety risks for aircraft have shown that runway excursions comprise a significant part of runway related accidents. Researchers have analyzed excursion accident data to identify the main contributing factor to excursion accidents. It was found that wet runway conditions are among the major causal factors for excursion accidents especially during landing (van Es, 2010; ATSB, 2008a, b; Benedetto, 2002). Wet runway conditions reduce the available friction for aircraft braking and directional control. In addition, the hazards faced by aircrafts are compounded due to other operational factors such as long landing, fast landing, and presence of cross wind etc., thereby increases the excursion risk significantly.

It is imperative for airports to implement an efficient runway friction management program to alleviate any friction related issues. Typical activities of friction maintenance and improvement include:

- Runway surface friction measurement and monitoring,
- Surface texture measurements where low friction values are reported,
- Repairing distresses that impede surface drainage,
- Removal of rubber deposit,
- Removal of contaminants that reduce friction levels, and
- Construction of runway grooving to improve friction performance under wet weather conditions.

Most of the maintenance decision making, prioritization, and severity assessments with respect to the above activities have been carried out based on subjective judgment from past experience, pavement condition determined from index method or measurement results comparisons with pre-determined criterion etc. Several shortcomings have been identified with such methods and there is a need to provide an improved to methodology to facilitate maintenance management decision making.

This research study evaluates runway distresses and surface characteristics on the basis of their impact on runway/aircraft tire friction performance under wet pavement conditions. A finite element model has been developed to analyze tire-pavement-fluid interaction and simulate hydroplaning and skid resistance for aircraft tires on runway pavement with surface water. This analysis incorporates distress, runway pavement, and aircraft operating characteristics in the simulation. The results enable one to identify the relative impacts that each of those factors has on skid resistance and hydroplaning of an aircraft tire.

Based on the type of distress and its impact on runway friction and ultimately aircraft performance, a failure criterion can be designated for each case analyzed. This forms the basis for assessing the risk that a distress or pavement condition poses to aircraft operations during wet runway conditions. Risk evaluation examines the failure criterion with respect to the various operating characteristics to identify the potential risks for aircraft safety. This approach allows for risk considerations to be incorporated into airport runway pavement maintenance management. The authorities can have a better understanding how a distress would impact pavement performance, the relative impacts of different distress severity levels, and the safety margins involved and improve the pavement maintenance management decision making.

This thesis presents a methodology to incorporate risk consideration into runway pavement maintenance management. Three main aspects of considerations namely, runway pavement management, aircraft runway safety risks, and analysis of wet pavement friction are integrated in the development of the methodology. As highlighted earlier, risk is referred to aircraft safety in the context of this research and the study primarily focused on runway friction related operational risks. Under this theme several distress and runway conditions are evaluated to apply the concepts developed. The following section will highlight the findings from each of these analyses.

8.1.1 Braking Distance Determination for Overrun Risk Evaluation in Runway Pavement Maintenance

The second part of the thesis focuses on aircraft skid resistance in wet weather conditions. A methodology to compute aircraft braking distance under wet-pavement conditions is developed. Finite element model is used to evaluate skid resistance variation with speed. It can incorporate the effects of key factors such as water film thickness, wheel load, pressure, and surface condition into the analysis of skid resistance and braking distance. The computed braking distances for different water film thicknesses show the impact wet pavement conditions have on aircraft performance during landing. This procedure offers an improved understanding of the factors affecting runway friction, which is an integral part of the aircraft braking distance computation and stopping distance estimation. The computed braking distances can be used to assess the overrun risk for different weather conditions and aircraft characteristics in an airport. It presents a useful tool for airport authorities in assessing the levels runway conditions for surface friction safety management as well as other safety measures to improve the overall safety performance of aircraft landing and takeoff operations.

8.1.2 Evaluation of Beneficial Effects of Runway Grooving

An analytical approach was developed to evaluate the beneficial effects of runway grooving on aircraft braking distances under wet pavement conditions. This approach is similar to the methodology adopted in the previous case to evaluate braking distance for smooth pavements. The proposed method employs a mechanistic based approach and uses finite element simulation to evaluate aircraft wet-pavement skid resistance on grooved pavements. The results show that there is a significant improvement in skid resistance for grooved pavements as compared to un-grooved. Furthermore the rate of reduction in skid resistance with speed is considerably less for grooved pavements.

The proposed method is able to incorporate the effects of key factors such as water film thickness, wheel load, pressure, and surface condition into the analysis of skid resistance and braking distance. The analysis considers the probabilistic nature of aircraft operational characteristics such as touchdown speed and landing weight. The beneficial effects of grooving are represented by comparing the braking distances on an un-grooved pavement. The comparison between the results for un-grooved and grooved pavements with different groove depths clearly demonstrates that pavement grooving significantly reduces aircraft braking distances.

The results for different groove depths demonstrate the change in runway pavement frictional characteristics with groove depth. The distribution of braking distances at each water film thickness provides a good indicator of the relative risk of aircraft overrun accidents under those conditions. The proposed method offers a valuable analytical tool for pavement groove design, and evaluation and assessment of the benefits of risk reduction by introducing grooving to existing runway pavements.

8.1.3 Risk Based Criteria for Maintenance Management of Rutting

A new approach was adopted to determine the critical rut depth threshold for pavement maintenance based on its impact on aircraft safety performance. From past studies on pavement rutting it was found that road vehicle safety becomes a major concern much earlier before ruts deteriorate to an extent when pavement structural failure would occur. Safety risks mainly arise as a result of water accumulation which can lead to frictional losses. Therefore hydroplaning risk and increase of braking distance were identified as the main safety concern for rutting and the basis on which rut severity could be assessed. For each rut depth the hydroplaning speed and the speed at which the braking distance exceeds the design braking distance were computed. These can be compared with normal operating speeds of a highway to identify the critical rut depth, where the hydroplaning speed exceeded or the braking distance passes safe limits. The critical rut depth analysis for highways clearly illustrates that if the frictional properties and the maximum allowed road vehicle speed along different pavement sections of a highway are not the same, their critical rut depths would also be different.

The critical rut depth analysis was next extended to runway pavement rut analysis. Hydroplaning and overrun potentials were used as the basis for risk assessment. Water accumulation in ruts and leading to hydroplaning and overrun was considered by many airport agencies as the main issues with rutting. Input parameters related to aircraft, runway and ruts are used in the finite element model developed in this study to evaluate hydroplaning speeds and skid resistance for different rut depths. These are compared with the aircraft's expected speed profile on the runway to identify the region where a rut of a certain depth can pose hydroplaning risk to the aircraft. This method can be applied to all the types of aircrafts operating on the runway and identify the hydroplaning risk potential for a rut depending on it depth and location, and determine the relative severity for maintenance planning.

Rutting can also adversely affect aircraft braking performance. Using the computed skid resistance, aircraft braking distances were calculated for different rut depths and compared with that calculated assuming a coefficient of friction equal to 0.2. This comparison enables to identify the rut depth which has frictional properties representing poor braking conditions with to $\mu = 0.2$. The two analysis presented (i.e. hydroplaning and overrun risks) provide a useful tool for airport pavement engineers to assess the impact of rutting on aircraft safety and assist them in their maintenance decision making.

8.1.4 Aircraft Landing Hydroplaning Risk Consideration for Runway Pavement Maintenance

The hydroplaning speed analysis used earlier in the research is applied to evaluate the case of hydroplaning risk during landing. Hydroplaning is a major safety concern during landing in wet weather. An aircraft is most susceptible to hydroplaning during the initial phase of landing where the speeds are high and wheel loads are low. A probabilistic-based hydroplaning risk computation method is adopted in this study for aircraft landing on a runway during wet weather. By considering the physical and operational characteristics of the aircraft, weather conditions, and the runway and pavement surface characteristics, hydroplaning risks for aircraft landing operations are computed. Using this method risk contours can be generated for the touchdown zone to evaluate the risk for aircraft. This information is useful to determine the sensitivity of hydroplaning risk depending on other factors such as rainfall intensity, runway cross slope, surface characteristics (e.g. surface texture, grooving), and also aircraft type. This would provide useful information for airport operators in assessment of runway friction improvement work carried out. It also give them an idea of the safety margin for the purpose of runway friction maintenance planning.

8.2 Recommendations for Further Research

There are several areas where further research could be done to improve the current analysis as well as applying this concept to other aspects of pavement performance.

1. In this research surface water film thickness was assumed or estimated using empirical methods. Runway friction management work such as grooving or

restoring texture improves pavement friction performance by (i) decreasing the surface water film thickness during rainfall, and (ii) increasing drainage capability between tire-pavement contact areas. If more advanced theoretically based water film thickness estimation methods are incorporated into this analysis, it would provide more insight to the authorities on the benefits of texturing or grooving improvements.

2. The other improvement can be in the area of finite element simulation of skid resistance. The research considers a locked wheel tire sliding case. If tire slip can be simulated, it would allow computation of friction coefficient under different slip conditions. This can be used to simulate the friction available during the entire braking process. Another possible improvement is the modeling of skid resistance of a yawed tire. These results can be of great benefit to assess performance of aircraft on a wet runway under cross wind conditions.
3. Aircraft mechanics such as directional control mechanisms of aircraft should be considered in the analysis to assess the safety risks and determine failure criterion in the case of differential friction on runway.
4. In this research the methodology for incorporating risk into runway pavement maintenance management was primarily focused on runway friction and its impact on aircraft safety. However as a concept it is applicable to the assessment of other types of risks such as structural failure risk. The same basic steps i.e. identify distress impact on pavement performance, mechanistic analysis, define failure criterion, and evaluate risk based on aircraft operating characteristics can be adopted to assess the risk and incorporate it into pavement maintenance management decision making.

REFERENCES

ADINA Inc. (2009). ADINA Theory and Modeling Guide volume I: ADINA Solids and Structures. Watertown, Mass.

Agrawal S. K. and Henry, J. J.. (1977). Technique for Evaluating Hydroplaning Potential of Pavements, Transportation Research Record, No. 633, pp. 1-7.

Agrawal, S.K. (1981). The Braking Performance of an Aircraft Tire on Grooved Portland Cement Concrete Surfaces. FAA-RD-80-78, Federal Aviation Administration, Washington, D.C.

Agrawal, S.K. (1983). The Braking Performance of an Aircraft Tire on Grooved and Porous Asphalt Concrete Surfaces, FAA-RD-82-147, Federal Aviation Administration, Washington, D.C.

Agrawal, S.K. (1986). Braking Performance of Aircraft Tires, Progr. Aerospace Sci. Vol. 23, pp. 105 -150.

Agrawal, S.K., and Daiutolo, H. (1981). Effects of Groove Spacing on Braking Performance of An Aircraft Tire. Transportation Research Record, No. 836, pp. 55-60.

American Association of State Highway and Transportation Officials (AASHTO). (2004). A Policy on Geometric Design of Highways and Streets: 5th Edition. Washington D.C.

American Association of State Highway and Transportation Officials (AASHTO). (1989). AASHTO Report of the AASHTO Joint Task Force on Rutting, Washington D.C.

American Society for Testing and Materials (ASTM) (2009). Standard Test Method for Airport Pavement Condition Index Surveys. ASTM D5340-04, Philadelphia.

ASTM. (2008). ASTM standards E 501-8. Standard specification for standard rib tire for pavement skid- resistance tests. ASTM standards sources (CD-ROM), Philadelphia.

Australian Transport Safety Board (ATSB). (2008a). Transport Safety Report: Aviation Research and Analysis Report - A worldwide review of commercial jet aircraft runway excursions. AR-2008-018(1), Sydney.

Australian Transport Safety Board (ATSB). (2008b). Transport Safety Report: Aviation Research and Analysis Report - Minimizing the Likelihood and Consequences of Runway Excursions. AR-2008-018(2), Sydney.

Bailey, G. (2000). Slippery When Wet. Flight Safety Australia. Issue: September-October. Australian Transport Safety Bureau, Canberra, Australia.

Baladi, G. Y., Novak, E. C. Jr. and Kuo, W. H. (1992). Pavement condition index remaining service life. Pavement Management Implementation, STP 1121, eds F. B., Holt and W. L., Gramling, American Society for Testing and Material, Philadelphia, pp. 63-90.

Balmer, G.G., and Gallaway, B.M. (1983). Pavement Design and Controls for Minimizing Automative Hydroplaning and Increasing Traction. Frictional Interaction of Tire and Pavement, ASTM STP 793, eds W.E. Meyer and J.D.Walter, pp 167-190. American Society for Testing and Materials, Philadelphia, PA.

Barksdale, R.D. (1972). Laboratory Evaluation of Rutting in Base Course Materials. Proceedings of the Third international Conference on the Structural Design of Asphalt Pavements, Vol. 1, London, pp. 161-174.

Barling, J.M. and Fleming, P. (2005). Safe Management of Airfield Pavements. Proceedings of the Institution of Civil Engineers: Transport, 158, Issue TR2, pp 97-106.

Barnes, T., DeFiore, T. and Micklos, R. (1999). Video Landing Parameter Survey—Washington National Airport. DOT/FAA/AR-97/106, Federal Aviation Administration, U.S. Department of Transportation.

Benedetto, A. (2002). A Decision Support System for the Safety of Airport Runways: The Case of Heavy Rainstorms. Transportation Research Part A. Volume 36, pp. 665-882.

Blythe, William and Seguin, Debra E. (2006). Commentary: Legal Minimum Tread Depth for Passenger Car Tires in the U.S.A. - Survey. Traffic Injury Prevention, 7 (2), 107 -110.

Boeing. (1985). Airplane Characteristics for Airport Planning, D6-58324, Boeing . <http://www.boeing.com/commercial/airports/727.htm.> (June 10, 2009).

Boeing. (2008). Statistical Summary of Commercial Jets Airline Accidents: Worldwide Operations 1959 – 2008. < http://www.boeing.com/news /news/techissues/pdf/statsum.pdf >. (Mar. 20, 2010).

Boeing. (2010). Statistical Summary of Commercial Jets Airline Accidents, Worldwide Operations 1959 – 2010, Boeing. < http://www.boeing.com/news /news/techissues/pdf/statsum.pdf >. (July 20, 2011).

Boeing. (2011). Current Market Outlook 2011-2030. Boeing <http://www.boeing.com/commercial/cmo/forecast_summary.html> (July 10, 2011).

Brilon, W., and M. Ponzlet. (1996). Variability of Speed-Flow Relationships on German Autobahns. Transportation Research Record 1555, Transportation Research Board, Washington, D.C.

Bullas, John C. (2004). Tyres, road Surfaces and Reducing Accidents: A review. The AA Foundation for Road Safety Research/County Surveyor's Society, UK. 45–50. < http://www.cssnet.org.uk/> (15.12.2010)

California Department of Transportation (Caltran). (2006). Maintenance Manual, Volume 1. Website: < http://www.dot.ca.gov/hq/maint/manual/ maintman.htm.> (Mar. 12 2010).

Central Massachusetts Metropolitan Planning Organization (CMMPO). (2006). Pavement Management Field Guide to Road Surface Distresses. <http://www.cmrpc.org/doc_download.aspx?document_id=71> . (March 24 2010).

Cepic, A. (2004). Hydroplaning of H-Type Aircraft Tires. 2004-1-3119, SAE International.

Christensen, P., and Ragnoy, A. (2006). The Condition of the Road Surface and Safety. TOI Report 840/2006, Transportokonomisk Institutt, Oslo.

Civil Aviation Authority (CAA) (2001). CAP 168: Licensing of Aerodromes. CAA, London.

Civil Aviation Authority (CAA). (2008). The Assessment of Runway Surface Friction Characteristics. CAP 683, CAA, West Sussex, United Kingdom.

Croll, J. and Bastian, M. (2004). Falcon 20 Aircraft Braking Performance on Wet Concrete Runway Surfaces. Publication TP 14273E, Transport Canada, Quebec.

Dreher, R.C., and Tanner, J.A. (1974). Experimental Investigation of Braking and Cornering Characteristics of 30x11.5-14.5- Type VII, Aircraft Tires with Different Tread Patterns, NASA TN D-7743, National Aeronautics and Space Administration, Washington, D.C.

Engineering Science Data Unit (ESDU). (2003). Development of a Comprehensive Method for Modelling Performance of Aircraft Tyres Rolling or Braking on Dry and Precipitation- Contaminated Runways. Transport Canada, TP 14289e.

Engineering Sciences Data Unit (ESDU). (1995). Frictional and Retarding Forces on Aircraft Tires Part II: Estimation of Braking Force, ESDU Data Item, No. 71206.

Engineering Sciences Data Unit ESDU. (1999). Statistical Analysis of Wet Runway Friction for Aircraft and Ground-test Machines. ESDU Report 99015.

European Aviation Safety Agency (EASA). (2010). Runway Friction Characteristics Measurement And Aircraft Braking (Rufab) - Volume 1. Germany.

Faber, M. H., and Stewart, M. G. (2003). Risk Assessment for Civil Engineering Facilities: Critical Overview and Discussion. Reliability Engineering & System Safety, Volume 80, Issue 2, pp. 173-184.

Federal Aviation Administration (FAA). (1997). Measurement, Construction and Maintenance of Skid-Resistant Airport Pavement Surfaces, AC 150/5320-12C, Washington D.C.

Federal Aviation Administration. (2004). PASER Manual: Asphalt Airfield Pavements. AC No: 150/5320-17, Washington D.C.

Federal Aviation Administration. (2006). Airport Pavement Management System (APMS). AC No: 150/5380-7A, Washington D.C.

Federal Aviation Administration. (2007). Runway Overrun Prevention. AC No: 91-79, Washington D.C.

Federal Aviation Administration. (2009a). Guidelines and Procedures for Maintenance of Airport Pavements. AC No: 150/5380-6A, Washington D.C.

Federal Aviation Administration. (2009b). Guidelines and Procedures for Measuring Airfield Pavement Roughness. AC No: 150/5380-9, Washington D.C.

Federal Aviation Administration. (2009c). Debris Hazards at Civil Airports. AC 150/5380-5B, Washington D.C.

Flight Safety Foundation (FSF). (2000 b). Approach and Landing Accident Reduction Tool Kit- Crosswind Landings. Flight Safety Digest, Aug-Nov 2000.

Flight Safety Foundation (FSF). (2000 c). Approach and Landing Accident Reduction Tool Kit- Wet or Contaminated Runway, Flight Safety Digest, Nov-Dec 2000.

Flight Safety Foundation (FSF). (2000a). Approach and Landing Accident Reduction Tool Kit- Braking Devices, Flight Safety Digest, Nov-Dec 2000.

Flight Safety Foundation (FSF). (2009). Runway Safety Initiative -Reducing the Risk of Runway Excursion.

Florida Department of Transportation (Florida DOT) (2006): Airfield Inspection Reference Manual, State wide Pavement Management Program, Florida. <http://www.floridaairportpavement.com/reports/FDOT_Field_Manual_Final_Report.pdf> (July 01, 2011)

Fwa, T. F., and Ong, G. P. (2007). Wet-Pavement Hydroplaning Risk and Skid Resistance: Analysis, Journal of Transportation Engineering, Vol. 134, No.5, pp. 184–190.

Fwa, T.F. and Shanmugam, R. (1998). Fuzzy Logic Technique for Pavement Condition Rating and Maintenance Needs, Proceedings of the 4th International Conference on Managing Pavements. Durban, South Africa.

Fwa, T.F., Chan, W.T., and Lim, C.T. (1997). Decision Framework for Pavement Friction Management of Airport Runways, Journal of Transportation Engineering, Vol. 123, No.6, pp. 429-435.

Fwa, T.F., Liu, S.B. and Teng, K.J. (2003). Airport Pavement Condition Rating and Maintenance Need K.J. s Assessment Using Fuzzy Logic, Proceedings of the Airfield Pavements: Challenges and New Technologies Conference, ASCE, Las Vegas, Nevada.

Gallaway, B. M., D. L. Ivey, G. G. Hayes, W. G. Ledbetter, R. M. Olson, D. L. Woods and R. E. Schiller. (1979). Pavement and Geometric Design Criteria for Minimizing Hydroplaning. Federal Highway Administration Report No. FHWA-RD-79-31.

Gallaway, R.M., Schiller, R.E., Jr., and Rose, J.G. (1971). The Effect of Rainfall Intensity, Pavement Cross Slope, Texture, and Drainage Path Length on Pavement Water Depths. Texas Transportation Institute, Texas A&M University Research Report No. 138-5.

Gendreau, M., and Soriano, P. (1998). Airport Pavement Management Systems: An Appraisal of Existing Methodologies. Transportation Res. A, Vol. 32, No. 3, pp. 197-214.

Goodyear Tire & Rubber Co. (2002) Aircraft Tire Data Book. Goodyear Tire & Rubber Co., Ohio.

Gray, W. E. (1963). Aquaplaning on Runways. Journal of Royal Aeronautical Society. (Tech. Notes), Vol. 67, No. 629, pp. 302-304.

Green, J., Shahin, M.Y. and Alexander, D.R. (2004). Airfield Pavement Condition Assessment. Transportation Research Record, No. 1889.

Hachiya, Y., Maekawa, R., and Su, K. (2008). Verification of Surface Condition Evaluation Subsystem for Airport Asphalt Pavement Management in Japan, In Transportation Research Board 87th Annual Meeting Compendium of Papers (CD-ROM), Transportation Research Board, Washington,D.C.

Hachiya, Y., Watanabe, T., and Kitaochi, K. (2009). Some Issues on Surface Distress of Airport Pavements in Japan, Service Center of Port Engineering (SCOPE), <http://www.scopenet.or.jp/main/thesis-article/pdf/ronbun_16.pdf > (August 3, 2011).

Hajek, J., Hall, J.W., and Hein, D.K. (2011). Common Airport Pavement Maintenance Practices, ACRP Synthesis 22. Transportation Research Board, Washington, D.C.

Hall, J.W. (2009). National Cooperative Highway Research Program (NCHRP): Guide for Pavement Friction. Transportation Research Board, Washington, D.C.

Hayes, G.G., Ivey, D.L., and Gallaway, B.M. (1983). Hydroplaning, Hydrodynamic Drag and Vehicle Stability. Frictional Interaction of Tire and Pavement, ASTM STP 793, W.E. Meyer and J.D.Walter, eds., American Society for Testing and Materials, pp. 151-166.

Henry, J.J. (2000). Evaluation of Pavement Friction Characteristics. NCHRP Synthesis 291, National Cooperative Highway Research Program, Washington, D.C.

Hicks, R. G., Seeds, S. and Peshkin, D. G. (2000). Selecting a Preventive Maintenance Treatment for Flexible Pavements. Report No. FHWA-IF-00-027, Federal Highway Administration, Washington, D.C.

Ho Sang, V. (1975) A. Field Survey and Analysis of Aircraft Distribution on Airport Pavements, Report FAA-RD-74-36. Federal Aviation Administration, U.S. Department of Transportation.

Horne, W. B. (1966). Interactions between Pneumatic Tire and Pavement Surface. NASA N63- 25343, National Aeronautics and Space Administration, Langley Research Center, Hampton, Va.

Horne, W. B. (1969). Results from Studies of Highway Grooving and Texturing at NASA Wallops Station, Pavement Grooving and Traction Studies, NASA SP-5073, National Aeronautics and Space Administration, Washington, D.C.

Horne, W. B. (1975). Wet Runways. NASA TM X-72650, National Aeronautics and Space Administration, Langley Research Center, Hampton, Va.

Horne, W. B., and Brookes, G.W. (1967). Runway Grooving for Increasing Tire Traction- The Current Program and an Assessment of Available Results. National Aeronautics and Space Administration, Langley Research Center, Hampton, Va.

Horne, W. B., and Dreher, R. C. (1963). Phenomena of Pneumatic Tire Hydroplaning. NASA T.N.D-2056, National Aeronautics and Space Administration, Langley Research Center, Hampton, Va.

Horne, W. B., and Joyner, U. T. (1965). Pneumatic Tire Hydroplaning and Some Effects on Vehicle Performance, In SAE International Automotive Engineering Congress, Detroit, Michigan, USA.

Horne, W.B. (1976). Status of Runway Slipperiness Research, Transportation Research Record, No. 624, pp. 95-121.

Horne, W.B., and Leland, T.J.W. (1962). Influence of Tire Tread Pattern and Runway Surface Condition on Braking Friction and Rolling Resistance of a Modern Aircraft Tire. NASA Technical Note TN D-1376, National Aeronautic and Space Administration, Washington, D.C.

Horne, W.B., and Whitehurst, E.A. (1969). Highway and Runway Traction Studies: The Problem, History and NASA Program, Pavement Grooving and Traction Studies. NASA SP-5073, National Aeronautic and Space Administration, Washington, D.C., pp. 3-19.

Horne, W.B., Yager, T.J. and Ivey, D.L. (1986). Recent Studies to Investigate Effects of Tire Footprint Ratio on Dynamic Hydroplaning Speed. The Tire Pavement Interface, ASTM STP 929, ASTM, Philadelphia, pp. 26-46

Horne, W.B., Yager, T.J., and Taylor, G.R. (1965). Recent Research to Improve Tire Traction on Water, Slush and Ice, Publication N66-83984, NASA, Langley Research Center.

Horne, W.B., Yager, T.J., and Taylor, G.R. (1968) Review of Causes and Alleviation of Low Tire Traction Wet Runways. NASA TN D-4406, Hampton, VA.

Hudson, S. W., Hudson, W. R., and Carmichael, R. F. (1992). Minimum Requirements for Standard Pavement Management Systems. In Pavement Management Implementation, eds F. B. Holt and W. L. Gramling, STP 1121, American Society for Testing and Material, Philadelphia, PA, pp.19-31.

Huebner, R. S., Reed, J. R., and Henry, J. J. (1986). Criteria for Predicting Hydroplaning Potential. J. Transp. Eng., Vol. 112, No. 5, pp. 549–553.

Ibrahim, A.T., and Hall, F.L. (1994). Effect of Adverse Weather Conditions on Speed Flow- Occupancy Relationships. Transportation Research Record 1457, Transportation Research Board, Washington, D.C.

Ihs, A., Velin, H., and Wiklund, M. (2002). Vägytans Inverkan Påtrafiksäkerheten. Data Från 1992-1998, VTI meddelande 909-2002, Statens vägoch Transportforskningsinstitut, Linköping.

International Civil Aviation Organization (ICAO) (2002). Airport Services Manual – Part 2: Pavement Surface Conditions. 4th Ed., Doc 9137 N/898.

International Civil Aviation Organization (ICAO) (2004). Annex 14 Aerodromes- Volume 1: Aerodromes Design and Operation.

Ivey, D. L., and Griffin, L. I. (1977). Development of a Wet Weather Safety Index. Texas Transportation Institute, Texas A&M University, College Station.

Jackson, P. (2001) Jane's All World Aircrafts 2001-2002. Jane's Information Group. McGraw Hill, New York.

Janic, M. (2000). An Assessment of Risk and Safety in Civil Aviation. Air Transport Management , No. 6, pp .43-50.

Kamplade, J. (1990). Analysis of Transverse Unevenness with Respect to Traffic Safety. Surface Characteristics of Roadways: International Research and Technologies, ASTM STP 1031, pp. 211–223.

Keyes, H.J. (1962). A Review of the Problems of Aircraft Wheel Braking on Wet Surfaces and a Description of a Method of Artificially Wetting Runways for Test Purposes. C.P. No. 592, Ministry of Aviation, London, U.K.

Kim, B. J., A. A. Trani, X. Gu, and C. Zhong. (1996). Computer Simulation Model for Airplane Landing Performance Prediction. Transportation Research Record, No. 1562, pp. 53-62.

Kirkland, I.D.L., Caves, R.E., Humphreys, I.M., and Pitfield, D.E. (2004). An Improved Methodology for Assessing Risk in Aircraft Operations at Airports, Applied to Runway Overruns. Safety Science, Vol. 42, pp. 891–905.

Kulakowski, B. T. and W. E. Meyer. (1989). Skid Resistance of Adjacent Tangent and Nontangent Sections of Roads, Transportation Research Record, No. 1215, pp. 132-136.

Kyte, M., Khatib, Z., Shannon, P., and Kitchener, F. (2001). Effect of weather on free-flow speed. Transportation Research Record 1776, Transportation Research Board, Washington, D.C., 60–68.

Leland, T.J.W., and Taylor, G.R. (1965). An Investigation of the Influence of Aircraft Tire-Tread Wear on Wet-Runway Braking. NASA Technical Note TN D-2770, National Aeronautic and Space Administration, Washington, D.C.

Lemer, A. C., and Moavenzadeh, F. (1971). Reliability of Highway Pavements. Highway Research Record 362, Highway ResearchBoard, Washington, D.C., pp.1–8.

Li, D.C.H., Fung, W.H.W., Widyatmoko, I., Elliot, R.C., Larsen, B.K. (2008). Planning Design and Implementation of Major Runway Resurfacing at Hong Kong International Airport, In Proceedings of 6th International Conference on Road and Airfield Pavement Technology.

Li, S., Zhu, K. Q., Noureldin, S., and Kim, D. (2004). Pavement Surface Friction Test Using Standard Smooth Tire: The Indiana Experience, In Transportation Research Board 83rd Annual Meeting Compendium of Papers (CD-ROM), Transportation Research Board, Washington, D.C.

Lim, C.T., Phillip, T.C.Y., Fwa, T.F., and Chen, W.T. (1996). A Graphical Database Management System for Airport and Road Network Operations, In

Proceedings of the First PES-CTR Annual Symposium on Pavement Technology, Singapore.

Lister, N.W., and Addis, R.R. (1977). Field Observations of Rutting and Practical Considerations, Transportation Research Record, No. 640, pp. 28-34.

Malaysia Airports. (2011). Case Study: Kuala Lumpur International Airport Pavement Maintenance, Airfield Engineering and Asset Maintenance 2011, Singapore.

Manuel, A. et al. (2011). Improved Models for Risk Assessment of Runway Safety Areas. ACRP Report 50, Transportation Research Board, Washington, D.C.

Mc Nerney, M.T. (2010). Evaluation of Map Cracking as Failure Mechanism in Airport Concrete Pavements, Transportation Research Board 89th Annual Meeting Compendium of Papers (CD-ROM), Transportation Research Board, Washington, D.C.

Meyer, W. E. (1991). Pavement Texture Significance and Measurement, ASTM Standardization News, Vol. 19, No. 2, pp. 28-31.

Meyer, W.E. (1982). Synthesis of Frictional Requirements Research. Report No. FHWA/RD- 81/159, Federal Highway Administration (FHWA), Washington, D.C.

Meyer, W.E., Hegmon, R., and Gillespie, T. (1974). Locked-Wheel Pavement Skid Tester Correlation and Calibration Techniques, NCHRP report 151.

Ministry of Transportation and Infrastructure, British Columbia (MTI BC). (2009). Pavement Surface Condition Rating Manual- 3rd Edition. British Columbia.

Moughabghab, M. (2006). Pavements Defects and Repair. Swift Conference 200, <http://www.captg.ca/presentations> (June 6, 2011).

Navneet, G., Guo, E., and McQueen, R. (2004). Operational Life of Airport Pavements. Report DOT/FAA/AR-04/46. Federal Aviation Administration, Washington, D.C.

Neubert, T.W., and Goff, B. (2006). Runway Friction Measurement and Reporting Procedures. 29th Annual Airport Conference. < http://www.faa.gov/ airports/eastern/airports_news_events/hershey/ >

Newell, B. (1991). Landing on Frictionless Surface, Proceedings in Aircraft/Pavement Interaction: an Integrated System, Kansas City, Missouri, pp. 112–120.

Ohio State Department of Transportation (OhDOT). (2006). Pavement Condition Rating System. Columbus, OH.

Okano, T., and Koishi, M. (2000). A New Computational Procedure to Predict Transient Hydroplaning on a Tire, 19th Annual Meeting and Conf. on Tire Science and Technology, The Tire Society, Akron, Ohio.

Ong, G. P. and Fwa, T. F. (2007a). Wet-Pavement Hydroplaning Risk and Skid Resistance: Modeling. ASCE Journal of Transportation Engineering, Vol. 133, Iss.10, pp. 590–598.

Ong, G. P., and Fwa, T. F. (2007b). Prediction of Wet-Pavement Skid Resistance and Hydroplaning Potential. Transportation Research Record, No. 2005, pp. 160-171.

Ong, G.P., and Fwa, T.F. (2008). Modeling and Analysis of Truck Hydroplaning On Highways. Transportation Research Record, No. 2068, pp. 99-108.

Ong and Fwa (2009). Runway Geometric Design Incorporating Hydroplaning Consideration. Transportation Research Record, No. 2106, pp. 118-128.

Oregon Department of Aviation (Oregan DOA) (2007). Pavement Maintenance Program. <http://www.oregon.gov/Aviation/pmp.shtml> (June 03, 2011)

Paine,D.A. (2004). Managing Pavements through Risk Analysis. Proceedings of the 6th International Conference on Managing Pavements.

Perrone, E., Clark, D., Ness, Q., Chen, X., and Hudson, S. (1998) Risk Based Life Cycle Cost Analysis for Project Level Pavement Management. Proceedings of the 4th International Conference on Managing Pavements.

Phillips, P.W. (1969). Calculated Airplane Stopping Distances Based on Test Results Obtained at the Landing Research Runway NASA Wallops Station. Pavement Grooving and Traction Studies, NASA SP-5073, National Aeronautic and Space Administration, Washington, D.C., pp. 101-114.

Ranganathan A. (2006). Wet Runway Overruns: Pilot Error? System Deficiency? ISASI Forum Volume 39, Number 1 International Society of Air Safety Investigators.

Reesaul, G. (2011). Pavement Management at an Airport: A Myth or Reality, Airfield Engineering and Asset Maintenance 2011, Singapore.

Reigle, J.A., and Zaniewski, J. (2002). Risk-Based Life-Cycle Cost Analysis for Project-Level Pavement Management. Transportation Research Record, No. 1816, pp. 34-42.

Rizenbergs, R. L., Burchett, J. L. and Warren, L.A.(1976). Accidents on Rural Interstate and Parkway Roads and their Relation to Pavement Friction. Kentucky Bureau of Highways, Lexington.

Russam, K. and Ross, N.F. (1968). The Depth of Rain Water on Road Surfaces. Road Research Laboratory, Ministry of Transport Report No. LR 236.

Shahin, M. Y. (1982). Airfield Pavement Distress Measurements and Use in Pavement Management. Transportation Research Record, No. 893, pp, 59-63.

Shahin, M. Y. (1994). Pavement Management for Airports Roads and Parking Lots. Chapman and Hall, New York.

Shilling, B. (1969). R.A.E. Aircraft Tests on Grooved, Open Graded and Asphalt Runways in Great Britain. Pavement Grooving and Traction Studies, NASA SP-5073, National Aeronautic and Space Administration, Washington, D.C., pp. 67-80.

Sousa, J.B., Craus, J. and Monismith, C.L. (1991). Summary Report on Permanent Deformation in Asphalt Concrete. SHRP-A/IR-91-104, Strategic Highway Research Program (SHRP). Washington D.C.

Start, M. R., Kim, J., and Berg, W. D.(1996). Development of Safety Based Guidelines for Treatment of Pavement Rutting. Proceeding of the Conference, Road Safety in Europe and Strategic Highway Research Program (SHRP) No. 4, Part 5.

Start, R. M., Joeng, K., and Berg, W. D. (1998). Potential Safety Cost Effectiveness of Treating Rutted Pavements. Transportation Research Record, No.1629, pp. 208-213.

Tanner, J.A, Sandy, J.M., and McCurry, J.L. (1981). Static and Yawed Rolling Mechanical Properties of Type VII Aircraft Tires. NASA Technical Paper 1863, NASA, Virginia.

Trafford, J.L.W., and Taylor, G.R. (1965). An investigation of the Influence of Aircraft Tire Tread Wear on Wet Runway Braking. NASA TN D-2770, National Aeronautics and Space Administration, Langley Research Center, Hampton, Va.

Trani, A. A., B. J. Kim, X. Gu, and C. Zhong. (1995). Runway Exit Designs for Capacity Improvement Demonstrations (Phase III). Virginia Polytechnic Institute and State University, Blacksburg.

Transport Canada. (2001). Wet Runway Friction: Literature and Information Review, TP 14002E, Quebec.

Transport Canada. (2004). Maintenance of Airport HMAC Pavements. ERD-125-1, Ontario.

Transport Canada. (2008). Evaluation of Airfield Pavement Surface Roughness (Smoothness),<http://www.tc.gc.ca/civilaviation/International/Technical/Pavement/evaluation/smoothness/smoothness.htm.> (Mar. 29, .2009).

Transport Canada. (2010). Evaluation of Pavement Surface Drainage, <http://www.tc.gc.ca/civilaviation/international/technical/pavement/evaluation/surface.htm.> (Mar. 29, .2010).

Transportation Research Board (TRB). (2009). Influence of Roadway Surface Discontinuities on Safety: State of the Art Report. Transportation Research Circular E-C134. Washington DC.

Transports Quebec. (2002). Standard: Airport Maintenance, Ministère des Transports, Quebec.

Van Es, G. W. H., Roelen, A. L. C., Kruijsen, E. A. C., Giesberts, M. K. H. (2001). Safety Aspects of Aircraft Performance on Wet and Contaminated Runways. NLRTP-2001-216, Netherlands National Research Laboratories.

Van Es, G.W.H. (2001). Hydroplaning of Modern Aircraft Tires. NLR-TP-2001-242, National Aerospace Laboratory NLR.

Van Es, G.W.H. (2005). Running out of Runways: Analysis of 35 years of Landing Overrun Accidents, Publication NLRTP-2005-498, Netherlands National Research Laboratories.

Van Es, G.W.H. (2010). A Study on Runway Excursions from European Perspective. NLR-CR-2010-259. Netherlands, NLR Air Transport Institute.

Van Es, G.W.H., and van der Geest P.J. (2001). Safety Aspects of Aircraft Operations in Crosswind. NLR-TP-2001-217, National Aerospace Laboratory NLR.

Van Es, G.W.H., Tritschler, K., and Tauss, M. (2009). Development of Landing Overrun Risk Index, NLR-TP-2009-280. Netherlands, NLR Air Transport Institute.

Walker, D., Entine, L., Kummer, S. (2002). Pavement Surface Evaluation and Rating (PASER), Asphalt Roads. Wisconsin Transportation Information Center, Madison, WI.

Wall Street Journal (WSJ) (2007). NTSB Weighs Measures to Improve Air Safety. Nov. 6 edition. New York.

Wambold, J.C., Henry, J.J. and Yeh, E.C. (1984). Methodology for Analyzing Pavement Condition Data, report FHWA/RD-83/094 prepared by the Pennsylvania Transportation Institute.

Washington State Department of Transportation (WsDOT). (1999). Pavement Surface Condition Field Rating Manual for Asphalt Pavements. Olympia, Washington.

Washington Department of Transportation. (Washington DOT). (n/a) Pavement Management Manual: Washington Airport Pavement Management System.

Weissmann, A.J., McCullough, B.F., and Hudson, W.R.. (1992). Reliability Assessment of Continuously Reinforced Concrete Pavements. Journal of Transportation Engineering, Vol 120, No.2, pp 178-198.

Williams, J.R. (1969). Aquaplaning. Pavement Grooving and Traction Studies. NASA SP-5073, National Aeronautic and Space Administration, Washington, D.C., pp. 81-100.

Williams, T. (1971) Skid Resistance of Runways. Aircraft Engineering and Aerospace Technology, Vol. 43, Iss. 9, pp.6 - 9.

Yager, T. J. (1969). Comparative Braking Performance of Various Aircraft on Grooved and Ungrooved Pavements at the Landing Research Runway - NASA Wallops Station. Pavement Grooving and Traction Studies, NASA SP-5073, National Aeronautic and Space Administration, Washington, D.C., pp. 35-66.

Yager, T. J. and Dreher, R.C. (1976). Traction Characteristics of a 30 x 11.5 Type VIII Aircraft Tire on Dry, Wet and Flooded Surfaces. NASA TMX-72805, National Aeronautic and Space Administration, Washington, D.C.

Yager, T. J. and McCarty, J. L. (1977). Friction Characteristics of Three 30 × l1.5 Type VIII Aircraft Tires with Various Tread Groove Patterns and Rubber Compounds. NASA Technical Paper 1080. The National Aeronautics and Space Administration, Washington. D.C.

Yager, T., Phillips, W.P., and Horne, W. (1970). A Comparison of Aircraft and Ground Vehicle Stopping Performance on Dry, Wet, Flooded Slush Snow and Ice-Covered Runways. NASA Technical Note TN D-6098.

Yager, T.A. and Byrdsong, T.J. (1973). Some Effects of Grooved Runway Configurations on Aircraft Tire Braking Traction under Flooding Runway Conditions. NASA TN D-7215, Langley Research Center, Hampton, VA.

Zhang, H., and Bathe, K. J. (2001). Direct and iterative computing of fluid flows coupled with structures. Computational Fluid and Solid Mechanics: Proc. 1st MIT Conf. on Computational Fluid and Solid Mechanics, K. J. Bathe, ed., Elsevier Science, New York, pp. 1440–1443.

Zhang, H., Zhang X., Ji, S., Guo, Y., Ledezma, G., Elabbasi, N. and deCougny, H. (2003). Recent Development of Fluid-Structure Interaction Capabilities in the ADINA System, Computers and Structures, Vol. 81, pp. 1071-1085.

Zmindak, M., and Grajciar, I. (1997). Simulation of the Aquaplane Problem. Comput. Struct., Vol .64(5/6), pp. 1155–1164.